The Dissertation Committee for Christopher Michael Bejger Certifies that this is the approved version of the following dissertation:

Tetrathiafulvalene Schiff-base Ligands and Anion Receptors

Committee:

_____
Jonathan L. Sessler, Supervisor

_____
Christopher W. Bielawski

_____
Dionicio R. Siegel

_____
Bradley J. Holliday

_____
Ananth Dodabalapur

_____
Stosh A. Kozimor

Tetrathiafulvalene Schiff-base Ligands and Anion Receptors

by

Christopher Michael Bejger, B.S.

Dissertation

Presented to the Faculty of the Graduate School of

The University of Texas at Austin

In Partial Fulfillment

of the Requirements

for the Degree of

Doctor of Philosophy

The University of Texas at Austin

December 2012

Acknowledgements

First of all, I am grateful to my advisor, Professor Jonathan Sessler, for giving me a chance after taking a year off before my graduate studies. Thank you Professor Sessler for welcoming me into your laboratory and allowing me to work on the chemistry that most interests me. I would also like to thank him for patiently editing the manuscripts we coauthored, including this Dissertation. During my stay in his research group, he has provided an influential contribution to my scientific pursuits and has always offered enthusiastic and encouraging advice.

I would like to thank Dr. Jung Su Park for his friendship and guidance over the beginning of my research career. Jung Su's positive reinforcement motivated me to work harder and to think outside the box in my approach to chemistry. I will never forget the good times, including the endless hours we spent bickering as we worked together in the old laboratory in Welch hall.

I am indebted to Christian for putting up with my endless complaining. Throughout my five years in the lab, Christian has always patiently listened to me vent about reactions that do not work, crystals that refuse to grow, and numerous general issues that are frustrating about graduate school.

One of the best parts of working in the Sessler group is having the privilege to work with a large number of diverse people from all over the world. I would like to thank Dustin, Candace, Mandy, Elizabeth, Sun Kuk, Vladimir, Jia Jia, Gabriela, Rob, Dong Sub, Murat, Christina, Jonathan, Brett, and Dani for all their help and support during my time in Austin. Additionally, I would like to thank the other two members of the "American Office", Eric and Nathan, for keeping me sane and upbeat for the past two years!

I would like to acknowledge Dr. Vince Lynch for refining most of the crystal structures in this Dissertation and for spending countless hours trying to solve crystals of poor quality that never made the cut.

I am also appreciative of several other collaborators that have been very hospitable in sharing their laboratories with me during my studies. First, I would like to thank Dr. Jason Love of the University of Edinburgh for his suggestions and help while working on Pacman complexes. I must also express my gratitude to Dr. Stosh Kozimor and his research group at Los Alamos National Laboratory for their support while I was pursuing actinide chemistry. Working with Stosh and everyone in the C-IIAC group at LANL has been a great experience and has helped bring my research to the next level.

Finally, I wish to thank my parents and two sisters, Kerri and Alexandra, for their love and support throughout the years in which I have been away from home working towards my degree.

Tetrathiafulvalene Schiff-base Ligands and Anion Receptors

Publication Number. _____

Christopher Michael Bejger, Ph.D.
The University of Texas at Austin, 2012

Supervisor: Jonathan L. Sessler

Over the last decade, the classic organic donor tetrathiafulvalene (TTF) has emerged as an important functionality in supramolecular systems and complex ligand chemistry. Due to synthetic advances, TTF is no longer a moiety strictly limited to the area of charge transfer salts in material science. In fact, many complex systems incorporating the electron rich donor system are known. More can be imagined. This doctoral dissertation describes the author's journey in designing, synthesizing, and studying various compounds in which the TTF moiety serves a practical purpose, often times giving known molecules new functions. The reported findings have led to a greater understanding of anion binding effects on TTF-containing anion receptors, the use of transition metals to pre-organize π-faces for through-space donor-acceptor interactions, and the introduction of actinide species to tetrathiafulvalene ligands.

The first Chapter provides a brief introduction and a short history of TTF chemistry. It also provides an overview describing the fundamental properties of TTF compounds, including TTF dimeric behavior and redox properties. Chapter 2, as the major focus of this dissertation, details the use of a flexible TTF-modified macrocyclic

ligand, which upon metallation can effectively preorganize two TTF units to interact when oxidized. Specifically, a new way to stabilize the through-space mixed-valence TTF dimer, in which a transition metal can affect the degree of interaction between the two TTF units, is described. The mixed-valence TTF species in question could see use as components in molecular machines and could play an important role as molecular organic conductors, and discussions along these lines are included in this chapter. These mixed-valence complexes were investigated by spectroscopic (^{1}H-NMR, UV-Vis NIR titrations, and EPR analysis) and X-ray single crystallographic analyses involving both the neutral and oxidized products. Chapter 3 introduces the synthesis, characterization, and electrochemistry of the first TTF-ligand to form a complex with an actinide cation. Chapter 4 details the synthesis, binding studies and X-ray single crystallographic analyses of a TTF-based electrochemical sensor for dihydrogen phosphate anion detection. Experimental procedures and characterization data are reported in Chapter 5.

Table of Contents

List of Tables

List of Figures

List of Schemes

Chapter 1

Introduction and Historical Overview

1.1 General Background: Molecular Organic Conductors

Although organic materials are often thought of as insulators, instances of their conductivity have been known since 1886 when Letheby obtained a partially conductive substance (suspected to be polyaniline) by anodic oxidation of aniline in sulfuric acid.[1] Much later in the 1950's, Akamatu reported that the polycyclic compound perylene could form a relatively stable radical-ion salt with halogens. Remarkably, this salt had the ability to carry a current due to the electron-hole pairs generated upon oxidation of the perylene.[2] This initial report on radical-ion salts led others to focus on designing additional new conductive crystals compromised of purely organic compounds. The resulting first generation organic conductive materials consisted of linear arrays of organic molecules, as evidenced from the respective crystal structures. They were generally found capable of forming radical ion salts or charge-transfer complexes, in which the components are partially oxidized and reduced.[3] In search for a superior high conducting molecular crystal during the years that followed, researchers prepared and tested many radical-ion salts and donor/acceptor pairs. Most of these were made up of π-conjugated molecules able to accept or donate electrons depending on their electron affinity or their ionization potential. Initial early crystals were based on the easily reduced

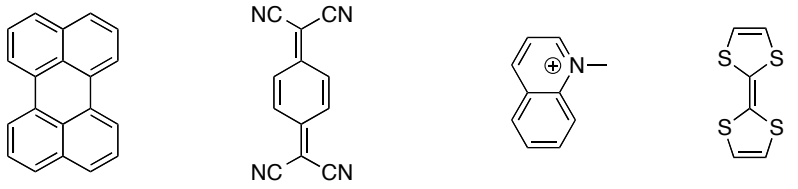

Perylene **TCNQ** **N-quinolium** **TTF, 1**

Figure 1.1 Organic molecules used in first generation conductive molecular crystals.

tetracyanoquinodimethane (TCNQ) and various quinolium and *N*-methylquinolium cations (Figure 1.1).[4] In 1970, a new π-donor was reported[5], called tetrathiafulvalene or TTF (**1**) for short. Its conduction properties were measured by Wudl along with that of the radical ion salt of $[TTF]^{\bullet+}$-Cl^{-}. Both species displayed semiconductor behavior.[6,7] In 1973 Ferraris and coworkers demonstrated that the charge transfer salt originating from a mixture of this newly reported electron donor (TTF) in conjunction with the hitherto known acceptor TCNQ, gave rise to an organic that displayed metallic conductivity in the solid state.[8]

Conductive molecular crystals with TCNQ and quinolium cations were known prior to the work with TTF, as noted above. However TTF was established as being a better donor for TCNQ due to their complementary HOMO-LUMO levels. In fact, significant conductivity over a wide temperature range was seen. It persisted down to 59 K, where a sharp metal insulator transition was observed.[9] The result of this metallic conductivity stems from the packing order of the crystals obtained, which leads to uniform segregated partially oxidized stacks of TTF lined up adjacent to stacks of partially reduced TCNQ. Within this arrangement the large sulfur heteroatoms present in the TTF moieties

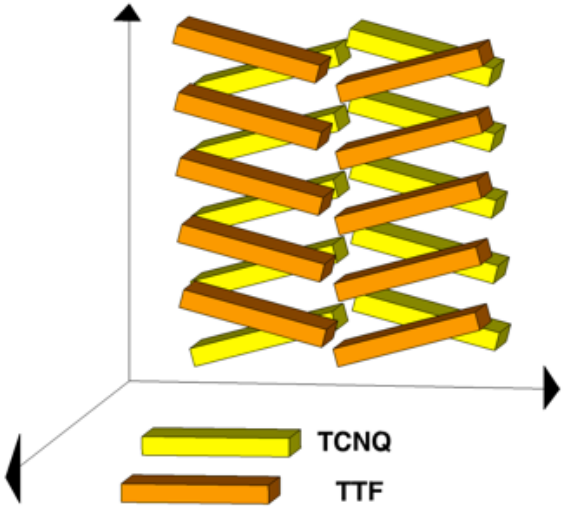

Figure 1.2 Packing representations of segregated stacks of partially oxidized TTF adjacent to partially reduced TCNQ in the charge-transfer salt.

presumably allow for a susbstantial "overlap" and strong intermolecular bonding (Figure 1.2). TTF-TCNQ is considered a one-dimensional conductor because the overlap of the molecular orbitals is largest along the stack direction and much weaker between the stacks.

Since this seminal discovery, there have been over 10,000 papers published on TTF, its derivatives, and conductive salts wherein TTF acts as the electron donor.[10] A major milestone in this field, which led to further interest in TTF chemistry, was the report of the first organic superconductor, the hexafluorophosphate salt of tetramethyltetraselenafulvalene (TMTSF) **2**, reported by Bechgaard and Jerome in 1980.[11] Another important compound BEDT-TTF **3**, also emerged from the search for higher temperature superconductors.[12] To this date, the highest reported T*c* values for organic superconductors have come from radical salts containing **3**. (Figure 1.3).

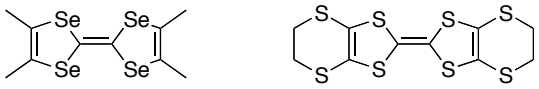

2 **3**

Figure 1.3 Organic superconductors TMTSF **2** and BEDT-TTF **3**

1.2 FUNDAMENTAL PROPERTIES OF TETRATHIAFULVALENE

Due to the central importance of TTF and TTF derivatives in this Dissertation, it is appropriate to discuss the key properties that endow these species with utility as an electron donor and as a building block for crystal engineering and various chemical applications. According to Wudl, the first to synthesize TTF, the initial objective was to prepare an electron-rich olefin with a lower oxidation potential than tetrakis(dimethylamino)ethylene (**4**).[13] Considering the structure of **4**, Wudl surmised that by substituting a more electronegative heteroatom for nitrogen, the olefin would, in turn, be a stronger reducing agent (Figure 1.4). However, after synthesizing TTF the converse was found to be true. Specifically, TTF proved to be a poorer electron donor than **2**. This was rationalized in terms of poor orbital overlap between the sulfur atoms and the central double bond, as well as possible electron withdrawing effects involving the sulfur atoms.[13] Despite these effects, the radical cation produced upon oxidation of TTF proved to be more stable than that produced from the oxidation of **4**.

1 **4**

Figure 1.4 Structural comparison of TTF and tetrakis(dimethylamino)ethylene.

To rationalize this stability, the "Hückel driving force" towards aromaticity was invoked. While TTF does indeed follow Hückel's 4n+2 rule for aromaticity of a 10 π-electron system, it is not planar and all bonds lengths are not equal. However, upon oxidation, the resulting isolated five membered ring cations, $TTF^{\bullet+}$ and TTF^{2+}, are

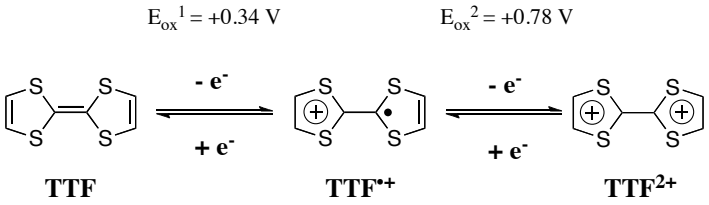

Figure 1.5 Reversible oxidations of TTF to the corresponding radical-cation and dication species. Oxidation potentials are reported *vs*. Ag/AgCl in CH_3CN.

formally 6 π-electron aromatic 1,3-dithiole ring systems. Apart from this aromatic stabilization, the polarizable sulfur atoms also reduce the energy of the radical cation $TTF^{\bullet+}$ and dication species TTF^{2+}. Therefore, due to the thermodynamic stability of the ensuing radical cation $TTF^{\bullet+}$ and dication species TTF^{2+}, TTF can be reversibly oxidized via two 1-electron steps at easily accessible potentials.

In conjunction with the rich redox chemistry that TTF exhibits, several additional fundamental properties make it an interesting building block in materials, macrocyclic, and supramolecular chemistry. These properties include the following: [14]

- Strong π-electron donor with high HOMO level;
- Oxidation of TTF to the radical cation $TTF^{\bullet+}$ and dication TTF^{2+} occurs sequentially and reversibly;
- The oxidation potentials of TTF can be fine tuned by attaching electron-donating or electron withdrawing substituents;
- Under many conditions the TTF radical cation $TTF^{\bullet+}$ and dication TTF^{2+} are thermodynamically stable species;
- The UV-Vis absorption spectra of TTF, $TTF^{\bullet+}$, and TTF^{2+} are distinctively different from one another;
- TTF is stable to many synthetic transformations, although it is important to avoid strongly acidic and oxidizing conditions;
- TTF derivatives readily form dimers, highly ordered stacks of two dimensional sheets, which are stabilized by π-π interactions and nonbonded sulfur-sulfur interactions.

1.2.1 TTF Dimeric Species

While a single TTF monomer displays novel electrochemical behavior, it is important to appreciate that intermolecular interactions between TTF units of different redox states, as well as those involving other redox active components, can also serve to form discrete species with unique properties. For example, the first organic metals, comprised of TTF-TCNQ (Figure 1.2), exist as arrays of partially-oxidized and partially-reduced long-bonded TTF units that interact through a "supramolecular-orbital" in the solid state.[8] In related TTF-halide[7] and TTF-pseudo-halide[15] (SCN^- and $SeCN^-$) salts, where there is only one stack (the TTF stack) the oxidation states of the interacting TTF units dictate whether the resulting crystal is a conductor or an insulator. In general, the appearance of metallic conductivity is contingent upon intrastack mixed-valence interactions, whereas an integer valence results in insulating materials.

Through-space dimers of TTF in different respective oxidation states can be regarded as the simplest model for the columnar stacks seen in conductive charge transfer and radical cations salts. However, because of their low stability, these systems are usually only observed[16] in solution at high concentration, at low temperatures, or in the solid state.[17] Two dimers are typically observed. They are the mixed-valence $(TTF)_2^{\bullet+}$ and the radical cation dimer, or π-dimer $(TTF^{\bullet+})_2$ (Figure 1.6). As a solution counterpart to charge-transfer and radical salts of TTF, the mixed-valence, or MV, $(TTF)_2^{\bullet+}$ species can be considered the conducting form and the π-dimer $(TTF^{\bullet+})_2$ as the insulating form. Beyond the three stable oxidation states of the parent TTF **1** (Figure 1.6) these two dimeric states of TTF exist as discrete weakly associated species and display their own distinct electrochemical and spectroscopic properties.

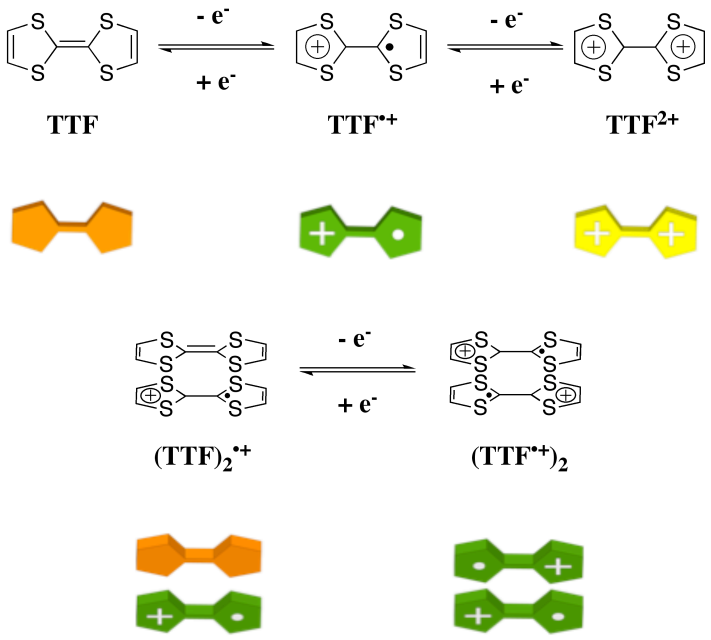

Figure 1.6 Illustration of the possible oxidation states of TTF including the two dimeric states formed under certain conditions $(TTF)_2^{\bullet+}$ and $(TTF^{\bullet+})_2$.

When taking into account the various oxidation states of TTF and its dimeric forms, the equilibrium constants for each state can help explain the electrochemical behavior.[18] When no dimers are formed, two reversible processes are seen under conditions of cyclic voltammetry (CV) as follows:

$$TTF \leftrightarrows TTF^{\bullet+} + e^- \ (E_1) \qquad (1)$$

$$TTF^{\bullet+} \leftrightarrows TTF^{2+} + e^- \ (E_2) \qquad (2)$$

In many cases, the oxidation steps can be followed by monitoring the formation of a mixed-valence dimer and/or a π-dimer by spectroscopic or electrochemical means. In

order to model the kinetic behavior of the mixed-valence dimer and π-dimer, the following equilibrium constants have been described:

$$TTF + TTF^{\bullet+} \leftrightarrows (TTF)_2^{\bullet+} \qquad K_{MV} = \frac{[(TTF)_2^{\bullet+}]}{[TTF][TTF^{\bullet+}]} \qquad (3)$$

$$2TTF^{\bullet+} \leftrightarrows (TTF^{\bullet+})_2 \qquad K_{\pi\text{-dim}} = \frac{[(TTF^{\bullet+})_2]}{[TTF^{\bullet+}]^2} \qquad (4)$$

Because the mixed-valence dimer $(TTF)_2^{\bullet+}$ and the π-dimer $(TTF^{\bullet+})_2$ are conjugated via through-space interactions, they are also in equilibrium characterized by the following equilibrium expression;

$$(TTF)_2^{\bullet+} \leftrightarrows (TTF^{\bullet+})_2 + e^- (E_3) \qquad (5)$$

Therefore, by subtracting the Nernst equations for the oxidation potentials E_1 and E_3, the redox potential E_3 may be related to E_1, K_{MV}, and $K_{\pi\text{-dim}}$ as follows;

$$E_3 - E_1 = \frac{RT}{F} \ln \frac{K_{MV}}{K_{\pi\text{-dim}}} \qquad (6)$$

Equation 6 can be used to explain perturbations in the CV that may signal formation of mixed-valence species. For example, when $K_{MV} = K_{\pi\text{-dim}}$, the potentials E_1 and E_3 become identical and the first oxidation process in the CV appears as a single wave. However, when $K_{MV} > K_{\pi\text{-dim}}$, $E_1 < E_3$. As a result, two waves are expected in the voltammogram, corresponding to the oxidation of TTF and subsequent oxidation of the mixed-valence

complex, respectively. Finally, $K_{MV} < K_{\pi\text{-dim}}$ implies that $E_1 > E_3$ and only one wave at position E_1 will be observed (Figure 1.7).

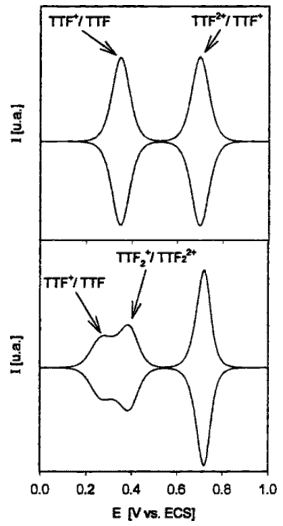

Figure 1.7 Simulated deconvoluted cyclic voltammograms of TTF systems. Top: Parent TTF **1**. Bottom: Bis-TTF system with through-space interactions leading to stabilization of dimeric states. Reprinted with permission from *J. Phys. Chem. B*. **1998**, *102*, 7776. Copyright 1998 American Chemical Society.

The simulated voltammograms shown in Figure 1.7 serve to illustrate differences in the electrochemical behavior between simple non-interacting TTF units and TTF's that have aggregated in solution. The top view shows the parent TTF **1** in which the expected two one-electron oxidations occur reversibly. The bottom voltammogram exemplifies the electrochemical consequences of dimerization according to the equilibrium constants in expressions (3) and (4). In this case, the first oxidation seen in the scan of **1** is split into two steps: The first involves oxidations of the neutral TTF to a mixed-valence dimer and the second reflects oxidation of the mixed-valence dimer to form the corresponding π-

dimer. The final oxidation wave is ascribed to a two-electron process wherein the π-dimer oxidizes to form two dicationic species that dissociate due to columbic repulsion.

In addition to different electrochemical signatures, electronically coupled TTF dimers also show distinct spectroscopic features. In 2005, Kochi developed a TTF salt comprised of a large non-coordinating permethylcarboranyl counterion (CB^-) to minimize ion-pairing effects in weakly polar solvents.[16d] The $TTF^{\bullet+}$ in the 1:1 salt was close to being a "free" cationic species in the solid state as well as in solution, thus allowing spectral observations in various solvent conditions for mixed-valence and π-dimers (Scheme 1.1). This seminal study is particularly noteworthy due to the fact that it represents the first instance where free dimers could be extensively studied in solution without the use of a host-cage or covalent stabilization.[19]

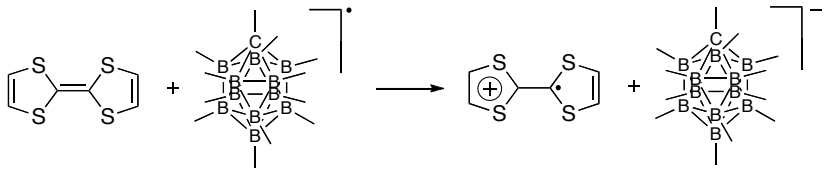

Scheme 1.1 Synthesis of the salt $TTF^{\bullet+}CB^-$

In the case of the mixed-valence dimer $(TTF)_2^{\bullet+}$ a distinct near-IR band that increased in intensity with lowering temperature was observed that reached saturation at a 1:1 TTF:$TTF^{\bullet+}$ stoichiometry. This intervalence charge-transfer band was found to be solvent dependent, with the formation of the mixed-valence dimer $(TTF)_2^{\bullet+}$ less favorable in polar solvents. The solvent dependence of the intervalence charge-transfer band, in accordance ab initio computations, was taken to mean that the dimer exists as a Class II mixed-valence system under the Robin-Day classification according to Müllken-Hush

analysis.[20] Briefly, this classification means that the TTF units are in two different oxidation states that interconvert readily.

Kochi also investigated the absorption properties of the π-dimer $(TTF^{\bullet+})_2$ in solution by cooling solutions of $TTF^{\bullet+}CB^-$. This study revealed a similarity between the absorption spectrum of the π-dimer in solution and in the solid-state. This allowed a direct correspondence to be drawn between the X-ray determined structure first reported by Torrance *et al*. and the species present in solution.[16b] Specifically, in both the solid and solution state the π-dimer exhibits a Davydov blue-shifted absorption[21] in comparison to the radical cation $TTF^{\bullet+}$, as well as a low energy band between the 650-850-nm range that shows no solvent dependence. Further spectroscopic evidence for formation of a π-dimer in solution came from an attenuation of the absorption band corresponding to the radical cation $TTF^{\bullet+}$ observed upon cooling. These spectroscopic studies were of paramount importance in establishing characteristic electronic absorption signatures for both TTF dimer species.

Not surprisingly, there are also several distinguishing solid state attributes that are exclusively characteristic of the mixed-valence dimer $(TTF)_2^{\bullet+}$ and π-dimer $(TTF^{\bullet+})_2$, respectively. These subtle differences are borne out by the X-ray crystallographic analysis of TTF-halide radical salts, where the TTF units form "infinite" stacks, as reported by Torrance *et al*.[16b]

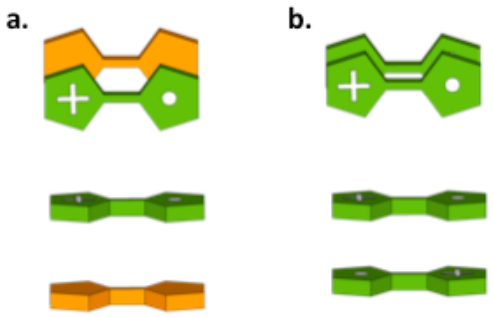

Figure 1.8 Top and side views of TTF dimers illustrating differences in overlap and intermolecular distance: **a.** Mixed-valence dimer and **b.** π-dimer.

In the mixed-valence halide salts of TTF, the distance between the π-faces (TTF•••TTF spacing) has an average distance of 3.57 Å. There is also a slight angle of offset between the two TTF units with respect to the C=C double bond. Therefore the TTF π-faces are not perfectly overlapping. However, upon further oxidation to the radical cation π-dimer the TTF units experience direct eclipsed overlap with no offset angle and a closer intermolecular distance of 3.34 Å (Figure 1.8). Another example of this intermolecular, intrastack bonding is seen in the TTF•TCNQ donor-donor acceptor complex. When compared to the structure of neutral TTF, wherein the interplanar separation between molecules along a given stack is 3.62 Å, the TTF•TCNQ structure shows a reduced interplanar distance of 3.47 Å.[22] Such a marked decrease in interplanar distances between the TTF units in charge-transfer complexes as compared to the typical TTF-halide salts is taken as a further indication of the cohesive nature of the various dimers. They exist in many cases as discrete species, despite the Columbic repulsion. In fact, the supramolecular interaction energy in these dimers has been estimated to be on the order of 2-3 kcal/mol.[13]

1.3 OBJECTIVE AND OUTLINE OF THIS DISSERTATION

A major thrust of modern supramolecular chemistry is the designing of molecules that incorporate both redox active units and metal or anion recognition sites. This strategy has produced many novel small molecule and macrocyclic systems with enhanced sensing and electron transfer properties. The main objective of this Dissertation is to explore the chemistry of redox active Schiff-base ligands and anion receptors constructed with TTF subunits.

It is hoped that this first chapter has served as a useful introduction to the history, properties, and applications of unfunctionalized TTF compounds. In this context, a detailed overview of dimeric-TTF species was included to illustrate the behavior and characterization of these dimers.

Chapter 2 describes the preparation of a new bis-TTF Schiff-base calixpyrrole macrocyclic ligand. The effect of metallation on the geometry and ensuing redox properties of this ligand are also explored. Part of this material has appeared in *Organic Letters* as a communication.[23] The electron paramagnetic resonance (EPR) studies were performed with the help of Christina M. Davis. Data analysis was done in collaboration with Jung Su Park.

Chapter 3 presents the preparation of a TTF-modified salphen ligand and subsequent uranyl complex. This complex represents the first time in which a TTF ligand is used for coordination of an actinide. A portion of these findings is currently being prepared as a manuscript in collaboration with Dr. Stosh A. Kozimor, Dr. Enrique Batista, and co-workers at Los Alamos National Laboratory.

Chapter 4 details the preparation and anion binding studies of a TTF-diindolylquinoxaline. The new anion receptor shows selective electrochemical and fluorescent response to the dihydrogen phosphate anion in solution. Evidence for self-

assembled dihydrogen-phosphate networks encapsulated within ordered arrays of the TTF-diindolylquinoxaline receptors is also observed in the solid state. The anion-mediated assembly of TTF units highlights the emerging roles of anion binding and hydrogen bonding in crystal engineering and construction of multi-TTF arrays. Part of this material has appeared in *Chemical Communications*.[24] Compound **4.14** was synthesized by Eric S. Silver.

The experimental procedures for the synthetic work described in this Dissertation are detailed in Chapter 5. The crystal structure refinements for **2.2**, $\mathbf{2.2^{\bullet+}(ClO_4)^-}$, and **4.1** were performed by Dr. Vincent M. Lynch of the X-ray Diffraction Laboratory of this Department. The crystal structure refinement for $\mathbf{4.1{\bullet}TBAH_2PO_4}$ was performed by Dr. Jung Su Park. Finally, Dr. Brian L. Scott of Los Alamos National Laboratory performed the crystal structure refinements for complex **3.1**. The resulting X-ray diffraction analysis data and refinement parameters are included in Appendix A.

References

1. Letheby, H. *J. Chem. Soc.*, **1862**, *15*, 161.

2. Akamatu, H.; Inokuchi, H.; Matsunaga, Y. *Nature,* **1954**, *173,* 168.

3. Jérome, D.; *Chem Rev*. **2004**, *104*, 5565.

4. (a) Acker, D. S.; Blomstrom, D. C., *J. Am. Chem. Soc.,* **1962**, *84*, 3370. (b) Burarov, L.; Fedutin, D.; Shchegolev, I. *Zh. Eksp. Teor. Fiz.* **1970**, *59*, 1125. (c) Shchegolev, I. *Phys. Status Solidi A* **1972**, *12*, 9.

5. TTF was actually first synthesized in 1965 and known as bis-1,3-Dithiolium, but only later realized to possess strong electron donating ability. Prinzbach, H.; Berger, H.; Luttringhaus, A. *Angew. Chem. Int. Ed. Engl.* **1965**, *4*, 435.

6. Three research groups independently and almost simultaneously reported the synthesis and associated studies of TTF (a) Wudl, F.; Smith, G. M.; Hufnagel, E. J. *J. Chem. Soc., Chem. Commun.* **1970**, 1453. (b) Coffen, D. L.; Chambers, J. Q.; Williams, D. R.; Garrett, P. E.; Canfield, N. D. *J. Amer. Chem. Soc.* **1971**, 109. (c) Hünig, S.; Kiesslich, G.; Scheutzow, D.; Zahradnik, R.; Carsky, P. *Int. J. Sulfur Chem. Part C*, **1971**, *6*, 109.

7. Wudl, F.; Wobschall, D.; Hafnagel, E. *J. Am. Chem. Soc.* **1972**, *94*, 670.

8. Ferraris, J.; Cowan, D. O.; Walatka, V. V., Jr.; Perlstein, J. H. *J. Am. Chem. Soc.* **1973**, *95*, 948.

9. Coleman, L. B.; Cohen, M. J.; Sandman, D. J.; Yamagishi, F. G.; Garito, A. F.; Heeger, A. J. *Solid State Commun.* **1973**, *12*, 1125.

10. (a) Yamada, J.-I., Sugimoto, T., Eds. *TTF Chemistry: Fundamentals and Applications of Tetrathiafulvalene*; Springer: Berlin, Germany, 2004. (b) Rovira, C. *Chem. Rev.* **2004**, *104*, 5289. (c) Mas-Torrent, M.; Hadley, P.; Bromley, S. T.; Crivillers, N.; Veciana, J.; Rovira, C. *Appl. Phys. Lett.* **2005**, *86*, 02110. (d) Mas-Torrent, M.; Durkut, M.; Hadley, P.; Ribas, X.; Rovira, C. *J. Am. Chem. Soc.* **2004**, *126*, 984. (e) Mas-Torrent, M.; Hadley, P.; Bromley, S. T.; Ribas, X.; Tarres, J.; Mas, M.; Molins, E.; Veciana, J.; Rovira, C. *J. Am. Chem. Soc.* **2004**, *126*, 8546. (f) Dressel, Mm; Drichko, N. *Chem. Rev.* **2004**, *104*, 5869. (g) Bendikov, M.; Wudl, F. Perepichka, D. F. *Chem. Rev.* **2004**, *104*, 4891. (h) Talham, D. R.; *Chem. Rev.* **2004**, *104*, 5479. (i) Kartsovnik, M. V. *Chem. Rev.* **2004**, *104*, 5737. (j) Gieser, U.; Schlueter, J. A. *Chem. Rev.* **2004**, *104*, 5203. (k) Enoki, T. Miyazaki, A. *Chem. Rev.* **2004**, *104*, 5449. (l) Shibaeva, R. P.; Yagubskii, E. B. *Chem. Rev.* **2004**, *104*, 5347. (m) Fourmigué, M.; Batail, P. *Chem. Rev.* **2004**, *104*, 5379. (n) Iyoda, M.; Hasegawa, M.; Miyake, Y. *Chem. Rev.* **2004**, *104*, 5085. (o) Yamada, J. I.; Akutsu, H.; Nishikawa, H.; Kikuchi, K. *Chem. Rev.* **2004**, *104*, 5057. (p) Kobayashi, H.; Cui, H. B.; Kobayashi, A. *Chem. Rev.* **2004**, *104*, 5265. (q)

Kobayashi, A.; Fujiwara, E.; Kobayashi, H. *Chem. Rev.* **2004**, *104*, 5243. (r) Mori, T. *Chem. Rev.* **2004**, *104*, 4947. (s) Fabre, J. M.; *Chem. Rev.* **2004**, *104*, 5133.

11. Jérome, D.; Mazaud, A.; Ribault, M.; Bechgaard, K. *J. Phys., Lett.* **1980**, *41*, L-95.

12. (a) Urayama, H.; Yamochi, H.; Saito, G.; Nozawa, K; Sugano, T.; Kinoshita, M.; Sato, S.; Oshima, K.; Kawamoto, A.; Tanaka, J. *Chem. Lett.* **1988**, 55. (b) Kini, A. M.; Geiser, U.; Wang, H. H.; Carlson, K. D.; Williams, J. M.; Kwok, W. K.; Vandervoot, K. G.; Thompson, J. E.; Stupka, D. L.; Jung, D.; Whangbo, M. H. *Inorg. Chem.* **1990**, *29*, 2555. (c) Williams, J. M.; Kini, A. M.; Wang, H. H.; Carlson, K. D.; Geiser, U.: Montgomery, L. K.; Pyrka, G. J.; Watkins, D. M.; Kommers, J. M.; Boryshuk, S. J.; Strieby Crouch, A. V.; Kwok, W. K.; Schirber, J. E.; Overmyer, D. L.; Jung, D.; Whangbo, M. H. *Inorg. Chem.* **1990**, *29*, 3272. (d) Williams, J. M.; Schultz, A. J. Geiser, U.: Carlson, K. D.; Kini, A. M.; Wang, H. H.; Kowk, W. K.; Whangbo, M. H.; Schirber, J. E. *Science,* **1991**, *252*, 1501. (e) Schlueter, J. A.; Williams, J. M.; Geiser, U.; Dudek, J. D.; Sirchio, S. A.; Kelly, M. E.; Gregar, J. S.; Kwok, W. K.; Fendrich, J. A.; Schirber, J. E.; Bayless, W. R.; Naumenn, D.; Roy, T. *J. Chem. Soc., Chem. Commun.* **1995**, 1311. (f) Williams, J. M.; Ferraro, J. R.; Thorn, R. J.; Carlson, K. D. Geiser, U.; Wang, H. H.; Kini, A. M.; Whangbo, M. H. *Organic Superconductors (Including Fullerenes) Synthesis, Structure, Properties, and Theory*; Prentice-Hall, Inc., New Jersey, 1992.

13. Wudl, F. *Acc. Chem. Res.* **1984**, *17*, 227.

14. (a) Jorgensen, T.; Hansen, T. K.; Becher, J. *Chem. Soc. Rev.* **1994**, *23*, 41. (b) Nielsen, M. B.; Lomholt, C.; Becher, J. *Chem. Soc. Rev.* **2000**, *29*, 153.

15. (a) Thomas, G. A.; Wudl, F.; DiSalvo, F.; Walsh, W. M., Jr.; Rupp, L. W.; Schafer, D. E. *Solid State Commun.* **1976**, *20*, 1009. (b) Wudl, F.; Schafer, D. E.; Walsh, W. M., Jr.; Rupp, L. W.; DiSalvo, F. J.; Waszczak, J. V.; Kaplan, M. L.; Thomas, G. A. *J. Chem. Phys.* **1977**, *66*, 377. (c) Wudl, F. *J. Amer. Chem. Soc.* **1975** *97*, 1962. (d) Somoano, R. B.; Gupta, A.; Hadek, V.; Novotny, M.; Jones, M.; Datta, T.; Deck, S. R.; Hermann, A. M. *Phys. Rev. B* **1977**, *15*, 595. (e) Kobayashi, H.; Kobayashi, K. *Bull. Chem. Soc. Jpn.* **1977**, *50*, 3127.

16. (a) Bozio, R.; Zanon, I.; Girlando, A.; Pecile, C. *J. Chem. Phys.* **1979**, *71*, 2282. (b) Torrance, J. B.; Scott, B. A.; Welber, B.; Kaufman, F. B.; Seiden, P. E. *Phys. Rev. B* **1979**, *19*, 730. (c) Khodorkovsky, V.; Shapiro, L.; Krief, P.; Shames, A.; Mabon, G.; Gorgues, A.; Giffard, M. *Chem. Commun.* **2001**, 2736. (d) Rosokha, S. V.; Kochi, J. K. *J. Am. Chem. Soc. 2007*, 129, 828.

17. (a) Yakushi, K.; Nishimura, S.; Sugano, T.; Kuroda, H.; Ikemoto, I. *Acta Crystallogr. B* **1980**, *36*, 358. (b) Kathirgamanathan, P.; Mazid, M. A.;

Rosseinsky, D. R. *J. Chem. Soc., Perkin Trans. 2* **1982**, 593. (c) Kondo, K.; Matsubayashi, G.; Tanaka, T.; Yoshioka, H.; Nakatsu, K. *J. Chem. Soc., Dalton Trans*. **1984**, 379. (d) Pyrka, G. J.; Fernando, Q.; Inoue, M. B.; Inoue, M. *Inorg. Chim. Acta* **1989**, *156*, 257. (e) Umeya, M.; Kawata, S.; Matsuzaka, H.; Kitagawa, S.; Nishikawa, H.; Kikuchi, K.; Ikemoto, I. *J. Mater. Chem.* **1998**, *8*, 295. (f) Tanaka, K.; Kunita, T.; Ishiguro, F.; Naka, K.; Chujo, Y. *Langmuir* **2009**, *25*, 6929.

18. (a) Huchet, L.; Akoudad, S.; Levillain, E.; Roncali, J.; Emge, A.; Bäuerle, P. *J. Phys. Chem. B* **1998**, *102*, 7776. (b) Spanggard, H.; Prehn, J.; Nielsen, M. B.; Levillain, E.; Allain, M.; Becher, J. *J. Am. Chem. Soc.* **2000**, *122*, 9486.

19. An in depth description of the various TTF-dimer stabilization strategies is given in Chapter 3.

20. Hankache, J.; Wenger, O. S.; *Chem. Rev.* **2011**, *111*, 5138.

21. (a) Davydov, A. S.; *Theory of Molecular Exitons* (Plenum, New York, 1971). (b) Craig, D. P.; Walmsley, S. H. *Exitons in Molecular Crystals* (Benjamin, New York, 1968).

22. Phillips, T. E.; Kistenmacher, T. J.; Ferraris, J. P.; Cowan, D. O. *J. Chem. Soc., Chem. Commun.* **1973**, 471.

23. Bejger, C.; Davis, C. M.; Park, J-S.; Lynch, V. M.; Love, J. B.; Sessler, J. L. *Org. Lett.*, **2011**, *13*, 4902.

24. Bejger, C.; Park, J-S.; Silver, E. S.; Sessler, J. L. *Chem. Commun.*, **2010**, *46*, 7745.

Chapter 2: Palladium Induced Macrocyclic Preorganization for Stabilization of a Tetrathiafulvalene Mixed-Valence Dimer

2.1 INTRODUCTION

A considerable effort has been devoted in recent years to the preparation and stabilization of synthetic TTF through-space dimeric systems.[1]

The fast growing interest in this field reflects a confluence of several factors. First, since TTF can form highly ordered stacks of weakly associated dimers upon oxidation (Chapter 1), which are responsible for the flow of conductivity (holes) through the crystal, synthetic systems that can control or stabilize such dimeric species are useful as model systems in the study of organic π-based conductivity. Second, the ability to stabilize different dimeric states of TTF gives access to more available oxidation states and thus greater control over the electronic properties of subsequent systems in which the interacting TTF π-faces play a role. Furthermore, the differences in ensuing association between the π-faces of such dimers, depending on their oxidation state, has implications in the production of molecular machines, chemical switches, and potential smart materials.[2] Lastly, many of the highest *Tc* organic superconductors based on organic charge-transfer salts exist in a packing order called the κ-phase that is comprised of an alternating pattern of orthogonal mixed-valence (MV) TTF dimers (Figure 2.1).[3] Therefore, for the purpose of engineering more robust organic crystals in which the electron rich TTF π-faces are preorganized in a dimeric fashion, it is imperative to design systems that have "built-in" TTF dimers that are preorganized to interact upon oxidation.

This Chapter describes the preparation, and spectroscopic characterization of a new TTF-modified Schiff-base calixpyrrole **2.1**, which upon homobinuclear palladium

metallation allows control over the formation of both mixed-valence and π-dimer oxidation states (Figure 2.2). The metal complex **2.2** described in the present Chapter will demonstrate the importance of the palladium induced preorganization on the stabilization of the two TTF π-faces in a dimeric arrangement.

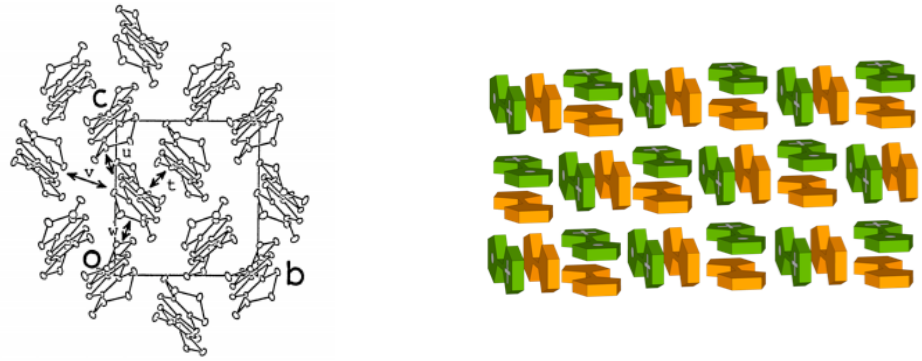

Figure 2.1 The crystal structure of an organic superconductor $(BEDT\text{-}TTF)_2Cu(NCS)_2$ (Tc =10.4 K) at 298 K determined by X-ray analysis and a representative packing illustration highlighting the checkerboard arrangement of the alternating dimers.[4]

The properties of the free ligand **2.1** and the homobinuclear complex **2.2** were examined using various spectroscopic techniques including EPR, ^{1}H NMR and UV-Vis-NIR spectroscopy, as well as electrochemically via cyclic voltammetry and differential pulse voltammetry. As will be detailed below, it was found that the free ligand **2.1** is too flexible to stabilize intramolecular mixed-valance and π-dimer states upon oxidation of the TTF units. In contrast, the rigid clip-like complex **2.2** enforces a close proximity between the two TTF π-faces. This geometric proximity presumably leads to stabilization of mixed-valence and as π-dimer states upon an appropriate degree of oxidation.

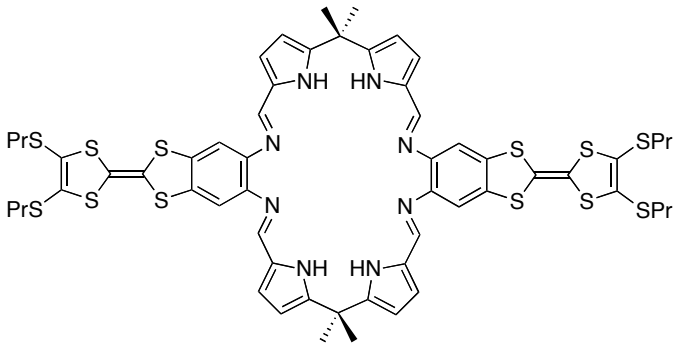

2.1

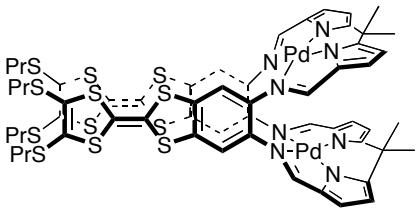

2.2

Figure 2.2 Tetrathiafulvalene-Schiff-base calixpyrrole ligand **2.1** and schematic representation of the dipalladium complex **2.2** that provides for the preorganization of the constituent TTF-dimers.

2.2 EFFORTS TOWARD STABILIZING TETRATHIAFULVALENE DIMERS IN SOLUTION

In the following section various strategies towards TTF-dimer stabilization will be discussed. The four main methods used to control interaction between TTF units are host stabilization, covalent attachment (including stimulus-induced preorganization), mechanical stabilization, and intermolecular assembly together with long-bonded aggregation phenomenon seen in organogels.

2.2.1 Host Stabilization

It is considered a formidable task to stabilize TTF dimers both in the solution and in the solid state. Nevertheless, there have been many elegant designs put forth to achieve this goal. Four main strategies have been used to stabilize TTF-dimers at room temperature in solution. The first approach uses the aid of a cavity or host-system in which TTF moieties can accumulate. Upon oxidation they interact with one another to form mixed-valence and π-dimers. Initial use of this method, as described by Kim *et al*., employed a cucurbit[8]uril as a hydrophobic host and a water soluble TTF derivative **2.3** that could assemble inside the host upon oxidation to form the π-dimer. This work marked the first time the stable radical species was observed in solution at room temperature (Scheme 2.1).[5]

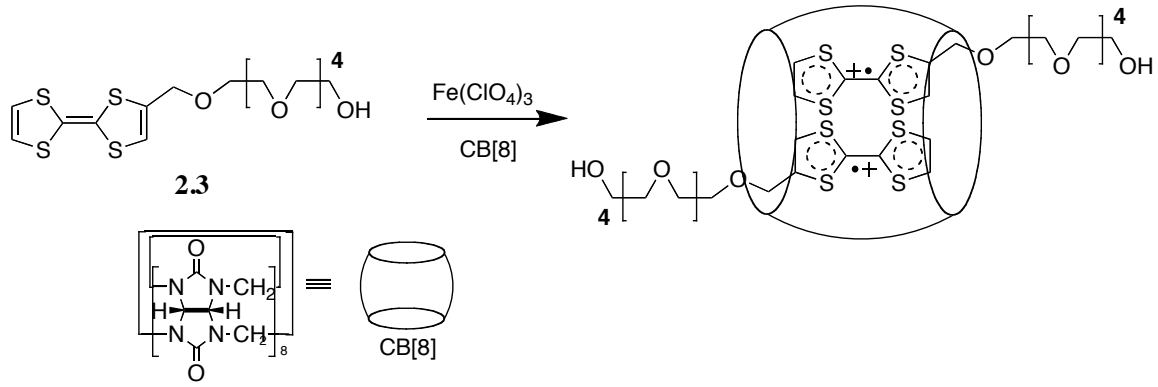

Scheme 2.1 Stable π-dimer of **2.3** encapsulated in the cavity of cucurbit[8]uril as reported by Kim *et al*.

The use of a stabilizing host, or in this case organic-pillared framework **2.4**, was exploited by Fujita *et al*. in the first observation of a TTF mixed-valence dimer in solution at room temperature.[6] In this instance, an electron deficient self-assembled cage of appropriate size acts as the host, allowing two TTFs to aggregate into the cavity. They are then preorganized for interaction upon oxidation. Specifically, it was found that upon electrochemical or chemical oxidation, one singly oxidized and one neutral TTF unit weakly associate forming a stable mixed-valence organic radical (Scheme 2.2).

Expanding upon this idea of cage molecules for TTF organization and stabilization, biporous uniform coordination networks were exploited recently by Fujita and shown to force pairs of TTF molecules into unique arrangements characterized by short S•••S contacts between the TTF faces.[7]

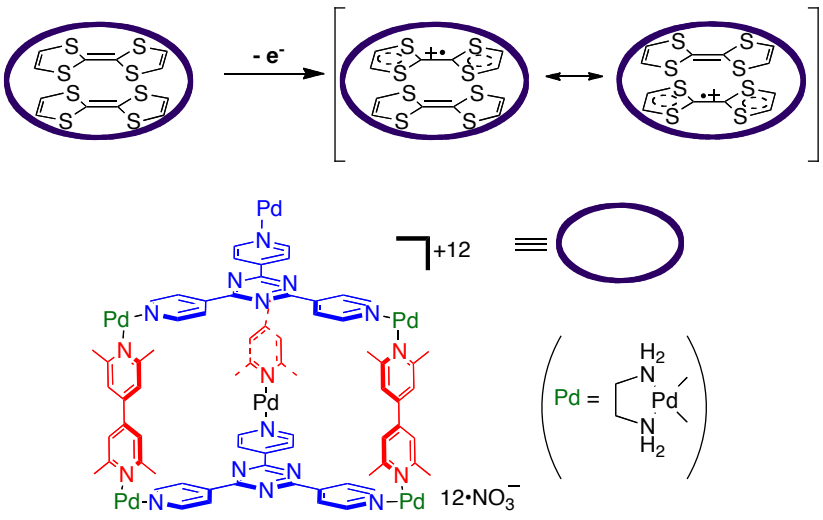

2.4

Scheme 2.2 Self-assembled tris(4-pyridyl)triazine based ligand **2.4** used to stabilize mixed-valence TTF dimers.

2.2.2 Covalent Attachment

The second major strategy employed in the stabilization of face-to-face interactions between TTFs is covalent linkage of two or more TTF units in close proximity to one another, thus avoiding the need for a host molecule or network to stabilize the resulting dimeric species. Many frameworks have been used to insure a through-space interaction between the neighboring TTFs. Some of the first attempts at implementing this covalent linkage strategy involved the use of the cyclophane type compound **2.5**.[8] More recent examples include a modified calixarene **2.6**,[9] the difunctionalized naphthalene derivative **2.7**,[10] and a trimeric-TTF complex **2.8**[11] with methylenedithio spacing units (Figure 2.5).

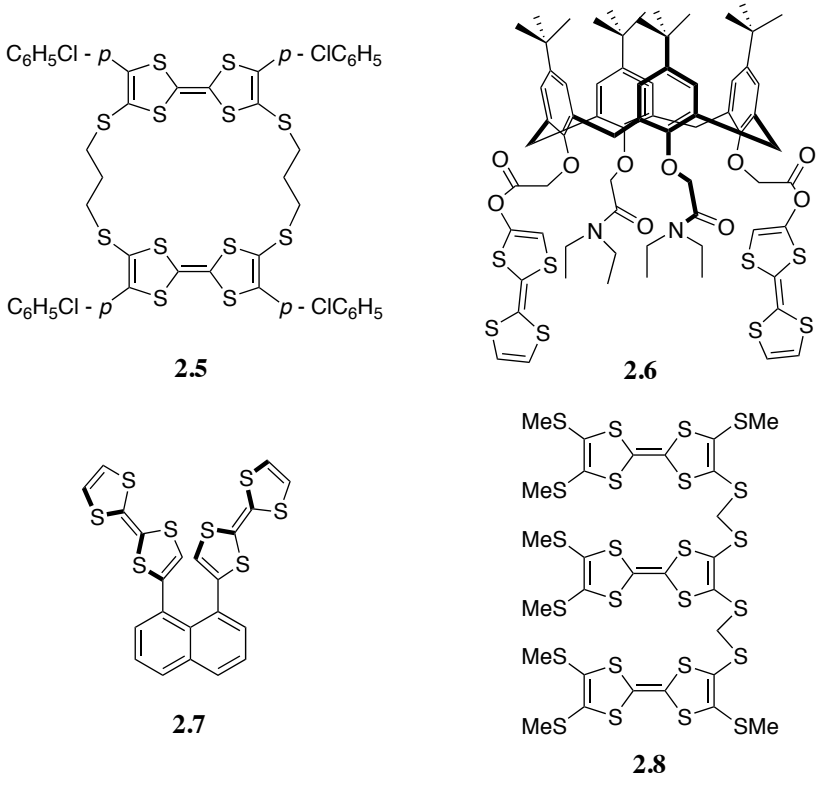

Figure 2.3 Examples of covalently linked TTF compounds: TTF-cyclophane **2.5**, TTF-calixarene **2.6**, bis-TTF-napthalene **2.7**, and trimeric-TTF **2.8** with methylenedithio spacers.

Another related mode of covalent linkage reported in the literature uses an external stimulus to induce a conformational change, which in turn preorganizes two TTF subunits for interaction upon oxidation. Sessler *et al*. have shown that by using the fluxional TTF-calix-[4]pyrrole **2.9**, an appropriate electron acceptor, and simple tetrabutylammonium anions, stabilization of a mixed-valence state is favored (Scheme 2.3).[12] This ion-mediated assembly provides the first example of a mixed-valence TTF dimer species characterized in the solid-state that was based on the use of a covalently linked system.

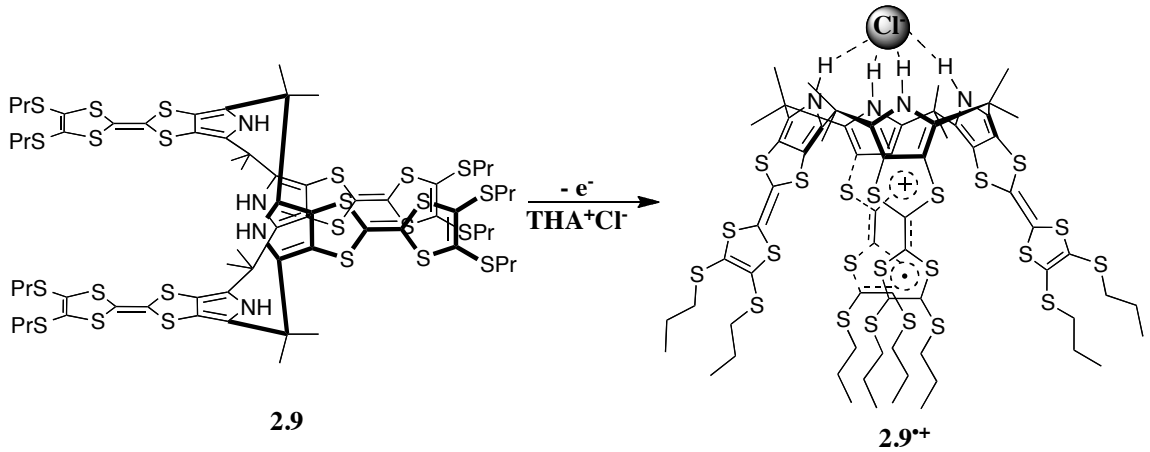

Scheme 2.3 Anion induced mixed-valence stabilization within the TTF-calix-[4]pyrrole **2.9**.

2.2.3 Mechanical-Stabilization

The most recent addition to the field of stabilizing TTF dimeric species consists of a hybrid between previously discussed host stabilization and covalent linkage techniques, and is often referred to as "mechanical stabilization". This strategy, pioneered

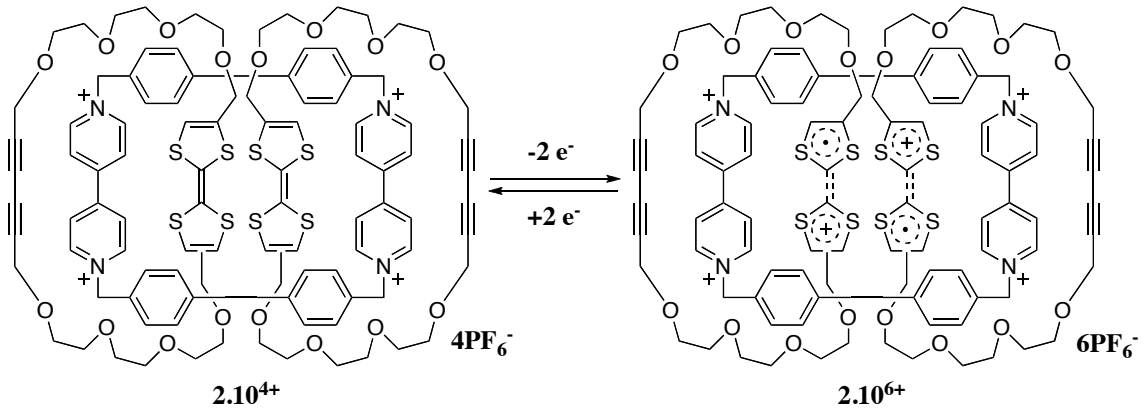

Scheme 2.4 Use of a "molecular-flask" [3]catenane **2.10** to stabilize TTF π-dimer upon oxidation.

by Stoddart and co-workers, utilizes complex interlocked molecules, such as catenane **2.10**, that contains TTF moieties covalently strung through electron deficient cavities.[13] In these so-called "molecular-flasks" the oxidation state of the TTFs dictate whether the TTF moieties are inside our outside of the cavity: TTF_2, $[TTF_2]^{\bullet+}$, and $[TTF]_2^{\bullet+}$ localize inside the host whereas the columbic repulsion is far too large in the case of $[TTF]_2^{2+}$ causing expulsion from the cavity. This fusion of covalent linkage and host accommodation can stabilize persistent dimeric states due both to the proximity of the neighboring TTF moiety and the stabilizing CT interaction between the electron deficient core and the electron rich TTF units (Scheme 2.4).

2.2.4 Intermolecular Dimerization and Aggregation

In contrast to neutral TTFs that easily dissociate in solution, π-extended TTF derivatives and TTFs having amphiphillic properties often self-associate, even in solution at appropriate concentrations. This results in the formation of dimeric species or gel-like extended nanostructures. Designing TTF molecules with extended π-faces results in

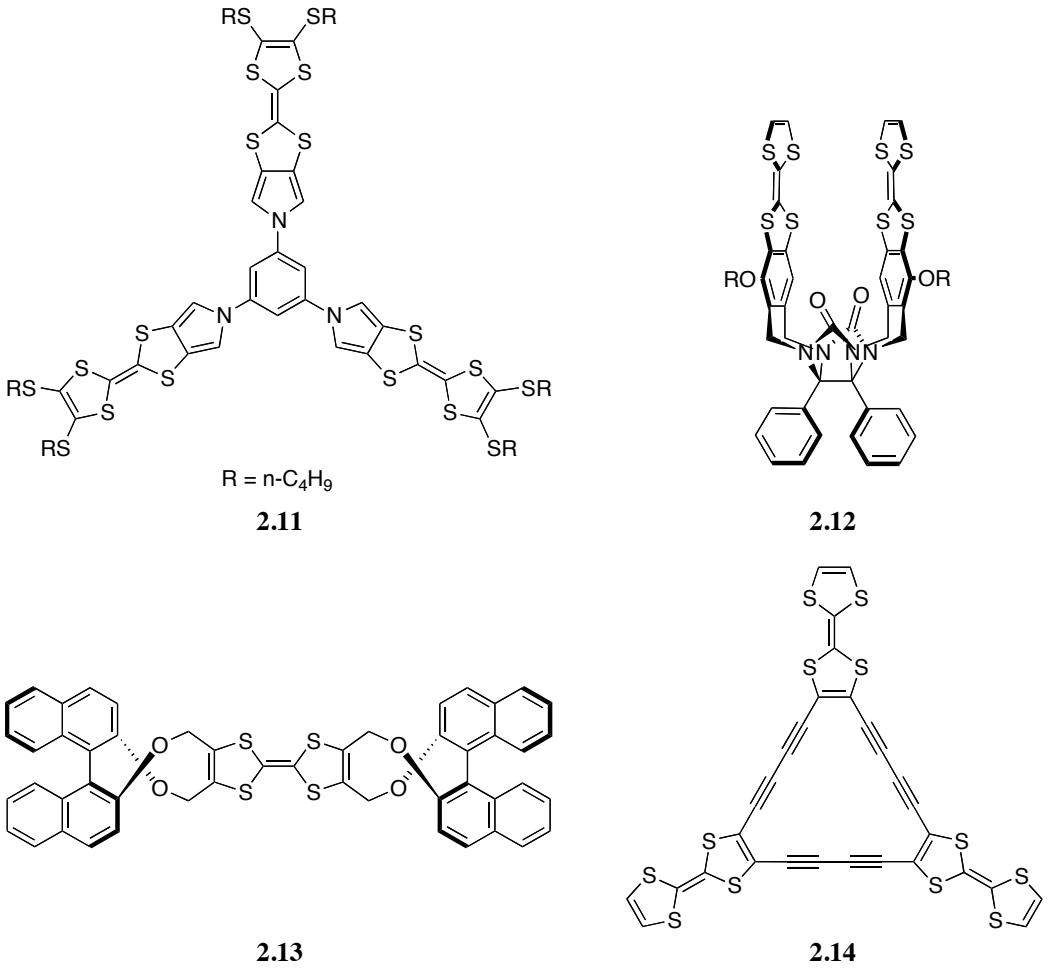

Figure 2.4 Examples of π-extended TTF compounds that demonstrate self association: TTF-star oligimer **2.11**, glyco-uril based TTF molecular-clip **2.12**, chiral *bis*-naphtho)-TTF **2.13**, and *tris*(TTF)dodecadehydro[18]annulene **2.14**.[14-17]

stronger intermolecular donor-acceptor interactions in solution, driving dimerization upon oxidation to the radical cation. Numerous such systems are known and several noteworthy examples are shown in Figure 2.4.[14-17] TTF derivatives **2.11**-**2.14** each demonstrate electrochemical evidence of intermolecular interaction upon oxidation and **2.11-2.13** also exhibit a strong absorbance in the NIR region upon oxidation due to formation of a stable mixed-valence radical. While derivatives **2.12** and **2.13** were shown

to form dimeric species only,[15,16] TTF-star oligimer **2.11** and *tris*(TTF) dodecadehydro[18]annulene **2.14** were investigated as aggregation-driven molecular wires; both display fibrous structures typical of nanoaggregates when analyzed by SEM (scanning electron microscopy) and semiconductor behavior upon doping with iodine vapors.[14,17]

Another approach towards achieving preorganized stacks of TTF moieties involves the formation of organogels.[18] The gel states allows for the construction of fibers in a homogenous medium (solvent), which can then be deposited on any surface. Organogels containing TTF units arrange through an assortment of noncovalent interactions including hydrogen bonds, amphiphilic beahvior, or through self-assembly between attached units. Figure 2.5 illustrates several TTF molecules capable of forming organogels.[19-22] The amphiphilic *bis*-TTF annulated macrocycle **2.15** can form a redox-active nanogel as well as electrically active nanowires and size controllable nanodots.[19] Hydrogen bonding amido groups in **2.16** provide an excellent scaffold, which leads to the formation of an organogel.[20] Further doping and annealing of the hydrogen bonded supramolecular structure leads to a bulk material that shows metal-like conductivity. Other systems with similar properties include the *bis*-arborol-TTF gel formed from **2.17** and the 1,3,5-trialkoxybenzoic acid-TTF derivative **2.18**, which after gellation and subsequent stacking, exhibits mixed-valence absorptions in the NIR spectral region upon doping.[21,22]

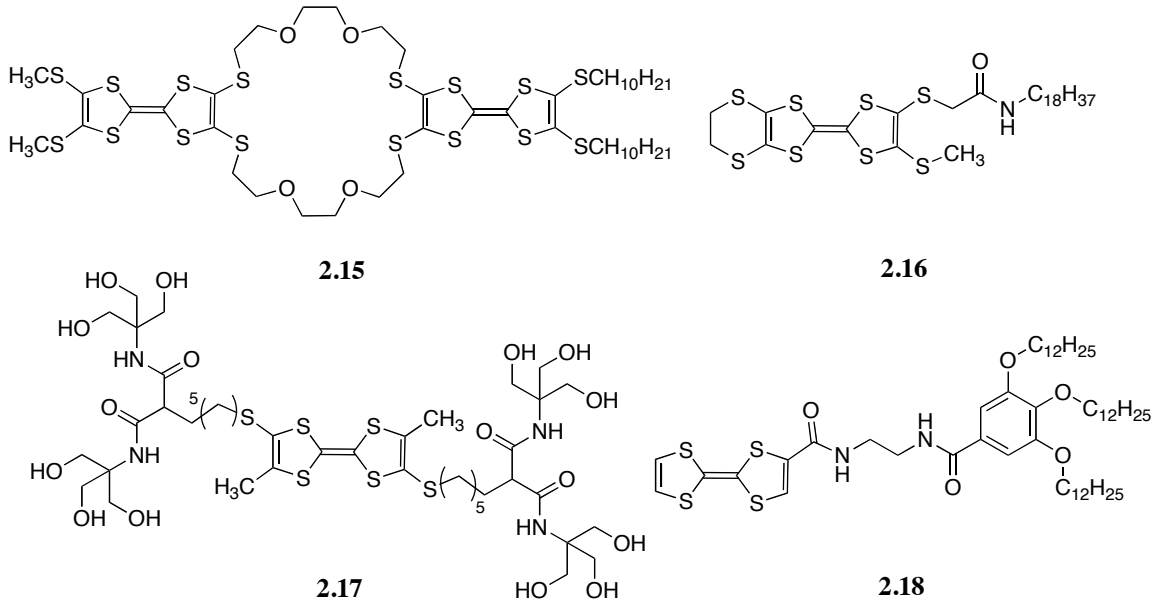

Figure 2.5 TTF functionalized redox-active organogelators **2.15**-**2.18**.

2.3 SCHIFF-BASE CALIXPYRROLE

2.3.1 History

In 1996 Sessler and coworkers first reported the use of tetrametric porphyrinogen **2.19** as an anion binding agent in organic solutions.[23] This macrocycle, originally reported by Baeyer[24] in 1886 and later studied for metal coordination[25] in the 1990s, was found to undergo conformational behavior similar to that of calix[4]arenes and thus the name calix[4]pyrrole was introduced. Since the initial report detailing the anion binding ability of **2.19**, many new calix[4]pyrrole-based anion receptors have been synthesized, ushering in a new branch of anion coordination chemistry.[26]

Although calix[4]pyrrole binds the fluoride anion strongly through four pyrrolic N-H hydrogen bonds, its cavity is too small to bind large anions well. In an effort to increase binding for larger anions, several expanded macrocycles incorporating the dipyrromethane unit, have been synthesized. One such system, also reported by Sessler and workers is macrocycle **2.20**. It contains both the flexible dipyrromethane component, that is present in calixpyrrole, as well as a Schiff-base linkage.[27] While **2.20** showed moderate binding affinity for larger anions, such as chloride, it was found to act as a better ligand for metal complexation, an area of research pioneered independently by the Sessler and Love research groups, and substantially developed by this latter group.[28]

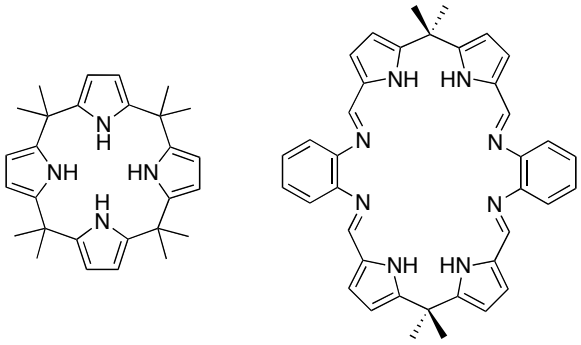

2.19 **2.20**

Figure 2.6 Polypyrrolic macrocyclic systems: calix[4]pyrrole **2.19** and Schiff-base calixpyrrole **2.20**.

Whereas the calix[4]pyrrole displays fluxional conformational behavior in the presence of anions, the Schiff-base calixpyrrole **2.20** undergoes a dramatic changes in geometry when coordinated to select transition metals (Scheme 2.5). For example, reacting **2.20** with 2 equivalents of Pd^{II}, Cu^{II}, or Co^{II} provides a binuclear complex that adopts a molecular cleft structure in the solid state similar to that of cofacial or Pacman

porphyrins (Figure 2.7).[29] X-ray crystallography revealed that without metals binding to **2.20**, the free ligand adopts a nonplanar bowl-like conformation.[28]

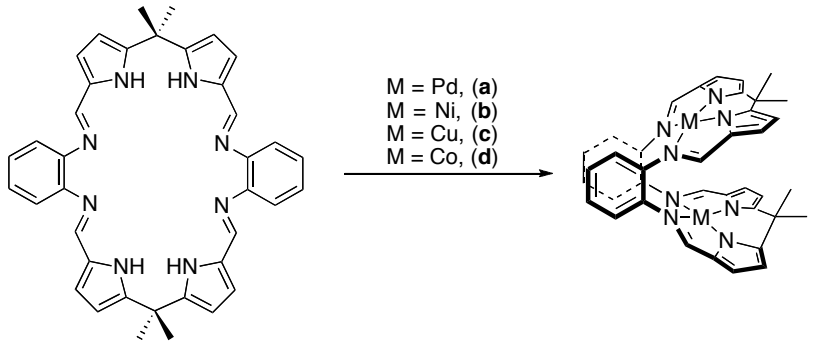

2.20 **2.21a-2.21d**

Scheme 2.5 Synthesis of binuclear transition metal complexes of **2.20**. Conditions: (**a**) $Pd(OAc)_2$, NEt_3, CH_2Cl_2; (**b**) KH, $NiCl_2(dme)$, THF,Δ ; (**c**) $Cu(BF_4)_2 \bullet xH_2O$. NEt_3, CH_2Cl_2; (**d**) $[Co(THF)\{N(SiMe_3)_2\}_2]$, THF.

Due to its similarity in shape and binuclear metallic coordination ability, Schiff-base calixpyrrole **2.20** can be seen as a structural analog to cofacial or Pacman porphyrin **2.22**. Noteworthy in this comparison is that the Schiff-base calixpyrrole offers a distinct advantage in synthetic ease compared to arduous multistep preparations of the latter porphyrin systems. In fact, Love and coworkers have studied the dibcobalt complex **2.21d** as a potential oxygen reduction catalyst, a major area of research dominated by the use of cofacial porphyrins.[29]

Due to the large size of the cavity and structural flexibility imparted by the sp^3 hybridized dipyrromethane units the Schiff-base calixpyrrole **2.20** is also emerging as a noteworthy dynanmic macrocycle that to date has proved capable of stabilizing not only binuclear transition metal complexes but also, those of *f*-elements.[30] as well as a magnesium hydroxide cubane.[31]

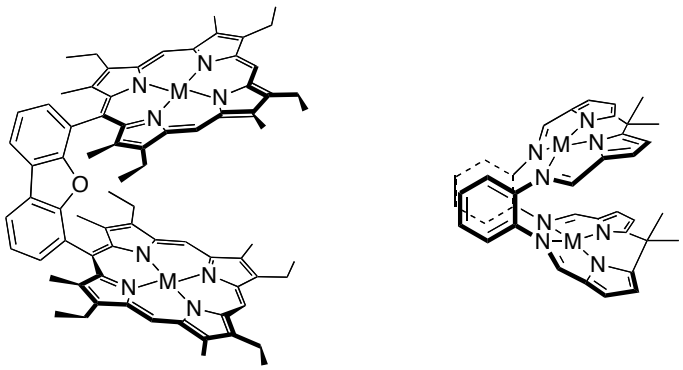

2.22 **2.21a-2.21d**

Figure 2.7 Structural similarities between two rigid binuclear metallic clefts; pacman diporphyrin **2.22** and Schiff-base calixpyrrole **2.21**.

2.4 DESIGN AND SYNTHETIC STRATEGY

In the following section, the preparation of a neutral pyrrolic macrocyclic ligand, *bis*TTF-Schiff-base calixpyrrole **2.1**, and homobinuclear palladium complex **2.2** will be described. The ability to stabilize and reversibly access mixed-valence and π-dimer states of TTF in the ensuing complex highlights the importance of preorganization in obtaining stable TTF dimeric states. Prior to this work, the parent Schiff-base calixpyrrole ligand **2.20** had been used to stabilize only metallic complexes. Thus, this study represents the first instance in which the ligand framework has been used to stabilize an "organic-metal".

Compound **2.1** was designed to take advantage of conformational changes in the ligand framework upon palladium complexation. The Schiff-base calixpyrrole **2.20** generally exists in a flexible bowl-like conformation due to the sp^3 hybridized *meso*-carbons in the dipyrromethane unit, wherein the aryl hinges are oriented on opposite sides of the macrocycle with no association between the π-faces (Scheme 2.5). Therefore

reaction with two equivalents of an appropriate transition metal can be expected to stabilize a folded form with a rigid clip-like geometry. In this form, the two electron rich π-faces of the TTF are lined up in an eclipsed fashion with a close π-π overlap between the two subunits. To the extent that these assumptions are true, the result would be an intramolecular TTF dimer that is "locked" into a conformation where the two TTF units are forced to interact.

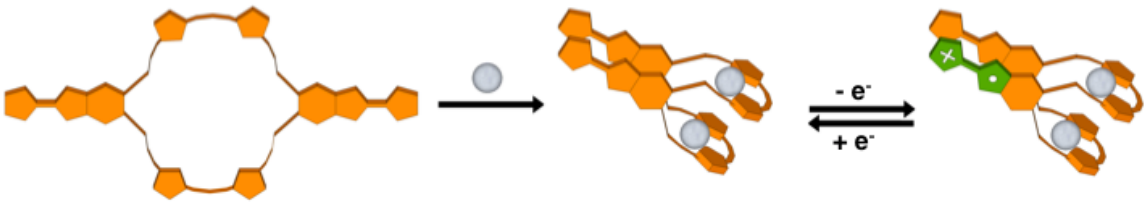

Scheme 2.6 A cartoon representation illustrating the expected ditopic metal complexation of TTF-Schiff-base calixpyrrole and resulting stabilization of a mixed-valence dimeric state.

2.5 SYNTHESIS AND CHARACTERIZATION

The synthesis of the TTF-Schiff-base calixpyrrole **2.1** is outlined in Scheme 2.7. The metal-free form of the TTF-Schiff-base calixpyrrole **2.1** was synthesized by condensing the known TTF-phenylenediamine **2.23**[32] with diformyldipyrromethane **2.24** in the presence of *para*-toluenesulfonic acid. These conditions are identical to those in the synthesis of **2.20**, substituting TTF-phenylenediamine for the simple *o*-phenylenediamine. No reaction takes place without an acid template, and as described by Sessler and coworkers, a variety of acids can mediate this [2+2] cyclization reaction. Love *et al*. have found that using *para*-toluenesulfonic acid generates clean and

crystalline products in the highest reproducible yields.[28g] Treatment of the suspended macrocyclic salt with triethylamine gave the free Schiff-base macrocycle **2.1** as an orange precipitate that could be isolated by filtration in 90% yield. A high-resolution ESI mass spectrum revealed an exact mass m/z 1253.16622 corresponding to the expected M^+ ion (calcd mass ($C_{58}H_{61}N_8S_{12}$) M^+1253.16661). The ^{1}H NMR spectrum (400 MHz) of **2.1** recorded in $CDCl_3$ at 298 K, showed a sharp singlet at δ = 8.00 ppm. This feature integrates to 4 H and can be assigned to the iminic NH protons. The signal arising from the methyl groups attached to the *meso*-position of the dipyromethane system in **2.1** appears at δ = 1.78 ppm in the form of a singlet integrating to 12 H.

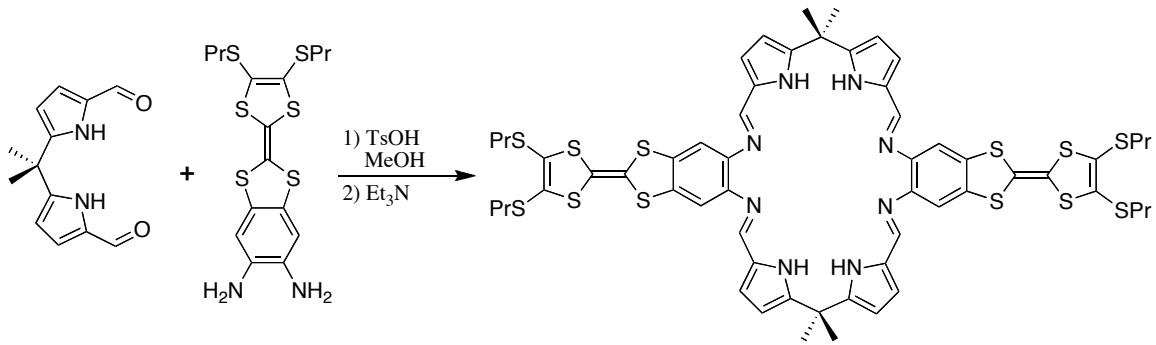

Scheme 2.7 Synthesis of TTF-Schiff-base calixpyrrole **2.1**.

Schiff-base calixpyrrole compounds are notoriously difficult to crystallize in their free base forms. For instance, solid state structural information is still not available for the parent free ligand **2.20**. Countless efforts using various conditions were made to obtain single-crystals of **2.1** suitable for X-ray diffraction. Unfortunately, under all attempted crystallization conditions, only amorphous solids were obtained.

The synthesis of the binuclear palladium complex **2.2** is summarized in Scheme 2.8. The homobinuclear metallation of **2.1** occurs under conditions similar to those used to metallate the parent Schiff-base calixpyrrole **2.20**.[28e] Briefly, **2.1** and two equivalents of palladium acetate were stirred in dichloromethane at room temperature in the presence of triethylamine (added to neutralize the acetic acid formed during the complexation reaction). After stirring overnight, pentane is added to the reaction. This gives rise to a precipitate that was then subject to column chromatography over silica gel. This provided **2.1** in 20% yield. A high-resolution matrix-assisted laser desorption/ionization mass spectrum showed an exact mass, m/z, at 1463.92879 amu.

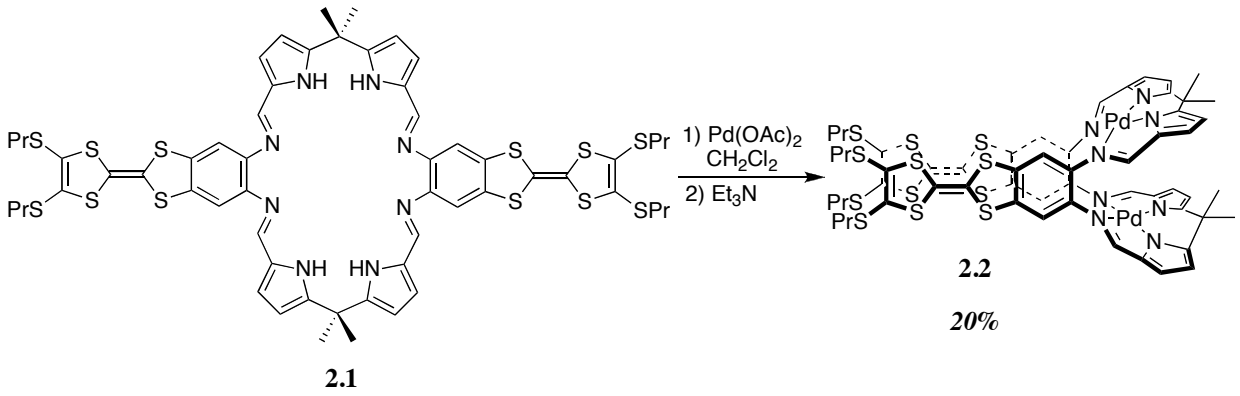

2.1 **2.2** ***20%***

Scheme 2.8 Synthesis of the *bis*-Pd(II) complex **2.2**.

2.5.1 ^{1}H NMR Spectroscopic Studies

Initial evidence for the conversion of **2.1** to **2.2** and the "Pacman"-like conformation of the latter species came from ^{1}H NMR spectroscopic measurements (Figure 2.8). Comparing the spectra of the metal-free ligand **2.1**, and the *bis*-Pd(II) complex **2.2**, recorded in $CDCl_3$ at room temperature, revealed the expected changes in the aromatic region. Also, splitting of the signal ascribed to the protons of the methyl

groups attached to *meso*-carbon was observed. This splitting is considered reflective of a loss in symmetry and can be rationalized by the resulting Pacman conformation in which two methyl groups points inside the cavity while two methyls are positioned outside. In the spectra of **2.1** only one set of signals is visible for the propyl group hydrogen atoms, as would be expected for a species of high inherent symmetry. In contrast, the spectrum of **2.2** recorded under analogous conditions revealed the presence of a set of nonequivalent signals at 2.86 and 2.75 ppm corresponding to the thiopropyl hydrogens. This latter nonequivalence is consistent with the presence of TTF subunits whose π-faces are proximate. To the extent in which this assignment is correct, this complex represents the first example of a Schiff-base calixpyrrole that loses symmetry along the aryl hinges as a result of homobinuclear metal complexation.

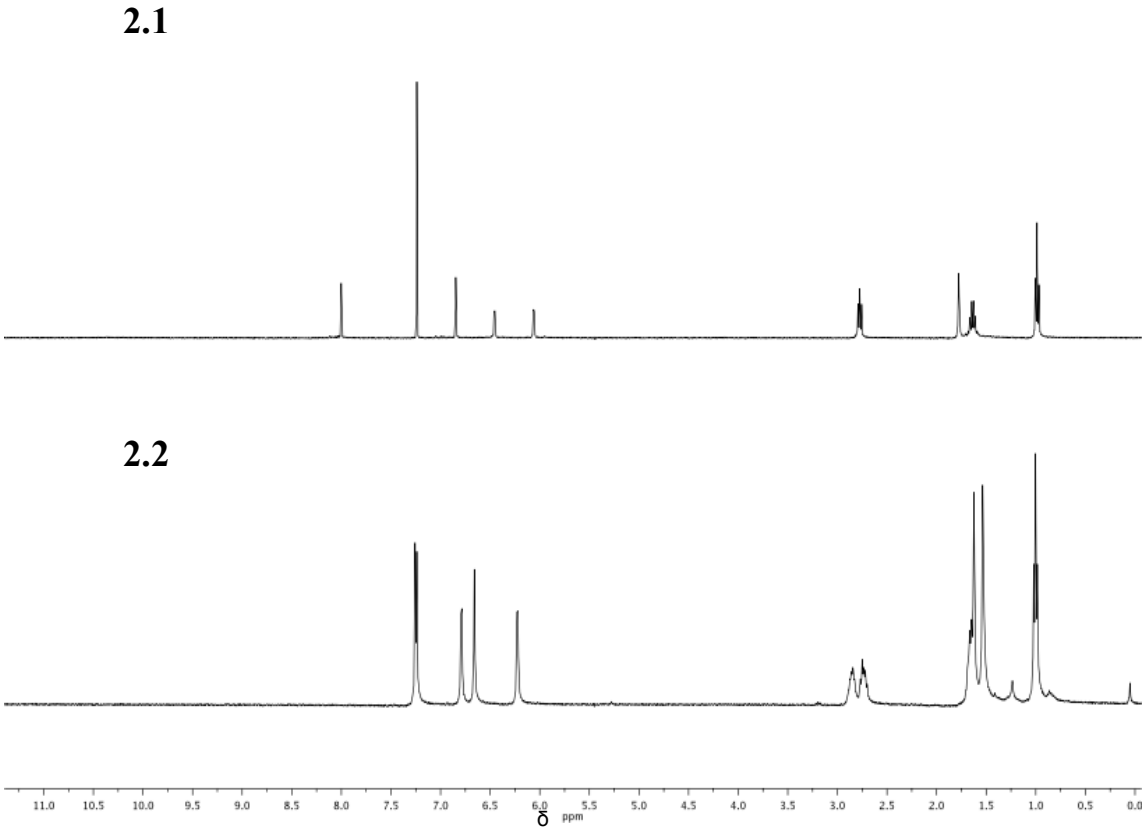

Figure 2.8 ^{1}H NMR spectra of **2.1** and **2.2** (400 MHz) recorded in $CDCl_3$ at 298 K.

2.5.2 X-ray Crystal Structure

Support for the Pacman structural assignment came from a single crystal X-ray structure determination of **2.2**. The resulting structure (Figure 2.9) confirms that **2.2** does indeed adopt the expected Pacman-like cleft structure, at least in the solid state. In **2.2**, each Pd(II) cation is bound to two deprotonated pyrrole nitrogen atoms of one dipyrromethane unit and to the two adjoining imine nitrogen donor atoms in an N4 co-ordination sphere. The Pd•••Pd distance is 3.40 Å. In comparison to the parent compound **2.21a**, the TTF-modified complex is characterized by a high level of coplanarity for the

aryl planes and a small offset angle of 2.9° between the two aryl hinges. The intraplanar distance between the two TTF mean planes is a relatively short 3.65 Å, leading to the inference that the two TTF π-faces are close enough to interact upon oxidation in a through space manner. This increased coplanarity and decreased intra-aryl separation presumably reflects several factors. Specifically, the extended π-faces of the tetrathiafulvalene moiety and stabilizing S•••S contacts lead to an increased intramolecular stacking via weak associative forces.

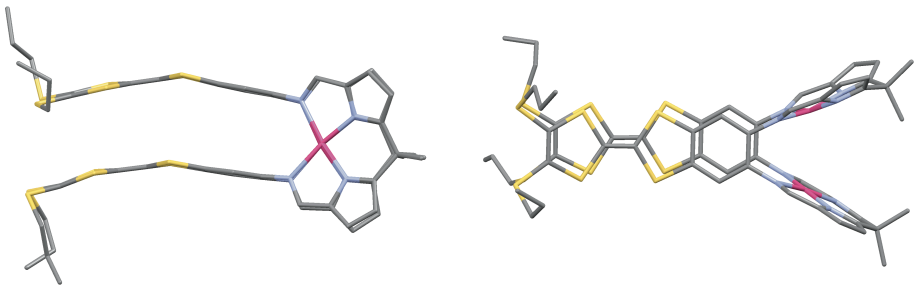

Figure 2.9 Top and side views of the X-ray crystal structure of *bis*-Pd(II) complex **2.2**.

Examining the expanded packing structure of **2.2** reveals the presence of an intermolecular dimer that exists between two molecules of **2.2** (Figure 2.10). This intermolecular dimer does not exhibit eclipsing of the TTF π-faces but rather exists in a slipped-stack orientation with a short 3.63 Å distance between the two aryl planes. The dimer unit repeats throughout the expanded structure with columns of non interacting dimers adjacent to stacks of orthogonal non-interacting dimers (Figure 2.11). However, each dimer is isolated and electronic communication does not flow through the stacks; *i.e*. there is no evidence of a long range interaction that might lead to conductivity. Nevertheless, the observed stacking behavior of the neutral compound gives insight into

how these systems might behavior once oxidized to the presumably conductive mixed-valence state. In fact, it is proposed that oxidation of the TTF units and subsequent planarization of the extended π-face could enhance the strength of these intromolecular dimers and potentially lead to highly conductive charge transfer salts.

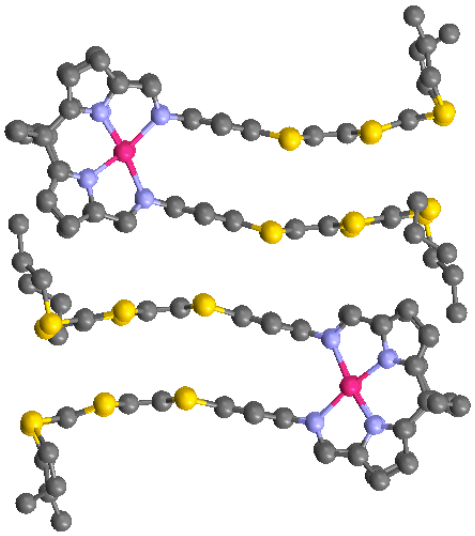

Figure 2.10 Intermolecular dimer involving two molecules of **2.2** as seen in the solid state.

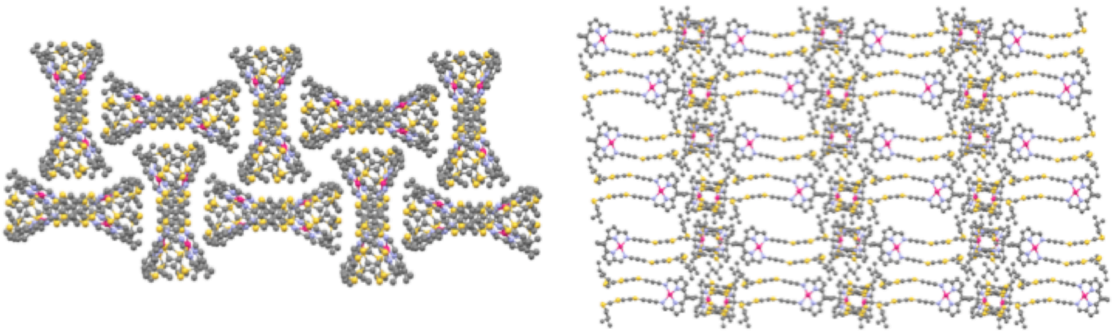

Figure 2.11 Packing structure of **2.2** highlighting the repeating orthoganol intermolecular dimers (top and side views). Hydrogens and solvent molecules (CH_2Cl_2) have been omitted for clarity.

2.5.3 Electrochemical Studies

To determine if palladium coordination and the attendant TTF preorganization would enhance the stabilization of a putative mixed-valence state, the electrochemical behavior of **2.1** and **2.2** were compared in dichloromethane (0.25 mM) using cyclic voltammetry (CV). As can be seen from an inspection of Figure 2.12, the CV of the free-ligand **2.1** shows two double-electron reversible redox waves at 590 and 990 mV, respectively. On this basis, we infer that there is little, if any, interaction between the two donor TTF moieties. In fact, the CV of **2.1** closely resembles that of the parent TTF **1**, further attesting to the lack of intramolecular interaction. In contrast, the CV of **2.2**, also shown in Figure 2.12, reveals three reversible redox waves at 490, 600, and 1130 mV, respectively. Analysis of the peak heights leads us to infer that the first two-electron oxidation of **2.1** at 590 mV is split into two one-electron oxidations in **2.2**. To the extent that this assignment is correct, it is most easily rationalized in terms of a stabilizing interaction between the two TTF planes that is made possible by their proximity. This proximity is, in turn, enforced by the "Pacman"-like conformation of this particular

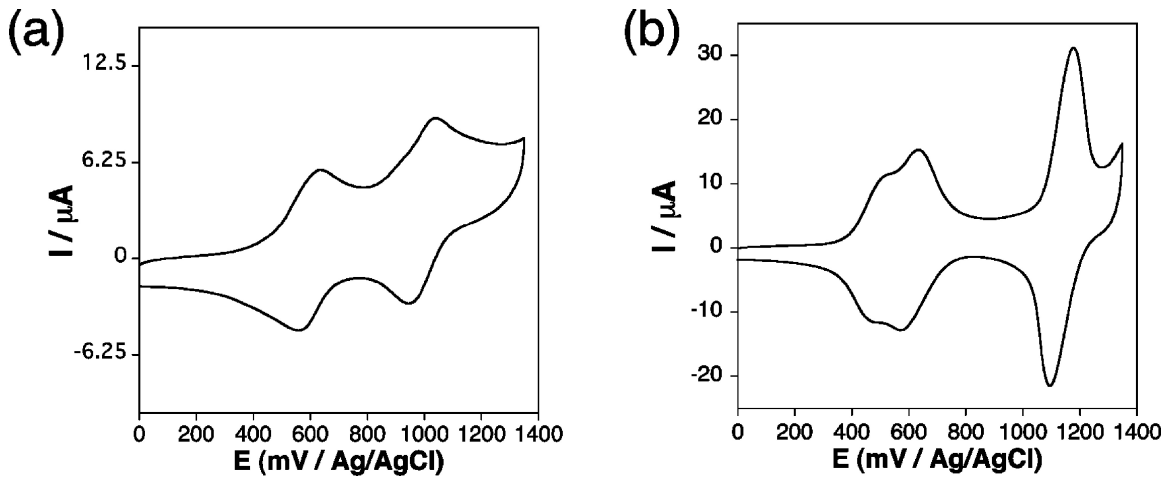

Figure 2.12 Cyclic voltammograms of (a) **2.1** and (b) **2.2** (0.25 mM) measured in CH_2Cl_2 using $TBA{\cdot}PF_6$ (0.2 M) as the supporting electrolyte, glassy carbon and Pt as the working and counter electrodes, respectively. Potentials were measured against a Ag/AgCl reference electrode at 100 mV/s.

binuclear Pd(II) complex. More specifically, we propose that electronic communication between the two TTF moieties allows for stabilization of the radical that is formed initially and which forms a weakly associated mixed-valence dimer. This association reduces the potential of the first oxidation step. Owing again to this imposed interaction between TTF units, the second one-electron oxidation in **2.2** at 600 mV ostensibly leads to a stabilized π-dimer. The stability of this dimeric species contributes to a significantly higher oxidation potential of the next and final redox process. This latter process corresponds to the third sharp oxidation seen in the CV of **2.2** at 1130 mV and is thought to involve a two-electron process that yields two dicationic TTF units. This oxidation process induces a destabilizing Coloumbic repulsion between the two doubly charged π-faces. Such a repulsion is enhanced due to the rigidly enforced proximity of the oxidized TTF moieties in **2.2** and accounts for the fact that the potential for this two electron

oxidation process is higher in the binuclear Pd(II) complex **2.2** than it is in the free ligand **2.1**. Considered in concert, the remarkable differences between the electrochemical signatures of **2.1** and **2.2** provide support for the proposed stabilization of the mixed-valence state. They also serve to underscore the benefit of preorganization in stabilizing intramolecular TTF interactions.

In an effort to further resolve the first two redox processes occurring in **2.2**, differential pulse voltammetry was performed in dichloromethane (0.5 mM) (Figure 2.13). From this study it is possible to see a three distinct oxidations occurring. This clear separation, specifically the clean splitting of the "first" oxidation is fully consistent with the formation of a mixed-valence state after oxidizing by one electron.

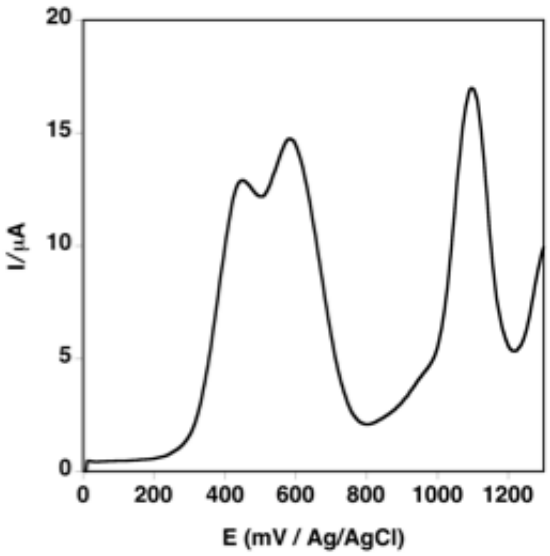

Figure 2.13 Voltammogram of **2.2** (0.5 mM / CH_2Cl_2) using TBA·PF_6 (0.1 M) as the supporting electrolyte, glassy carbon and Pt as the working and counter electrodes, respectively. The potential was measured against a Ag/AgCl reference electrode at 20 mV/s.

In the free ligand **2.1** there is no preference as to which TTF unit is oxidized first, since both TTFs are equivalent. However, upon metallation, the TTF moieties are no longer equivalent, due to the stabilizing through space interaction, and therefore one TTF can be oxidized preferentially.

2.5.4 UV-vis-NIR Absorption Studies

It is well known that the MV radical of TTF displays a characteristic absorbance centered between 1500 and 2500 nm.[33] Such an optical feature was thus expected when complex **2.2** was subject to oxidation but not when **2.1** was treated in the same way. The UV–vis–NIR spectra of both compounds were recorded upon titration with the chemical oxidant *tris*(4-bromophenyl)aminium hexachloroantimonate. The oxidant, known as "Magic Blue" was chosen in this case due to its known solubility in dichloromethane. Magic Blue exists as a stable radical species and becomes neutral upon reduction. (Figure 2.14). These chemical oxidation titrations were carried out at low concentration to avoid intermolecular dimerization or aggregation upon oxidation. As expected, when 0 to 1.0 equiv of this oxidant were added to a solution of **2.2**, strong absorption features were seen to emerge at 925 and 2000 nm, respectively (Figure 2.16). Further addition beyond 1.0

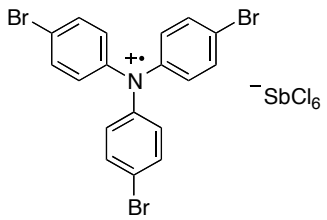

Figure 2.14 Structure of *tris*(4-bromophenyl)aminium hexachloroantimonate (Magic Blue).

equiv led to a systematic disappearance of the intervalence-charge transfer band at 2000 nm ascribed to the MV state but continued growth of the peak at 925 nm. The continued growth of this latter signal and literature precedent leads us to assign the peak at 925 nm to the simple $TTF^{\bullet+}$ cation radical, which is in equilibrium with the MV state. In accord with this latter assignment, the spectrum of the free ligand **2.1** recorded in the presence of increasing quantities of oxidant is also characterized by a continued growth in the feature centered at 927 nm. However, in the case of this metal-free species, no MV signal is observed in the near-IR region.

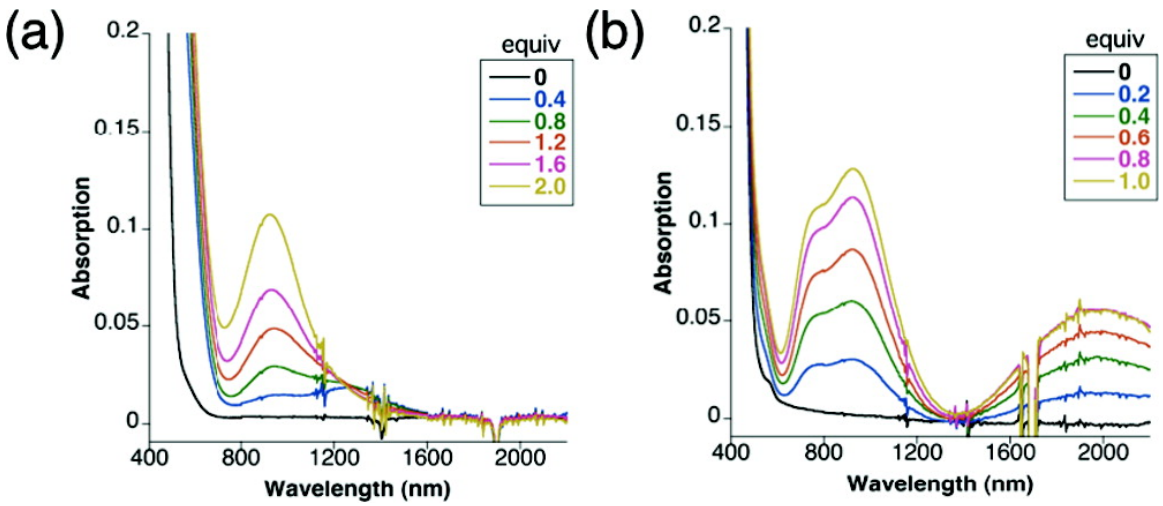

Figure 2.15 UV–vis–NIR absorption spectra of (a) **2** and (b) **3** (0.20 mM in CH_2Cl_2) recorded upon stepwise addition of Magic Blue.

More detailed examination of the electronic absorption spectra of **2.1** and **2.2** recorded in the presence of Magic Blue reveals slight differences in the 925 nm spectral regions for the two species. Specifically, a broadening and slight

splitting of this signal is seen in the case of palladium complex **2.2** but not for the free ligand **2.1**. Such a finding is in accord with the formation of a π –dimer, $(TTF^{\bullet+})_2$, in the case of **3**. This species, which has been shown to absorb between 740 and 1000 nm, presumably exists in equilibrium with the monomeric radical cation, $TTF^{\bullet+}$, at appropriate oxidant concentrations. In contrast, in the case of **2.1**, it is the monomeric radical cation, $TTF^{\bullet+}$, that is formed under all conditions.

The absorption analysis of **2.1** and **2.2** were also measured in situ using spectroelectrochemistry (Figure 2.16). The experimental set-up consisted of a quartz cuvette and a typical three-electrode set-up. However, in order to facilitate bulk electrolysis a fine-mesh platinum electrode is used as the working electrode. The free

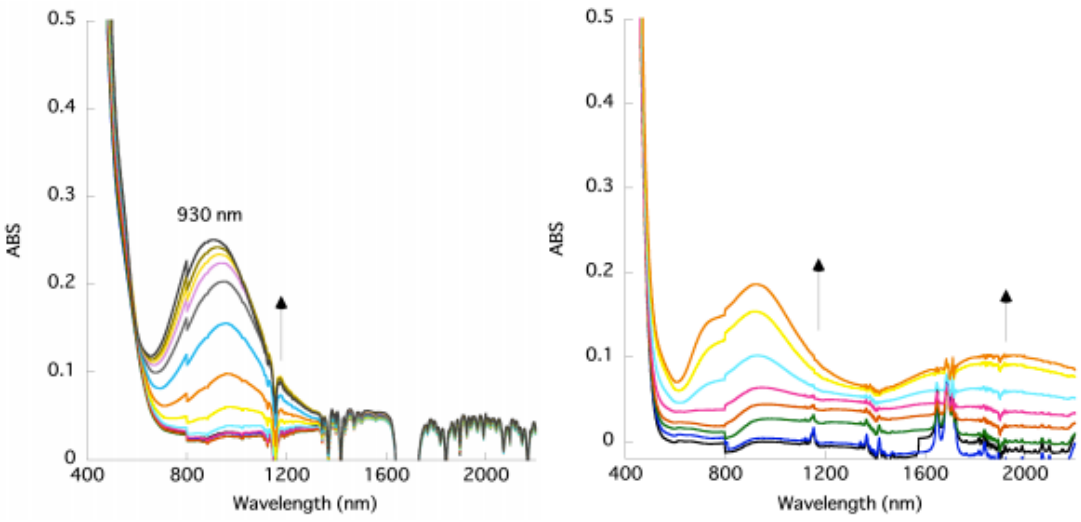

Figure 2.16 UV-vis-NIR absorption of **2.1** (left) and **2.2** (right) (0.25 mM / CH_2Cl_2) in a spectroelectrochemical quartz UV cell upon bulk electrolysis of the cell contents at various potentials using TBA•PF6 (0.2 M) as the supporting electrolyte, glassy carbon and Pt as the working and counter electrodes, respectively. Potentials were measured against a Ag/AgCl reference electrode at 100 mV/s.

ligand and metal complex were subjected to gradual electrochemical oxidation from 0 to 850 mV at room temperature in dichloromethane. In this way, it proved possible to observe directly the absorbance change that occurs as the neutral TTF species are oxidized to ones that have undergone a loss of 2.0 electrons. The resulting UV–vis–NIR absorption spectra show similar features as produced under the conditions of chemical oxidation as shown in Figure 2.15. Specifically, the oxidized form of **2.1** produced via chemical oxidation displays spectral features that are ascribable only to the production of a $TTF^{\bullet+}$ radical cation (absorbance centered around 925 nm). In contrast, electrochemical oxidation of **2.2** gives rise to a spectrum characterized by an intervalence charge-transfer band at 2000 nm, ascribable to the expected TTF-MV state, as well as absorbances at ca. 925 nm characteristic of the $TTF^{\bullet+}$ and $(TTF^{\bullet+})_2$ radicals.

2.5.5 EPR Studies

To provide further support for the proposal that the two TTF moieties interact in **2.1** but not in **2.2**, room-temperature EPR titrations were carried out using the chemical oxidant "Magic Blue". Upon titration with this oxidant, we observed marked differences between the two compounds. While the maximum EPR signal intensity is only seen after the free ligand **2.1** is treated with 2.0 equiv of oxidant (Figure 2.17), only 1.0 equiv of oxidant is required to reach this same maximum in the case of the Pd(II) complex **2.2** (Figure 2.18).

We rationalize the above differences between **2.1** and **2.2** in structural terms. In **2.1** the TTF units do not interact appreciably. Therefore, neither one is oxidized preferentially, and a full two equiv of oxidant are required to reach signal saturation. Addition of oxidant beyond 2.0 equiv leads to a reduction in the EPR signal intensity as

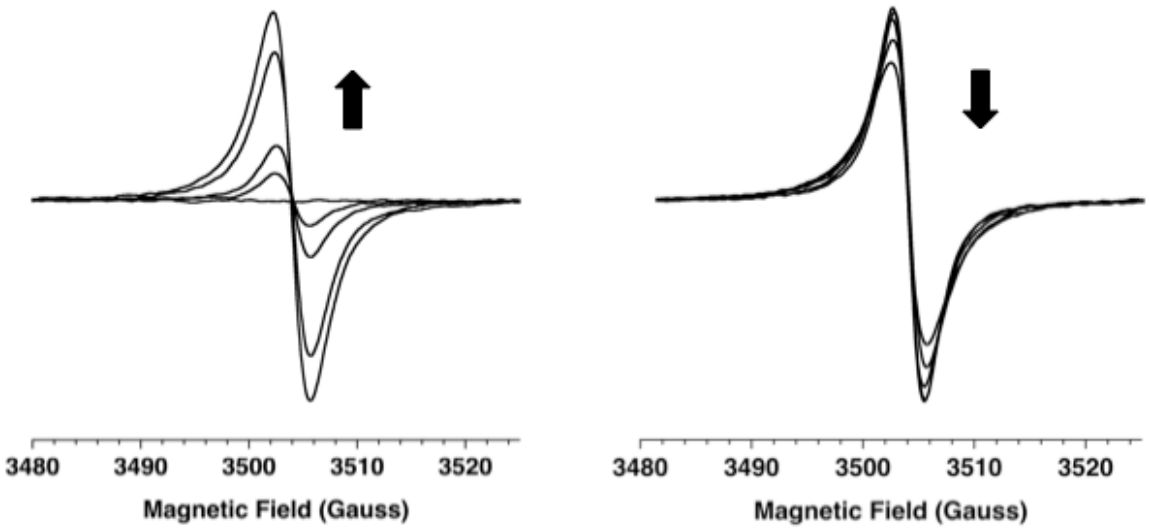

Figure 2.17 EPR spectra of **2.1** (0.2 mM / CH_2Cl_2, 295 K) recorded upon oxidation with (a) 0–2.0 equiv and (b) 2.0–4.0 equiv of "Magic Blue".

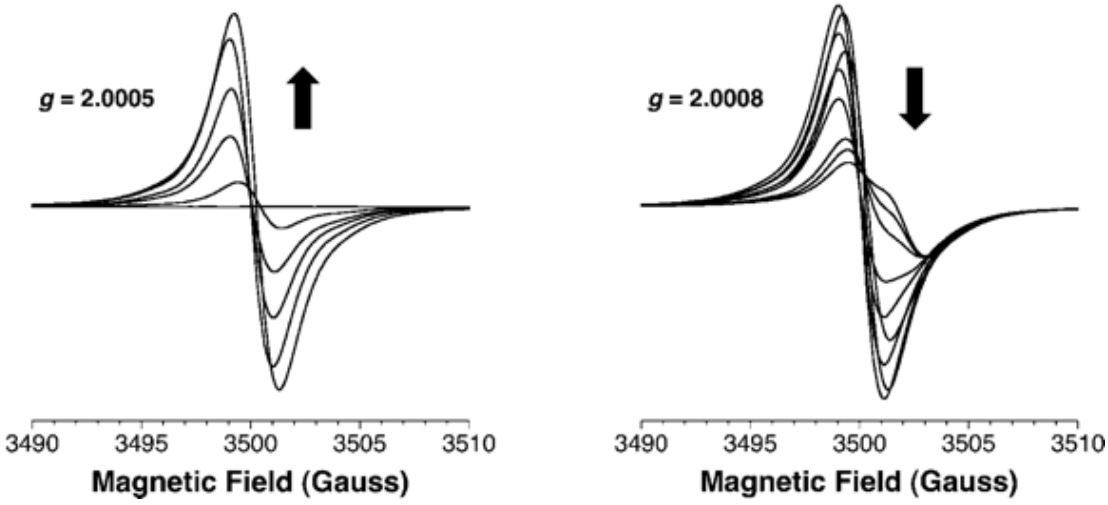

Figure 2.18 EPR spectra of **2.2** (0.2 mM / CH_2Cl_2, 295 K) recorded upon oxidation with (a) 0–1.0 equiv and (b) 1.0–4.0 equiv of "Magic Blue".

the two TTF units are increasingly converted to the corresponding dicationic species, which are EPR silent. However, due to the low solubility of the tetracationic species, precipitation occurred after approximately 2.6 equiv had been added. Nevertheless, the attenuation of the signal after 2.0 equiv is consistent with the creation of the EPR silent tetracationic species $(TTF)_2^{4+}$.

In contrast, the EPR signal of **2.2** saturates after the addition of only 1.0 equiv of the oxidant. We ascribe this result to the proximity between the TTF subunits, which allows for the preferential oxidation of only one TTF and the concomitant formation of a stabilized MV state. Addition of more oxidizing equivalents, from 1.0 to 2.0 equiv, leads to a decrease in the TTF-radical signal, as would befit formation of the corresponding EPR silent spin-paired π-dimer $(TTF^{\bullet+})_2$. Adding further oxidant, up to first 3.0 and then 4.0 equiv to **2.2** leads to further modifications in the EPR signal intensity as would be expected for the initial formation and then further oxidation of nonpaired radical species. However, as would be inferred from the CV analysis, which reveals a third redox process that is not split into two clear one-electron steps, the EPR changes induced by the addition of >2.0 equiv of oxidant are not "clean" and thus difficult to interpret via a simple first-order analysis. Nevertheless, the key point, namely that both MV radical $(TTF_2)^{\bullet+}$ state and a π-dimer $(TTF^{\bullet+})_2$ are accessible upon the addition of 1.0 or 2.0 equivs of oxidant, is fully supported by the EPR analyses of complex **2.2**.

2.5.6 Redox Mediated Molecular Motion

The synthesis of a new *bis*-Pd(II) Schiff-base calixpyrrole, **2.2**, offers the opportunity to compare structure function relationships across a series of known *bis*-Pd(II) Schiff-base calixpyrrole systems and further determine the structural effects

stemming from subtle changes in ligand framework. The structure of **2.2** can be compared to those of similar molecules by defining three variables: the metal–metal separation (M•••M), the "bite" angle, and the corresponding torsional twist angle between the two MN_4 compartments (Figure 2.19); these have been determined for all of the structurally characterized complexes in which the aryl hinge unit is varied and the dipyrromethane units remain constant (beta-unfunctionalized pyrroles and methyl groups attached to the *meso*-bridging carbons). For the previously reported systems it has been shown that the intermetallic separation in *bis*-Pd(II)Schiff-base calixpyrrole complexes appears to be intrinsically linked to both the bite angle and degree of torsional twisting, factors that are both dependent on ligand substitution patterns. Based on this prior work, a better offset, and improved face-to-face π-stacking overlap of the hinge aryl groups causes an increase twist angle and a decreased bite angle, which result in shorter Pd•••Pd distances.[28e]

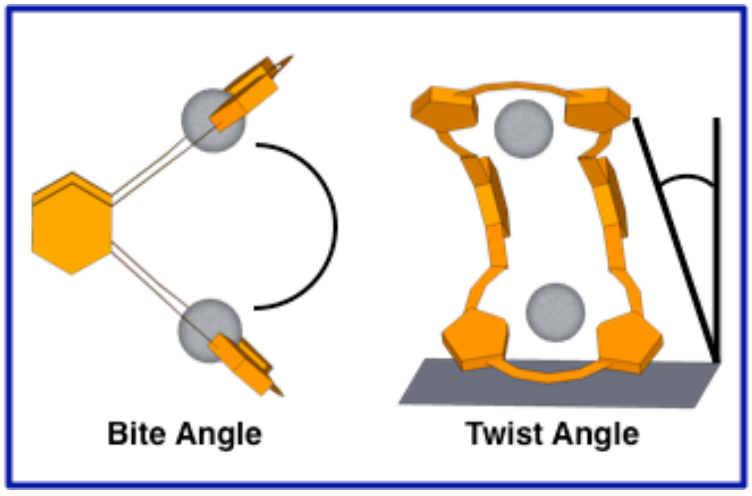

Figure 2.19 Schematic showing how the bite angle and torsional twist angle are defined.

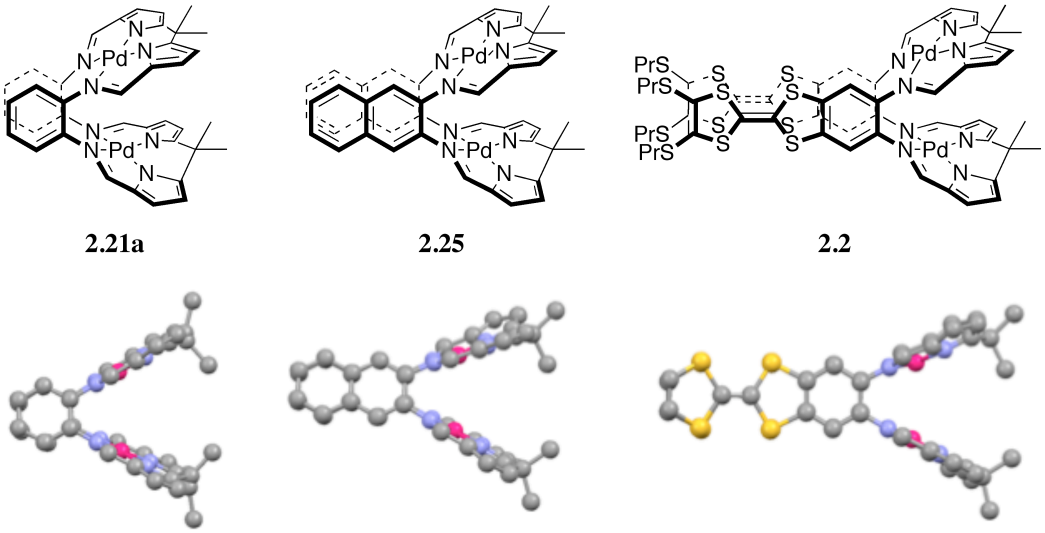

Figure 2.20 Structures of bis-Pd(II) Schiff-base calixpyrroles **2.21a**, **2.25**, and **2.2**. Hydrogen atoms and solvent molecules omitted for clarity. For sake of comparison, the thiopropyl groups of **2.2** have been omitted.

The addition of **2.2** to the lexicon of *bis*-Pd(II) Schiff-base calixpyrrole complexes, where *o*-phenylenediamine is the hinge aryl group, serves to reinforce further some aspects of the trend that expanded π-face units have on the resulting structural features of the complex. That is, better-offset π-π stacking in the hinge aryl groups leads to a shortened Pd•••Pd separation and a smaller bite angle for the Pacman mouth. Specifically, of the series of *bis*-Pd(II) Schiff-base calixpyrroles, **2.2** exhibits the largest delocalized π-faces throughout the TTF backbones. In turn, **2.2** also displays the shortest intermetallic palladium separation of these systems. This close Pd-Pd separation also coincides with the sharpest known bite angle of the Pacman mouth (Table 2.1).

The solid-state data of **2.2** reinforces the correlation between bite angle and π-π overlap in the hinge aryl groups of *bis*-Pd(II) complexes derived from Schiff-base calixpyrroles. Presumably, a fine level of synthetic control is available when creating

complexes in which tailored bite angles and intermetallic palladium separation values are desired. Furthermore, the ability to change these structural parameters *in situ* could be possible in systems where variation of the electronics and geometry of the π-aryl group can be made upon addition of an outside stimulus.

Aryl Hinge Group	Bite Angle [°]	M•••M [Å]
Benzene	56.5	3.762
Naphthalene	53	3.544
TTF-Benzene	44.2	3.397

Table 2.1 Comparison of aryl hinge group in bis-Pd(II) Schiff-base calixpyrroles showing bite angle and M•••M separation as a function of π-π stacking.

It is well known that TTF units undergo reversible structural changes, such as increased planarity, when the oxidation state is varied. The intramolecular distance between electronically coupled TTF-units is also understood to vary as different levels of oxidation take place. Therefore, complex **2.2** might be considered a dynamic *bis*-Pd(II) Pacman system. Complex **2.2** is unique in that the two redox-active TTF units are coupled in a through-space manner, leading to stable dimeric states. Because TTF dimers also have assorted electronic and structural states, differing from those of non-interacting TTF units, compound **2.2** offers the possibility to control the extent of π•••π stacking by toggling the oxidation state of the ligand. Increasing and decreasing the interactions and overlap of these aryl hinge groups could, in turn, increase or decrease the bite angle of the Pacman mouth.

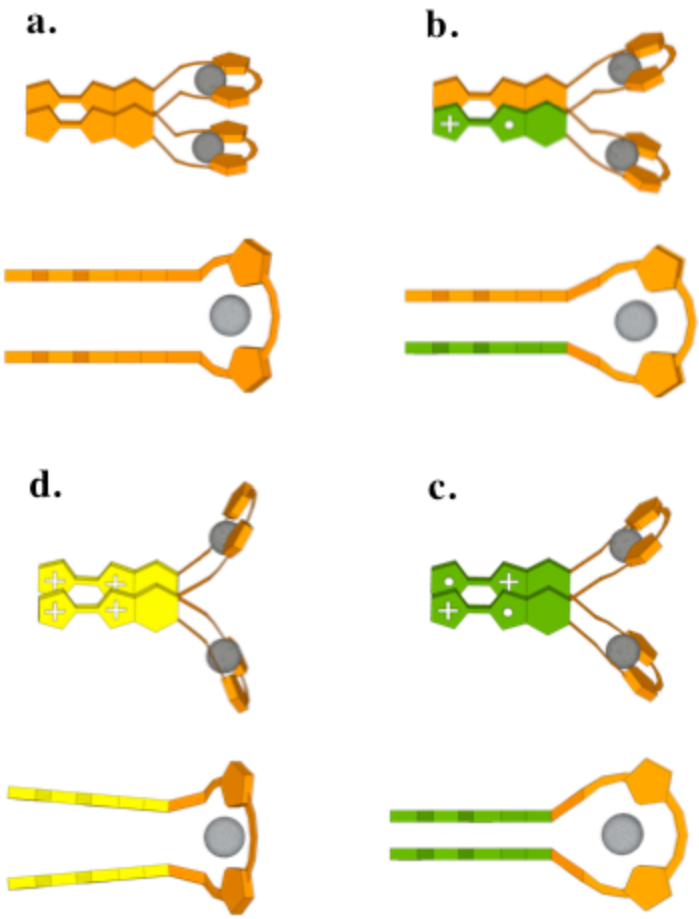

Figure 2.21 Graphical representation for the predicted conformational and oxidation states of **2.2** side and top views: **a.** neutral complex, **b.** mixed-valence dimer, **c.** π-dimer, **d.** tetracationic complex.

The impetus behind such a prediction is based the crystallographic evidence of related dimeric systems and CT conducting salts. TTF units that are coupled in a through-space manner are known to undergo a series of structural changes upon oxidation. Specifically, the distance between the two TTF units decreases as the system goes from neutral $(TTF)_2$ to mixed valence $(TTF_2)^{\bullet+}$, to π-dimer $(TTF^{\bullet+})_2$. The tetracationic species $(TTF_2)^{2+}$ is thought to have a highly destabilizing Columbic repulsion and thus greatest distance between the two TTF units. Apart from the change in distance between the TTF

π-faces upon oxidation, there is also marked change in the angle of offset between the TTF units as well as the vertical offset between the two, with decreasing offset values moving from neutral to π-dimer due to better overlap. This eclipsing has even led to predictions that in TTF π-dimers a partial covalent bond is forming between the central C atoms of the two TTF units as a result of radical overlap.[13b,34] This increased overlap along the backbone aryl hinge groups of the ligand may lead to changes in the MN_4 compartments, *i.e*. the so called "pacman mouth". For instance, variation of twist angle and therefore intermetallic Pd•••Pd separation might occur when the ligand is oxidized from neutral to mixed-valence to π-dimer. Presumably, the tetracationic state would give the largest bite angle and furthest Pd•••Pd separation (Figure 2.21).

In an effort to determine whether the change in oxidation state of the TTF backbone can stimulate a fluxional disposition in the Pacman mouth of these systems, attempts to grow single crystals of the mixed-valence form of **2.2** were undertaken. By titrating exactly one equivalent of $Fe(ClO_4)_3$, as a solution in acetonitrile, into a toluene solution of **2.2**, the mixed-valence state can be accessed. Subsequent vapor diffusion of hexanes into the complex solutions in toluene/acetonitrile yielded dark single crystals of **2.2**$^{\bullet+}$ suitable for X-ray analysis.

As expected, changes in the planarity of the TTF aryl hinge groups upon oxidation are evident from the structure of **2.2**$^{\bullet+}$. The top and side views of **2.2** and **2.2**$^{\bullet+}$ illustrate these differences clearly (Figure 2.22). Specifically, the structure of the neutral complex shows the two TTF units bent 24°with the respect to the diaminobenzene hinge groups whereas the mixed-valence species adopts a more uniform planarity throughout the extended π-face and a bend angle of 0°. This increase in planarity is also accompanied by a decrease in the TTF-TTF through-space distance. In the neutral complex the distance between the aryl planes is 3.79 Å. This distance is shortened to 3.43

Å in **2.2**$^{\bullet+}$. Presumably, the decrease in TTF-TTF separation is due to the weak association between the TTF subunits in the mixed-valence state. The degree of overlap between the two TTF-aryl groups, as evidenced in the side view of **2.2**, also undergoes a change when the TTF groups adopt a mixed-valence state. The TTF units in **2.2** display a near perfect overlap in which the sulfur atoms and central C=C bonds are close to fully eclipsed. However, the TTF subunits in **2.2**$^{\bullet+}$ are more offset (Figure 2.22b).

Stemming from this increased planarity and decreased overlap between the TTF subunits are changes to the "mouth" of the pacman ligand (Figure 2.22c). For instance, the palladium cations and dipyrromethane compartments in **2.2** are directly aligned, with an intermetallic separation of 3.40 Å between the two palladium cations. This alignment is related to the near perpendicular nature of the aryl hinge groups and subjects **2.2** to no twist angle as defined by Figure 2.19. Conversely, the TTF subunits in **2.2**$^{\bullet+}$, which display enhanced rigidity upon oxidation, lead to an increase in the twist angle of the complex. As a result of this twisting, the dipyrromethane top and bottom "mouth" compartments are no longer aligned and the Pd-Pd separation increases to 3.70 Å.

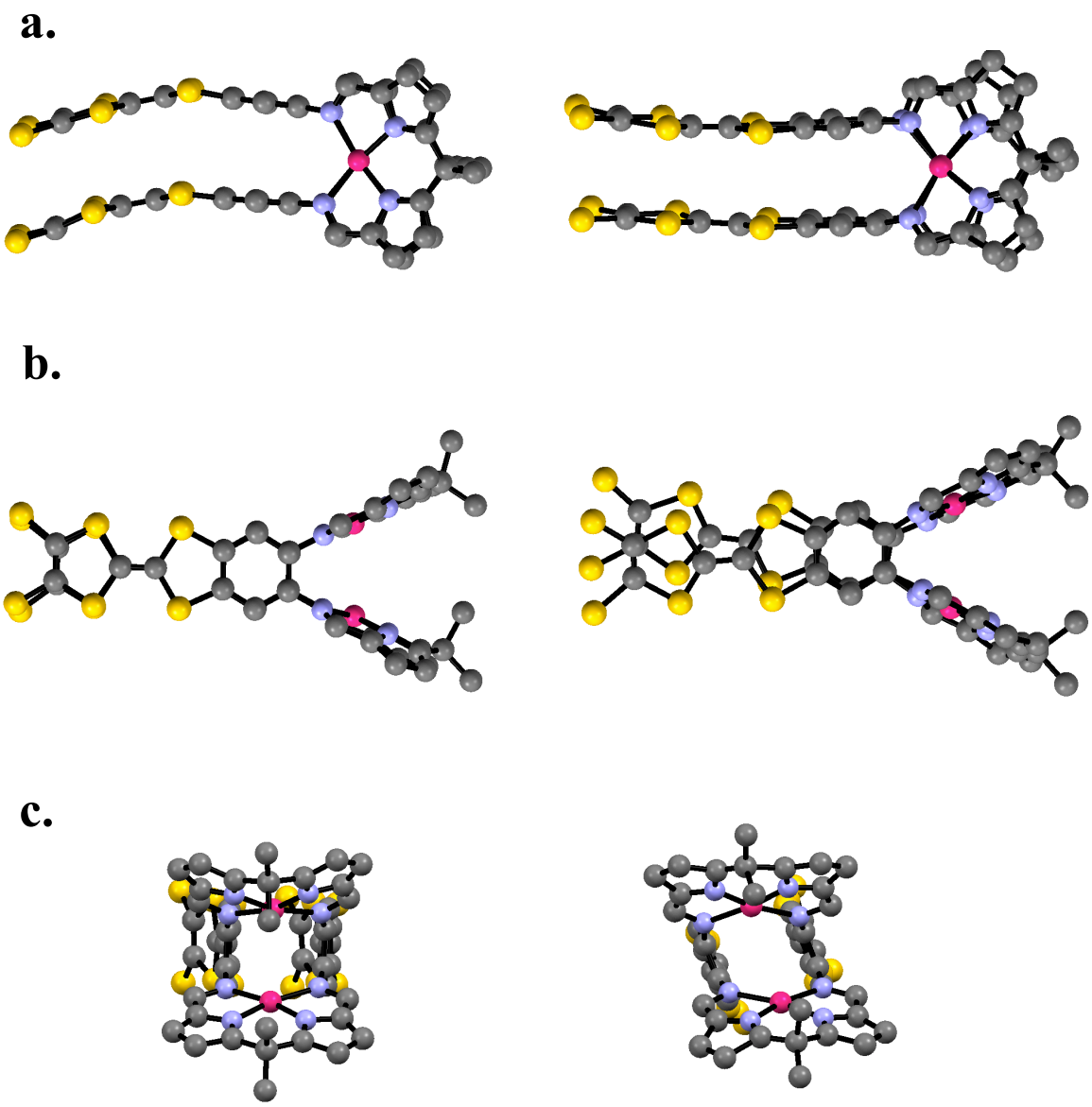

Figure 2.22 Top (a), side (b), and front (c) views of the structures of neutral **2.2** (left) and mixed-valence **2.2**$^{\bullet+}$ (right). Hydrogen atoms and solvent molecules omitted for clarity. Perchlorate counteranions omitted in the case of the mixed-valence species. For sake of comparison, the thiopropyl groups of **2.2** have been omitted.

2.6 CONCLUSION

In conclusion, the first example of metal induced stabilization in a synthetic dimeric TTF system has been detailed. Homobinuclear metalation of a flexible macrocycle, **2.1**, serves to bring together two otherwise independent TTF units and arrange them in such a manner that both the MV radical and radical cation π-dimer states may be stabilized upon oxidation. The preorganization of the TTF units in **2.2** was confirmed by X-ray crystal structure analysis where the extended π-faces are eclipsed when viewing the structure from the side view.

The difference in electronic structure between **2.1** and **2.2** that occurs upon the metalation-induced change in macrocyclic conformation was borne out via CV, UV–vis–NIR spectrscopic, and EPR studies. The free ligand **2.1** exhibits electrochemical behavior reminiscent of the parent TTF **1**, leading us to believe that the two TTF units are independent of one another. Conversely, the cyclic voltammetry and differential pulse voltammetry studies of **2.2** reveal the presence three redox processes, leading us to infer that there is an intramolecular stabilization of radical dimers formed upon oxidation.

Chemical and electrochemical oxidation UV-vis-NIR studies served to underscore further the importance of metallation and rigidity in linking the two TTFs in a through-space manner. While the flexible free ligand **2.1** did not show any features ascribable to an interaction, complex **2.2** gave a characteristic intervalence charge-transfer absorption centered around 2000 nm during both chemical and electrochemical oxidations.

These findings were additionally reinforced by EPR evidence of a stable mixed-valence state in **2.2** and not in **2.1**, after chemical oxidation. Moreover, EPR proved to be the determining factor in establishing evidence for the existence of a π-dimer state in **2.2**, The signal of the mixed-valence radical steadily decreased after the addition of more than

one equiv of chemical oxidant, indicating the presence of a spin-paired radical cation dimer.

Comparing the structural features of **2.2** to other *bis*-Pd(II) Schiff-base calixpyrrole complexes provides support for the notion that better π•••π stacking in the aryl hinges of *bis*-(Pd)II complexes leads to smaller bite angles and closer Pd-Pd distances. This finding, coupled with the redox-active nature of **2.2**, has lead to preliminary solid-state evidence that oxidizing the TTF subunits of the ligands can induce structural changes in the degree of intermetallic separation.

The rigid inseparable TTF faces in complex **2.2** make it an ideal system for studying and exploiting dimeric through-space interactions linking TTF units. The use of a Pd(II) as a stimulus for the preorganization event warrants the use of transition metals in building more complex TTF scaffolds for nanowires and complex organic electronic assemblies.

2.7 FUTURE WORK

The versatility of the Schiff-base calixpyrrole **2.20** as a ligand for transition metals, *f*-elements, and other metal centers means that there are numerous possibilities for TTF-derivatives, such as **2.1**, in which the ligand framework can take on various stable oxidation states with different structural geometries.

In light of the results from this chapter, it would be of great interest to study the effects on ligand **2.1** when the transition metal is varied, especially in complexes that are known to adopt the ditopic Pacman geometry. The most logical approach in this case would consist of first studying other group 10 transition metals complexes such as **2.1-Ni**

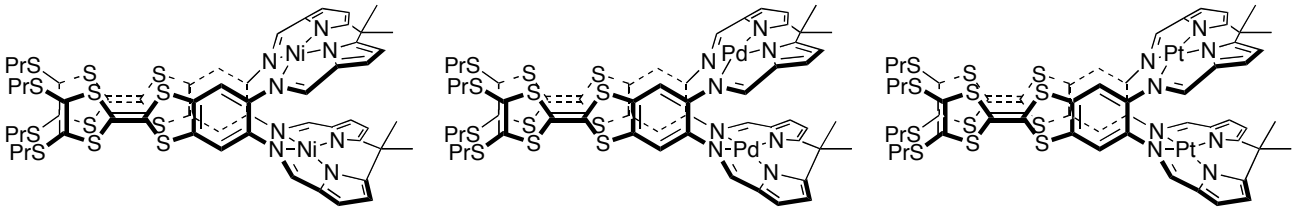

2.1-Ni **2.2** **2.1-Pt**

Figure 2.23 TTF-Pacman bis-Pd(II) complex **2.2** and proposed group 10 TTF-Pacman complexes **2.1-Ni** and **2.1-Pt**.

and **2.1-Pt** (Figure 2.23). Transition metals smaller than Pd(II), such as Ni(II), might be expected to force the two TTF aryl hinge units into closer proximity and offer more communication or stabilization upon oxidation. On the other hand, larger cations, such as Pt(II) may do the opposite. Whereas the parent *bis*-Ni(II) Schiff-base calixpyrrole complexes are known (**2.21b**), there are no reported *bis*-Pt(II) complexes with Schiff-base calixpyrrole **2.20**.

Aside from establishing a trend in these TTF-Pacman complexes of group 10 metals, a *bis*-Pt(II) platinum complex, such as **2.1-Pt**, could prove interesting electrochemical luminescent switches. For example, it has been shown that for homobinuclear *bis*-Pt(II) complexes the separation between the luminescent metal centers dictates the wavelength of emission due to perturbations in the MMCT interactions.[35] Therefore, in **2.1-Pt** it could be possible to tune the distance between the Pt metals by oxidizing and reducing the ligand. This change in Pt•••Pt distance would presumably alter the emission wavelength.

Another way to increase the stabilization of the contiguous radical dimers in TTF-Pacman complexes is to expand the π-faces. This strategy could be implemented by replacing the propylthio groups on **2.2** with aryl units, such as in **2.26**. The expected increase in intramolecular π-π overlap could also lead to more pronounced structural

changes in the systems upon oxidation. In fact, drastic structural changes in these systems might occur if a 2-[9-(1,3-dithiol-2-ylidene)anthracen-10(9H)-ylidene]-1,3-dithiole (exTTF) unit were covalently linked to the aryl hinges **2.27** (Figure 2.24). The exTTF covalently links a "conjugated *p*-quinoid spacer" unit between two 1,3-dithiole rings. Upon the loss of 2 electrons the "spacer" gains aromaticity and planarity and undergoes a geometrical change from a butterfly shaped neutral state to a planar di-cationic structure.[36] The steric strain of the resulting di-cationic complex could be exploited to impart dramatic structural changes in the Pacman geometry.

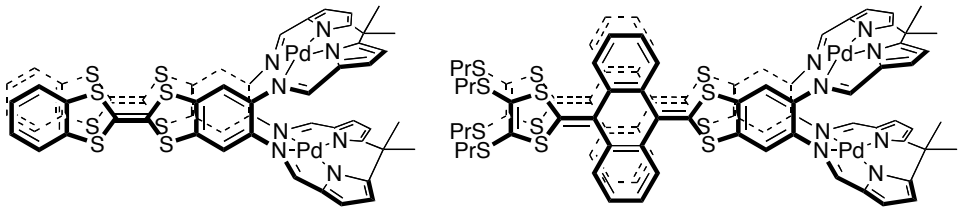

Figure 2.24 π-extended *bis*-Pd(II) TTF-Schiff-base calixpyrrole complexes: Benzo-annulated bis-Pd(II) TTF-Pacman **2.26** and exTTF *bis*-Pd(II) TTF-Pacman **2.27**.

Finally, it is safe to predict that the chemistry of bimetallic TTF Schiff-base calixpyrrole complexes will continue to provide new opportunities to investigate the fundamental properties and use of TTF dimers in molecular machines. In particular, we envision that variation of the metal and arylation of the TTF subunits will provide interesting analogues with augmented properties.

References and Notes

1. For Reviews on TTF-cyclophanes and TTF-oligimeric systems see: (a) Jeppesen, J. O.; Nielsen, M. B.; Becher, J. *Chem. Rev.* **2004**, *104*, 5115. (b) Iyoda, M.; Hasegawa, M.; Miyake, Y.; *Chem. Rev.* **2004**, *104*, 5085.

2. (a) Hasegawa, M.; Iyoda, M. *Chem. Soc. Rev.* **2010**, *39*, 2420. (b) Amabilino, D. B.; Puigmartí-Luis, J. *Soft Matter* **2010**, *6*, 1605. (c) Canevet,, D.; Sallé, M.; Zhang, G.; Zhu, D. *Chem. Commun.* **2009**, 2245. (d) Iyoda, M.; Hasegawa, M.; Enozawa, E. *Chem. Lett.* **2007**, *36*, 1402.

3. See Chapter 1 reference 12f.

4. Urayama, H.; Yamochi, H.; Saito, G.; Nozawa, K. Sugano, T.; Kinoshita, M.; Sato, S.; Oshima, K.; Kawamoto, A.; Tanaka, J. *Chem. Lett.* **1988**, 55.

5. Ziganshina, A. Y.; Ko, Y-H.; Jeon, W-S.; Kim, K. *Chem. Commun.* **2004**, 806.

6. Yoshizawa, M.; Kumazawa, K.; Fujita, M. *J. Am. Chem. Soc.* **2005**, *127*, 13456.

7. Martí-Rujas, J.; Islam, N.; Hashizume, D.; Izumi, F.; Fujita, M.; Song, H. J.; Choi, H. C.; Kawano, M. *Angew. Chem. Int. Ed.* **2011**, *50*, 6105.

8. Bertho-Thoraval, F; Robert, A.; Souizi, A.; Boubekeur, K.; Batail, P. *J. Chem. Soc., Chem. Commun.* **1991**, 843.

9. Lyskawa, J.; Sallé, M.; Balandie, J-Y.; Le Derf, F.; Levillain, E.; Allain, M.; Viel, P.; Palacin, S. *Chem. Commun.* **2006**, 2233.

10. Hasegawa, M.; Daigoku, K.; Hashimoto, K.; Nishikawa, H.; Iyoda, M. *Bull. Chem. Soc. Jpn.* **2012**, *85*, 51.

11. Nakamura, K.; Takashima, T.; Shirahata, T.; Hino, S.; Hasegawa, M.; Mazaki, Y.; Misaki, Y. *Org. Lett.* **2011**, *13*, 3122.

12. Park, J. S.; Karnas, E.; Ohkubo, K.; Chen, P.; Kadish, K. M.; Fukuzumi, S.; Bielawski, C. W.; Hudnall, T. W.; Lynch, V. M.; Sessler, J. L. *Science* **2010**, *329*, 1324.

13. (a) Coskun, A.; Spruell, J. M.; Barin, G.; Fahrenbach, A. C.; Forgan, R. S.; Colvin, M. T.; Carmieli, R.; Benítez, D.; Tkatchouk, E.; Friedman, D. C.; Sarjeant, A. A.; Wasielewski, M. R.; Goddard, W. A., III; Stoddart, J. F. *J. Am. Chem. Soc.*, **2011**, *133*, 4538. (b) Spruell, J. M.; Coskun, A.; Friedman, D. C.; Forgan, R. S.; Sarjeant, A. A.; Trabolsi, A.; Fahrenbach, A. C.; Barin, G.; Paxton, W. F.; Dey, S. K.; Olson, M. A.; Benítz, D.; Tkatchouk, E.; Colvin, M. T.; Carmielli, R.; Caldwell, S. T.; Rosair, G. M.; Hewage, S. G.; Duclairoir, F.; Seymour, J. L.; Slawin, A. M. Z.; Goddard, W. A., III; Wasielewski, M. R.; Cooke, G.; Stoddard, J. F. *Nat. Chem.* **2010**, *2*, 870.

14. Takase, M.; Yoshia, N.; Nishinaga, T.; Iyoda, M. *Org. Lett.* **2011**, *13*, 3896.

15. (a) Cheng, P-N.; Chiang, P-T.; Chiu, S-H. *Chem. Commun.* **2005**, 1285. (b) Chiang, P-T.; Chen, N-C.; Lai, C-C.; Chiu, S-H. *Chem. Eur. J.* **2008**, *14*, 6546.

16. Saad, A.; Barriére, F.; Levillain, E.; Vanthuyne, N.; Jeannin, O.; Fourmigué, M. *Chem. Eur. J.* **2010**, 16, 8020.

17. Enozawa, H.; Hasegawa, M.; Takamatsu, D.; Fukui, K-I.; Iyoda, M. *Org. Lett.* **2006**, *8*, 1917.

18. (a) Terech, P.; Weiss, R. G. *Chem. Rev.* **1997**, *97*, 3133. (b) Fages, F. *Low Molecular Mass Gelators* In *Topics in Current Chemistry* Ed.; Springer: Berlin, Heidelberg, New York, 2005; Vol. 256.

19. Akutagawa, T.; Kakiuchi, K.; Hasegawa T.; Noro, S.; Nakamura, T.; Hasegawa, H.; Mashiko, S.; Becher, J. *Angew. Chem. Int. Ed.* **2005**, *44*, 7283.

20. Puigmartí-Luis, J.; Laukhin, V.; Pérez del Pino, A.; Vidal-Gancedo, J.; Rovira, C.; Laukhina, E.; Amabalino, D. B. *Angew. Chem. Int. Ed.* **2007**, *46*, 238.

21. Jørgensen, M.; Bechgaard, K. *J. Org. Chem.* **1984**, *59*, 5877.

22. Kitahara, T.; Shirakawa, M.; Kawano, S.; Beginn, U.; Fujita, N.; Shinkai, S. *J. Am. Chem. Soc.* **2005**, *127*, 14980.

23. Gale, P. A.; Sessler, J. L.; Král, V.; Lynch, V. *J. Am. Chem. Soc.* **1996**, *118*, 5184.

24. Baeyer, A. *Ber. Dtsch Chem. Ges.* **1886**, *19*, 2184.

25. Floriani, C.; Floriani-Moro, R. *Porphyrin Handbook* **2000**, *3*, 385.

26. Gale, P. A.; Anzenbacher, P., Jr.; Sessler, J. L. *Coord. Chem. Rev* **2001**, *222*, 57.

27. Sessler, J. L.; Cho, W-S; Dudek, S. P.; Hicks, L.; Lynch, V. M.; Huggins, M. T. *Journal of Porphyrins and Phthalocyanines **2003**, 7*, 97.

28. (a) Givaja, G.; Blake, A. J.; Wilson, C.; Schröder, M.; Love, J. B. *Chem. Commun.* **2003**, 2508. (b) Givaja, G.; Blake, A. J.; Wilson, C.; Schröder, M.; Love, J. B. *Chem. Commun.* **2005**, 4423. (c) Veauthier, J. M.; Tomat, E; Lynch, V. M.; Sessler, J. L.; Mirsaidov, U.; Markert, J. T. *Inorg. Chem.* **2005**, 44, 6736. (d) Tomat, E.; Cuesta, L.; Lynch, V. M.; Sessler, J. L. *Inorg. Chem.* **2007**, 46, 6224. (e) Givaja, G.; Volpe, M.; Leeland, J. W.; Edwards, M. A.; Young, T. K.; Darby, S. B.; Reid, S. D.; Blake, A. J.; Wilson, C.; Wolowska, J.; McInnes, E. J. L.; Schröder, M.; Love, J. B. *Chem.—Eur. J.* **2007**, 13, 3707. (f) Cuesta, L.; Tomat, E.; Lynch, V. M.; Sessler, J. L. *Chem. Commun.* **2008**, 3744. (g) Love, J. B. *Chem. Commun.* **2009**, 3154.

29. (a) Collman, J. P.; Wagenknecht, P. S.; Hutchinson, J. E *Angew. Chem.* **1994**, *106*, 1620. (b) Dempsey, J. L.; Esswein, A. J.; Manke, D. R.; Rosenthal, J.; Soper, J. D.; Nocera, D. G. *Inorg. Chem.* **2005**, *44*, 6879. (c) Chang, C. J.;

Loh, Z.-H.; Shi, C.; Anson, F. C.; Nocera, D. G. *J. Am. Chem. Soc.* **2004**, *126*, 10013. (d) Chang, C. J.; Deng, Y.; Shi, C.; Anson, F. C.; Nocera, D. G. *Chem. Commun.* **2000**, 1355. (e) Guilard, R.; Brandès, S.; Tardieux, C.; Tabard, A.; L'Her, M.; Miry, C.; Gouerec, P.; Knop, Y.; Collman, J. P. *J. Am. Chem. Soc.* **1995**, *117*, 11721. (f) Proniewicz, L. M.; Odo, J.; Goral, J.; Chang, C. K.; Nakamoto, C. K. *J. Am. Chem. Soc.* **1989**, *111*, 2105 (g) Durand, R. R.; Bencosme, Jr., C. S.; Collman, J. P.; Anson, F. C. *J. Am. Chem. Soc.* **1983**, *105*, 2710. (h) Collman, J. P.; Denisevich, P.; Konai, Y.; Marrocco, M.; Koval, C.; Anson, F. C. *J. Am. Chem. Soc.* **1980**, *102*, 6027. (i) Hodgkiss, J. M.; Chang, C. J.; Pistorio, B. J.; Nocera, D. G. *Inorg. Chem.* **2003**, *42*, 8270. (j) Pistorio, B. J.; Chang, C. J.; Nocera, D. G. *J. Am. Chem. Soc.* **2002**, *124*, 7884. (k) Rosenthal, J.; Luckett, T. D.; Hodgkiss, J. M.; Nocera, D. G. *J. Am. Chem. Soc.* 2006, **128**, 6546. (l) Rosenthal, J.; Pistorio, B. J.; Chng, L. L.; Nocera, D. G. *J. Org. Chem.* **2005**, *70*, 1885.

30. (a) Arnold, P. L.; Potter, N. A.; Carmichael, C. D.; Slawin, A. M. Z.; Roussel, P.; Love, J. B. *Chem. Commun.* **2010**, 1833. (b) Arnold, P. L.; Blake, A. J.; Wilson, C.; Love, J. B. *Inorg. Chem.* **2004**, *43*, 8206. (c) Arnold, P. L.; Patel, D.; Pécharman, A.-F.; Wilson, C.; Love, J. B. *Dalton Trans.* **2010**, *39*, 3501. (d) Arnold, P. L.; Patel, D.; Wilson, C.; Love, J. B. *Nature* **2008**, *451*, 315. (e) Arnold, P. L.; Pécharman, A.-F.; Hollis, E.; Yahia, A.; Maron, L.; Parsons, S.; Love, J. B. *Nat. Chem.* **2010**, *2*, 1056. (f) Arnold, P. L.; Hollis, E.; White, F. J.; Magnani, N.; Caciuffo, R.; Love, J. B. *Angew. Chem., Int. Ed.* **2011**, *50*, 887.

31. Leeland, J. W.; White, F. J.; Love, J. B. *J. Am. Chem. Soc.* **2011**, *133*, 7320.

32. Jia, C.; Liu, S. X.; Tanner, C.; Leiggener, C.; Neels, A.; Sanguinet, L.; Levillain, E.; Leutwyler, S.; Hauser, A.; Decurtins, S. *Chem.–Eur. J.* **2007**, *13*, 3804.

33. Spanggard, H.; Prehn, J.; Nielsen, M. B.; Levillain, E.; Allain, M.; Becher, J. *J. Am. Chem. Soc.* **2000**, 122, 9486.

34. Wang, F. F.; Wang, F.; Wang, B. Q.; Wang, Y. F.; Ma, F.; Li, Z. R. *Sci. China Ser. B: Chem.* **2009**, *52*, 1980.

35. Ma, B.; Li, J.; Djurovich, P.; Yousufuddin, M.; Bau, R.; Thompson, M. E. *J. Am. Chem. Soc.*, **2005**, *127*, 28.

36. (a) Yamashita, Y.; Kobayashi, Y.; Miyashi, T. *Angew. Chem., Int. Ed. Engl.* **1989**, *28*, 1052. (b) Bryce, M. R.; Moore, A. J.; Hasan, M.; Ashwell, G. J.; Fraser, A. T.; Clegg, W.; Hursthouse, M. B.; Karaulov, A. I. *Angew. Chem., Int. Ed. Engl.* **1990**, *29*, 1450.

Chapter 3: Synthesis and Characterization of a Tetrathiafulvalene-salphen Actinide Complex

3.1 INTRODUCTION

Ligands incorporating the classic organic donor tetrathiafulvalene (TTF) have been shown to form metal complexes that are promising compounds for the development of cooperative systems where the redox-active TTF ligand is in electronic communication with the metal ion.[1] The observation of cooperative behavior in compounds containing the organic donor tetrathiafulvalene (TTF) and 3*d* transition metals has sparked interest in the development of new multifunctional materials that display both conductivity across the delocalized TTF π-system and magnetic moments arising from unpaired metal spins.[2] Extending this concept into the realm of 4*f* elements is appealing. Typically, members of the lanthanide series display a greater number of unpaired spins, a more pronounced anisotropy, and unique luminescent properties compared to their transition metal counterparts. Accordingly, it has been proposed that electronic and magnetic coupling between the 4*f*-lanthanide electrons and the delocalized electrons in the TTF π-orbitals may lead to hybrid materials with more desirable properties than the corresponding 3*d*-analogues.[3] Assuming through-bond interactions, it seems likely that high spin ground states that are well isolated in energy could be more readily accessed with enhanced metal ligand orbital mixing. From this perspective, substitution of the central lanthanide ion for an actinide, which has more radially extended and accessible 5*f* orbitals,[4] offers opportunity to enhance the electronic communication between the ligand the central metal. However, only a few actinide complexes have been reported with redox active

ligands and, to the best of our knowledge, there are no examples of actinide-TTF compounds.[5] Our long term objective is thus to develop new actinide complexes containing TTF moieties and to explore their properties.

In pursuit of this long-range goal, this Chapter reports the synthesis of the first TTF-actinide complex **3.1**. The properties of this complex have been examined by single crystal X-ray defractometry, cyclic voltammetry, ^{1}H-NMR, ^{13}C-NMR, and IR spectrometry. As detailed below, the results could provide an opportunity to expand TTF chemistry to transuranic elements. More specifically, they serve to establish the use the TTF-salphen^{2-}dianionic ligand as a platform for complexation of the uranyl cation. This has allowed initial insights into the electronic coupling between a specific actinide cation and a classic redox active subunit.

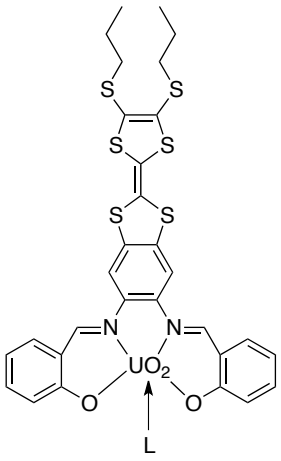

3.1

Figure 3.1 Structure of the (Tetrathiafulvalene-salphen)UO_2(L) **3.1**.

3.2 TETRATHIAFULVALENE MULTIFUNCTIONAL MATERIALS

A major goal of modern materials science is to create systems that exhibit multifunctionality. One way to impart this multifunctionality in a single solid is to emplace two or more physical properties into the same crystal lattice. Molecular organic conductors comprised of TTF have been thoroughly investigated as building blocks for the preparation of multifunctional molecular solids in which conductivity is coupled with magnetic bistability. Introduction of magnetic ions as the charge-compensating anion in solids formed by partially oxidized TTFs has afforded compounds that display the coexistence of paramagnetism and superconductivity, antiferromagnetism and superconductivity, and also ferromagnetism and metallic conductivity.[2d,e]

Inorganic chemistry provides a plethora of metal complexes of various nuclearities and dimensionality that can be used as counterions when constructing conductive cation-radical salts. It is possible to use simple mononuclear anions, cluster-type complexes, dithiolate chain complexes, or bimetallic layered structures. In fact, a layered radical cation system comprised of oxalate-bridged Mn^{2+} and Cr^{3+} ions and bis(ethylenedithio)tetrathiafulvalene (BEDT-TTF) represents one of the most notable examples of a hybrid magnetic conductor, wherein metallic conductivity and ferromagnetism are seen in the same material (Figure 3.2).[2f] In this case, the use of a counteranion that exists in the form of infinite layers of oxalate-bridged hexagonal networks was decisive in obtaining bulk magnetism. (BEDT-TTF)[$MnCr(C_2O_4)_3$] shows magnetic behavior below a critical temperature, T_c, of 5.5 K and metallic behavior down to 2 K.

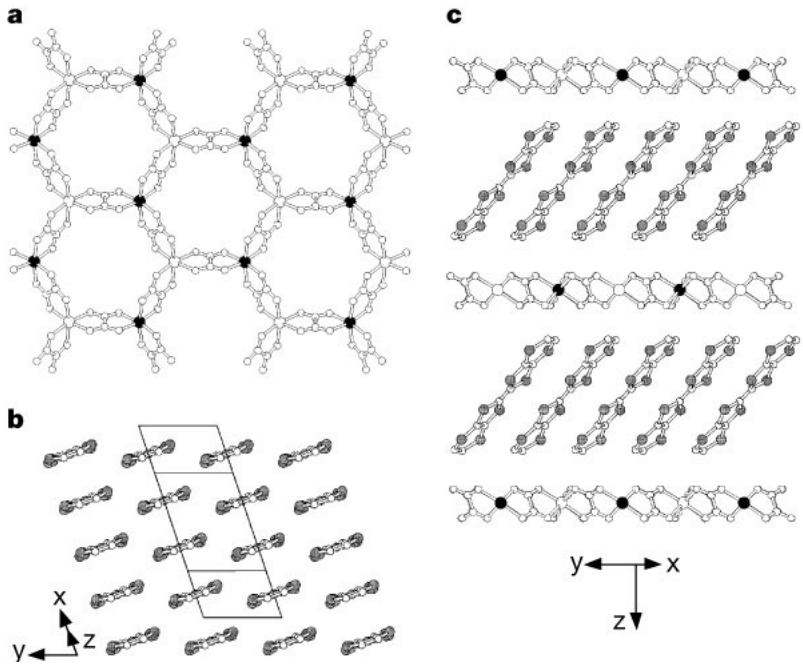

Figure 3.2 Packing of (a) the $[MnCr(C_2O_4)_3]^-$ anion layer, (b) the BEDT-TTF layer, and (c) the alternating organic and inorganic layers in the hybrid structure. Reprinted with permission from *Nature* **2000**, 408, 447. Copyright 2000 Nature Publishing Group.

3.3 TETRATHIAFULVALENE LIGANDS

The interactions between the TTF units and the paramagnetic inorganic counterions are often weak or non-existing. This lack of strong interaction often represents the most significant limitation in the construction of multifunctional systems.[2f] To overcome the lack of interaction within in these hybrid TTF-contatining compounds increased effort has been devoted to the design of ligands that covalently link the TTF moiety to the metal center.[1,3] It is proposed that direct coordination can provide stronger electronic communication between the metal and the TTF subunits, thereby enhancing the synergy in the resulting molecular solid. The two most widely developed

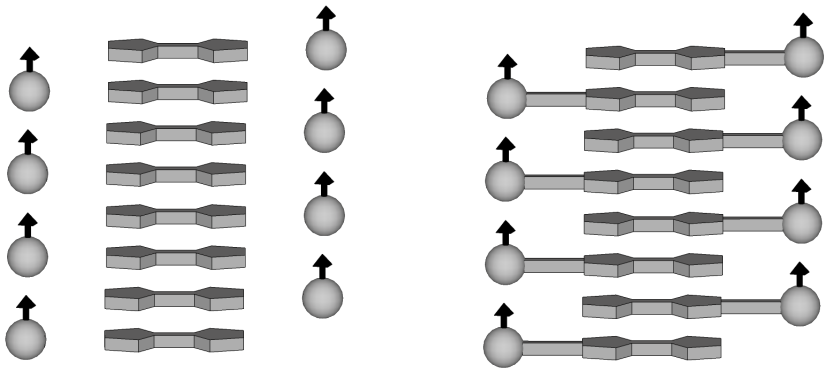

Figure 3.3 Representations of the indirect exchange mechanism; (left) through space interaction, (right) through bridge interaction.

strategies for obtaining magnetic conductors based on TTF subunits is shown in Figure 3.3. It is thought that better long-range magnetic coupling between localized spins can be achieved by the through bridge interaction (Figure 3.3 right).

3.3.1 Tetrathiafulvalene Ligands for Transition Metals

The first TTF ligand used for metal complexation was the thiolate dianion **3.3**. In 1979 Rivera *et al*. described the synthesis of a nickel dithiolate complex. However, at that time, the structure and the conducting properties of the oxidized material were not reported.[6] These complexes were studied widely in the 1990s.[7] In 2001, Kobayashi *et al*. reported the first single component molecular metal $[Ni(tmdt)_2]$ (tmdt, trimethylenetetrathiafulvalenedithiolate) **3.4**.[8] This complex behaved as a 3-D conductor displaying room temperature conductivity of 400 S cm^{-1} as well as metallic behavior down to 0.6 K. More recently, it was reported by Kobayashi and co-workers that at $[Cu(dmdt)_2]$ (dmdt, dimethyltetrathiafulvalenedithiolate) **3.5** is also a single-component molecular conductor. This system is of interest because if contains magnetic moments that are arranged in a three-dimensional fashion and delocalized throughout the π-system (Figure 3.4).[2a]

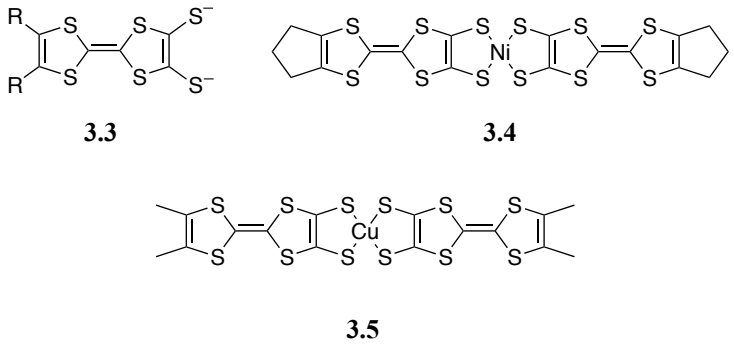

3.3 **3.4**

3.5

Figure 3.4 Early TTF derivative ligand, thiolate **3.3** and single component molecular conductors [Ni(tmdt)$_2$] **3.4**, and [Cu(dmdt)$_2$] **3.5**.

Of the numerous TTF derivatives that have been designed in as hybrid organic-inorganic materials, those containing pyridine or phosphine are the most extensively studied thus far (Figure 3.5).[9] The 1-D coordination polymer reported by Liu *et al.*, which uses TTF-pyridine ligand **3.6** and contains chains of chloro-bridged Mn^{2+} ions, is an elegant example of a system structurally prearranged to support magnetism and conductivity (Figure 3.6).[10] However, despite the stacking of the TTF units in the direction parallel to the chains and the bridging between Mn^{2+} centers, the TTF units remain neutral and there is only weak ferromagnetic coupling between the Mn^{2+} centers.

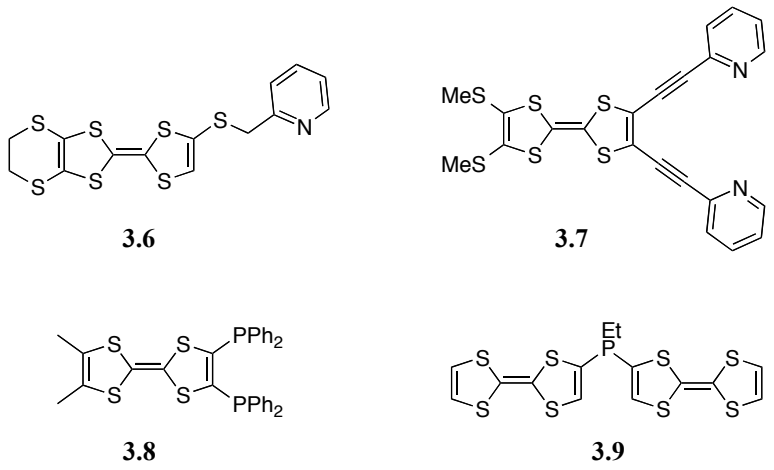

Figure 3.5 Representative TTF-pyridine ligands **3.6** and **3.7** and TTF-phosphine ligands **3.8** and **3.9**.

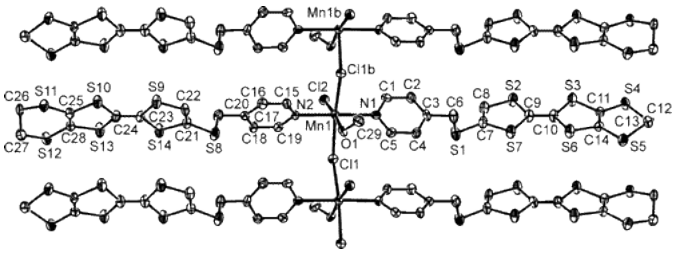

Figure 3.6 ORTEP (50% probability ellipsoids) showing the structure of the coordination polymer formed from ligand **3.6** and $MnCl_2$. Hydrogen atoms are omitted for clarity. Reprinted with permission from *Inorg. Chem.* **2006**, 45, 3152. Copyright 2006 American Chemical Society.

More recently, metal complexes derived from TTF-modified carboxylates, [11] β-diketonates, [12] and increasingly novel *N*-heterocyclic ligands[13] have been reported (Figure 3.7). Ongoing advances in synthetic TTF-chemistry are allowing ligands of increasing complexity to be prepared; including those stabilizing macrocyclic complexes,[14] precatenates,[15] and self-assembled cages[16] (Figure 3.8).

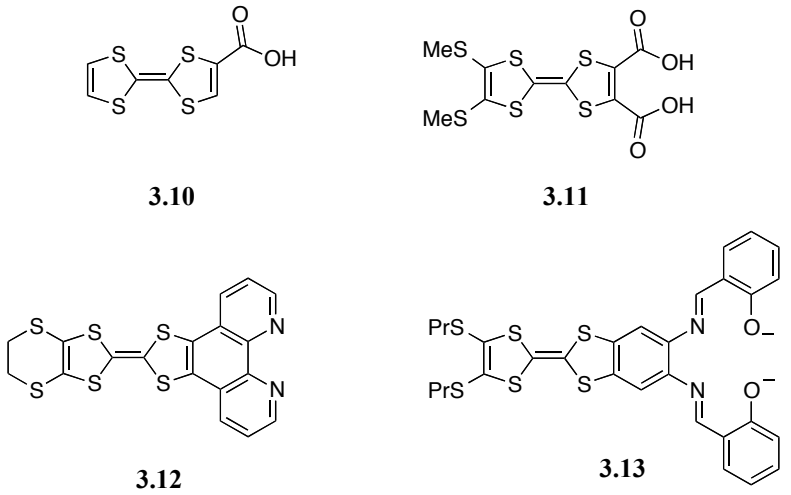

Figure 3.7 TTF-carboxylates **3.10** -**3.11** and *N*-heterocyclic-TTF ligands **3.12**-**3.13**.

However, despite the wide array of new ligands and complexes, the preparation of conductive materials has been successful only in a few cases, aside from the TTF-dithiolates. Many TTF-metal complexes lack good electron transport properties upon oxidation. Presumably, this reflects an absence of effective long range stacking between the TTF units, with the net effect that crystals of these hybrid systems are insulating. One exception is a Cu^{I} complex of a pyrazinodiselandithiafulvalene (pyra-STF) **3.17**, which

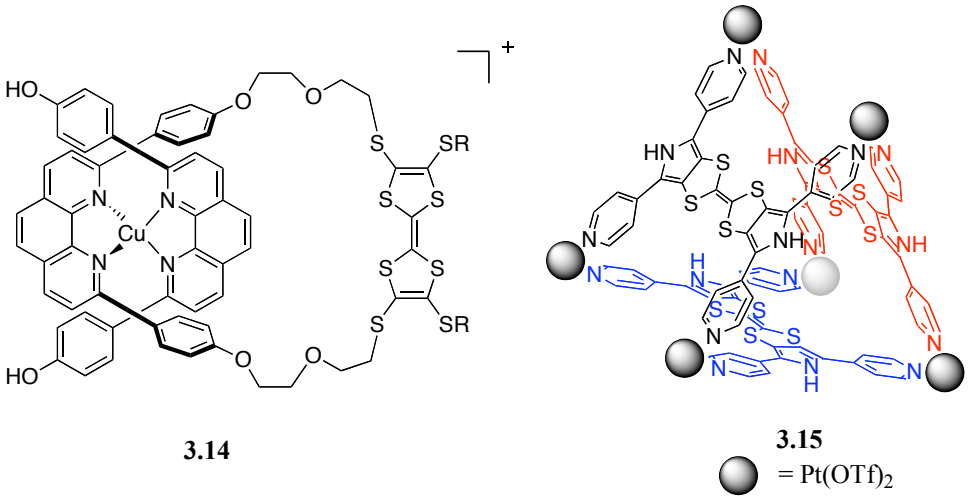

3.14

3.15
= $Pt(OTf)_2$

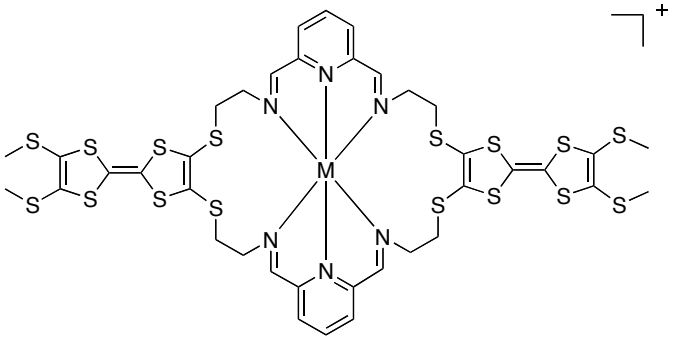

3.16
(M = Fe^{II}, Co^{II}, Ni^{II}, Zn^{II})

Figure 3.8 Examples of sophisticated TTF-ligand complexes: Cu^{II}-TTF-precatenane **3.14** , *bis*(pyrroly)TTF-Pt^{II}-trigonal-prismic-cage **3.15**, and TTF-Schiff-base macrocycle **3.16**.

shows high room temperature conductivity of 25 S cm^{-1}.[17] Similar to the 1-D coordination polymer reported by Liu[10] (Figure 3.6), the structure of $CuCl_{1.5}$•**3.17** consists of an infinite chain of metal centers bridged by a chloride anion. As opposed to the TTF-pyridine•$MnCl_2$ complex, which remains neutral and exhibits insulating behavior, the TTF moieties in $CuCl_{1.5}$•**3.17** are oxidized. The oxidized ligands coordinate to the copper centers and are organized in a stacking manner with π•••π separations of 3.5

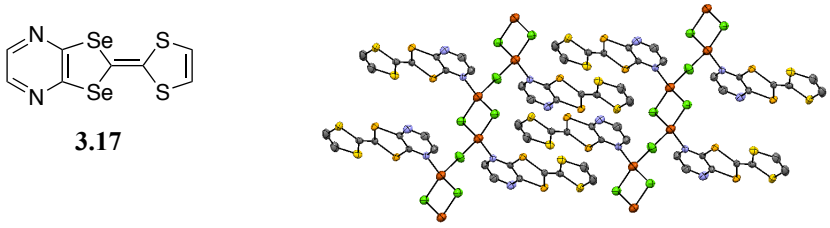

3.17

Figure 3.9 Pyra-STF ligand **3.17** and crystal structure of the conducting solid derived from it, [$CuCl_{1.5}$(pyra-STF)].

Å. This reinforces the required long range interaction imperative for conductivity (Figure 3.9).

3.3.2 Tetrathiafulvalene 4f-ligands

In the search for more advanced multifunctional materials, rare-earth elements offer unique characteristics in comparison to 3*d* transition metals. For example, the 4*f* orbitals of rare earth metals exhibit a more enhanced localized character than 3*d* transition metals resulting in strong correlation and the high degeneracy.[3a-d] The 4*f* lanthanide valence electrons are also well shielded by outer closed shell electrons and can have very large anisotropic magnetic moments, as a result of the strong spin-orbit coupling and multiple degeneracy. Several attempts to incorporate 4*f*-elements into the conductive solids formed by TTF donors were initially made by taking the traditional through-space approach in which the lanthanide counterions were expected to interact with the delocalized π-system through Van der Waals interactions.[3a-d] However, due to an absence of synergism in the resulting TTF-lanthanide radical-cation salts, ligands that covalently attach the lanthanide to the TTF unit are currently being explored.

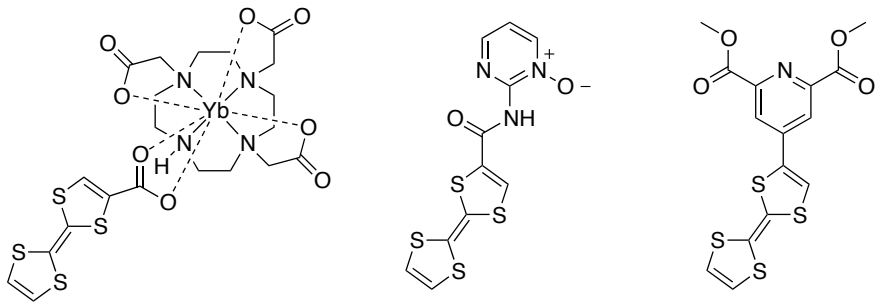

3.18 **3.19** **3.20**

Figure 3.10 First TTF-lanthanide complex studied for luminescence Yb(III) complex **3.18**. Early TTF-based ligands **3.19** and **3.20** used for lanthanide complexation.

The first complexes to be reported that included a TTF ligand linked to a lanthanide were prepared for the purpose of achieving near-infared (NIR) lanthanide luminescence.[3e-i] Thus, lanthanide compounds have a weak absorption originating from dipole forbidden *f-f* transitions.[18] The goal of these studies was to employ a TTF subunit, which absorbs strongly in the UV-visible region, as a luminescence sensitizer. Faulkner and co-workers prepared the first TTF-lanthanide complex, a ternary ytterbium complex with an appended TTF carboxylate **3.18** (Figure 3.10). [3g,h] This system was used to probe the mechanism of energy transfer from TTF subunit to the ytterbium(III) center. Later, Ouahab *et al*. synthesized 4*f* gadolidium(III) complexes with TTF-amido-2-pyrimidine-1-oxide ligand **3.19**. The antenna ligand 4-TTF-2,6-pyridinedicarboxylic acid dimethyl **3.20** was also reported by Ouahab and co-workers for the purpose of erbium(III) luminescence sensitization (Figure 3.10).[3e,f]

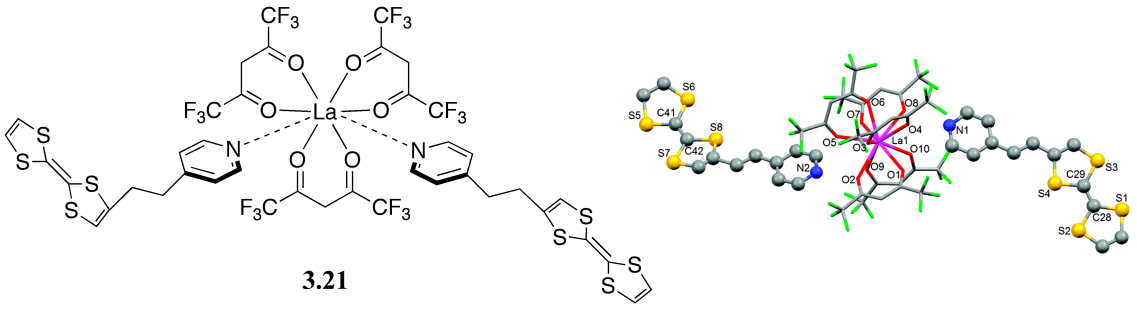

3.21

Figure 3.11 Ln(III) complex **3.21** and crystal structure of the asymmetric unit of **3.21**. The radical cation donors are drawn as balls and sticks; the anionic coordination complex of La(III) is drawn as capped sticks. Reprinted with permission from *Inorg. Chem.* **2009**, 48, 7421. Copyright 2009 American Chemical Society.

Several complexes have also been reported for the purpose of investigating the magnetic behavior of TTF-lanthanide compounds and their radical-cation salts In 2009, Ouahab used the redox active 4-(2-tetrathiafulvalene-ethenyl)pyridine ligand **3.21** to form complexes with lanthanum and neodymium ions.[3k] Reaction of **3.21** with La(III)(hfac)$_3$ and Nd(III)(hfac)$_3$ (hfac = 1,1,1,5,5,5-hexafluoroacetylacetonate) lead to spontaneous oxidation of the TTF-ligand giving radical-salts in which each TTF unit was singly oxidized (Figure 3.11). Due to this partial oxidation and a propensity to form dimers and tetramers in the solid state, these salts were determined to be insulators. Moreover, both strong anti-ferromagnetic interactions and quasi-diamagnetic behavior was observed for the organic network present in these complexes. Presumably, these features reflect the short contacts between the sulfur atoms of the donors within the radical salt.

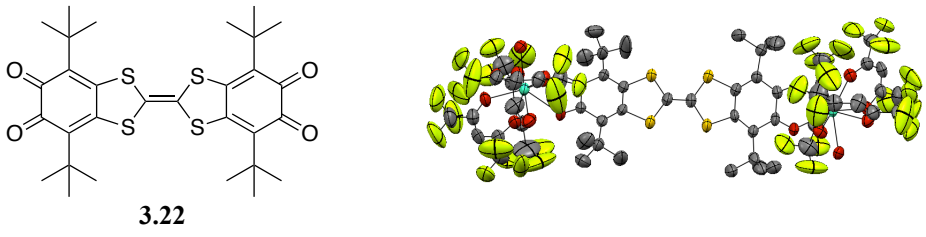

3.22

Figure 3.12 Novel donor-acceptor ligand **3.22** and an ORTEP view of the dinuclear $Dy(hfac)_3$ complex derived from it. Thermal ellipsoids are drawn at 50% probability level. Hydrogen atoms have been omitted for clarity.

Ouahab and co-workers also reported two TTF-lanthanide complexes that exhibit single-molecule magnetic behavior. The first of the compounds is a dinuclear complex formed from the TTF *N*-oxide ligand **3.19** and dysprosium$(tta)_3$ (tta^- = 2-thenoyltrifluoroacetate anion).[3k] The second complex is also a dinuclear Dy(III) compound.[3l] However, this complex uses a fused quinone-TTF-quinone (acceptor-donor-acceptor) ligand (**3.22**) to bridge two $Dy(hfac)_3$ moieties (Figure 3.12).[3j]

3.3.3 Tetrathiafulvalene-3d-4f Heterobimetallic Systems

Heterometallic 3*d*-4f complexes are of interest in the study of molecular magnetism. This research area can be traced to 1985, when Gatteschi *et al*. reported ferromagnetic interactions between Cu^{II} and Gd^{III} ions stabilized by a Schiff-base ligand.[19] Since this seminal study, interest has moved more towards using lanthanides exhibiting high anisotropy, such as Tb^{III}, Dy^{III}, and Ho^{III}, in an effort to design single-molecule magnets (SMM) or single-chain magnets (SCM).[20] When 3*d* ions interact with lanthanide cations characterized by high anisotropy, the spin-ground state of the resulting complex is effectively increased and there is a net enhancement in the intramolecular magnetic exchange interactions. Ligands containing both TTF and appropriate coordination sites

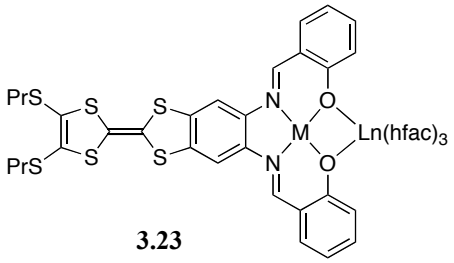

3.23

a. M = Cu , Ln = Gd
b. M = Cu , Ln = Tb
c. M = Cu , Ln = Dy
d. M = Ni , Ln = Gd
e. M = Ni , Ln = Tb
f. M = Ni , Ln = Dy

Figure 3.13 TTF-salphen-3d-4f heterobimetallic complexes **3.23a-f** (hfac = hexafluoroacetylacetone).

that promote heterometallic 3*d*-4*f* complexes offer the possibility of introducing the magnetic benefits of 3*d*-4*f* systems into conducting materials. In this vein, Ouahab *et al*. have reported the first TTF-3*d*-4*f* heterobimetallic complexes using the TTF-salphen ligand **3.13**.[21] Five new complexes using **3.13** were reported and as expected there is a ferromagnetic interaction between the Cu and Gd^{III} ions mediated by the phenolate bridges of the ligand (Figure 3.13). The conductivity of these systems remains unexplored but the stability of the complexes in solution should allow for electrocrystallization and future studies in their conductivity.

3.4 ACTINIDE CHEMISTRY

Whereas the filling of the 4*f* atomic orbitals is a feature of the lanthanides series, the chemistry of the actinides is dominated by the gradual filling of the 5*f* atomic orbitals. The *f*-orbitals are responsible for the chemical and physical properties of the lanthanide and actinide elements. Filling the *f*-orbitals results in a systematic decrease in the radii of the *f*-sub-shell as the nuclear charge increases.[4] This decrease in atomic radii across the series is known as the lanthanide contraction in the case of the 4*f* and the actinide contraction in the case of the 5*f*-orbitals, respectively. However, there are differences. Typically, the 4*f* atomic orbitals are deeply buried (*i.e*., nearer to the nucleus) and are considered "core-like". In the case of early actinides (*i.e*., Th to Pu), the 5*f* atomic orbitals

are more radially extended. As a consequence, they are thought to participate in more covalent bonding interactions.[4, 22]

3.4.1 Actinyl Ions

As opposed to the dominant III oxidation state of lanthanides, the early actinide cations can exist in a range of oxidation states.[4] For example; uranium is most stable in the VI oxidation state, neptunium in the V oxidation state, and plutonium in the IV oxidation state.[23] Normally the actinyl ion $(AnO_2)^{n+}$ (n = 1,2) is the most prevalent form of actinide elements in oxidation states above IV. The actinyl O=Ac=O bonds are linear, very robust, and are thought of as relatively covalent.[23] Due to the stability of the linear Ac=O bonds, ligands tend to coordinate to actinyl ions in the equatorial plane, resulting usually in a pentagonal bipyramidal coordination geometry, when the O=Ac=O bonds are considered. Of the actinyl ions, the uranyl ion, UO_2^{2+} is the most widely studied due to its chemical stability and availability in the depleted form, which poses a relatively low radiological hazard.

3.4.2 Uranyl(VI) Complexes with Tetradentate Ligands

There are many salicylaldehyde derivatives reported in the literature that form tetradentate complexes with UO_2^{2+}.[24] The most common of these are the $salen^{2-}$ or $salophen^{2-}$ Schiff-base ligands ($salen^{2-}$ = *N,N'*- disalicylidene-1,2-ethylenediaminate, $salophen^{2-}$ = *N,N'*-disalicylidene-1,2-phenylenediaminate). These complexes are particularly easy to prepare and they have an extensive history. For instance, in 1971, Vigato *et al*, prepared the UO_2(salophen)EtOH complex **3.24** through a condensation of *o*-phenylenediamine and salicylaldehyde in the presence of uranyl nitrate hexahydrate.[25]

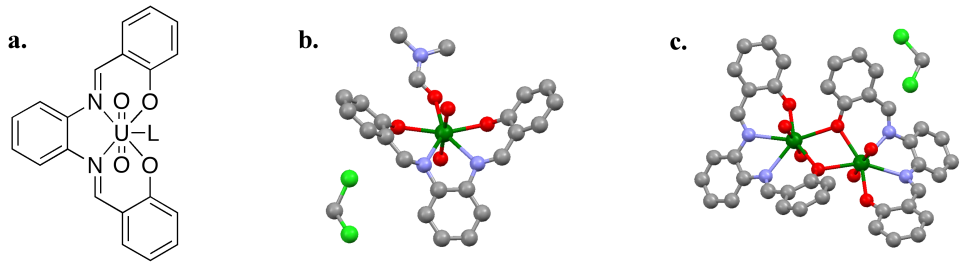

3.24

Figure 3.14 **a.** Structure of UO_2(salophen)L **3.24**. Ball and stick views of **b.** UO_2(salophen)DMF-CH_2Cl_2 and **c.** racemic $[UO_2(salophen)]_2$- CH_2Cl_2. Hydrogen atoms have been omitted for clarity.

It was determined that the N_2O_2 cavity of the ligand chelates the UO_2^{2+} adopting a tetra-coordinate geometry. The favored coordination geometry of the UO_2^{2+} cation equatorial plane allows for the binding of a monodentate ligand within the equatorial plane (Figure 3.14). This monodentate ligand, which is usually a molecule of solvent, is labile and can undergo facile ligand exchange. Exploitation of this labile ligand exchange coupled with the Lewis acidity of the uranyl species has led to derivatives of UO_2(salophen) finding use as anion / ion-pair sensors and electrodes.[26] In the absence of coordinating solvent the complex forms a racemic mixture of the dimeric compound $[UO_2(salophen)]_2$, in which the UO_2(salophen) fragments are held together by a phenoxy bridge (Figure 3.13).[27a] It is also worth noting that in contrast to uni- or bidentate ligands, the tetradentate ligand framework of the salophen^{2-} is capable of stabilizing quasireversible electrochemical reduction of the UO_2^{2+} to UO_2^{1+} in non aqueous solvents.[27b] This combination of features provided an incentive to prepare a TTF-containing complex of these venerable complexes. The authors work along these lines is summarized below.

3.5 SYNTHESIS AND CHARACTERIZATION

The synthesis of the (TTF-salphen)UO_2(EtOH) complex **3.1** is outlined in Scheme 3.1. One equivalent of uranyl nitrate hexahydrate [$UO_2(NO_3)_2$•$6H_2O$] acts as both a template and a Lewis acid catalyst in the condensation reaction between the known TTF-phenylenediamine **2.23** and 2 equivs of salicylaldehyde in ethanol. These conditions, which produce the desired complex in *73%* yield, are identical to those used for the synthesis of complex **3.24**. The only difference is that a TTF-phenylenediamine is used in lieu of the simple *o*-phenylenediamine. It is also possible to synthesize the known TTF-salphen free ligand **3.13** by omitting $UO_2(NO_3)_2$•$6H_2O$ from the reaction conditions. In both reactions, the desired products precipitate from the ethanol solution after several hours and are isolated using suction filtration.

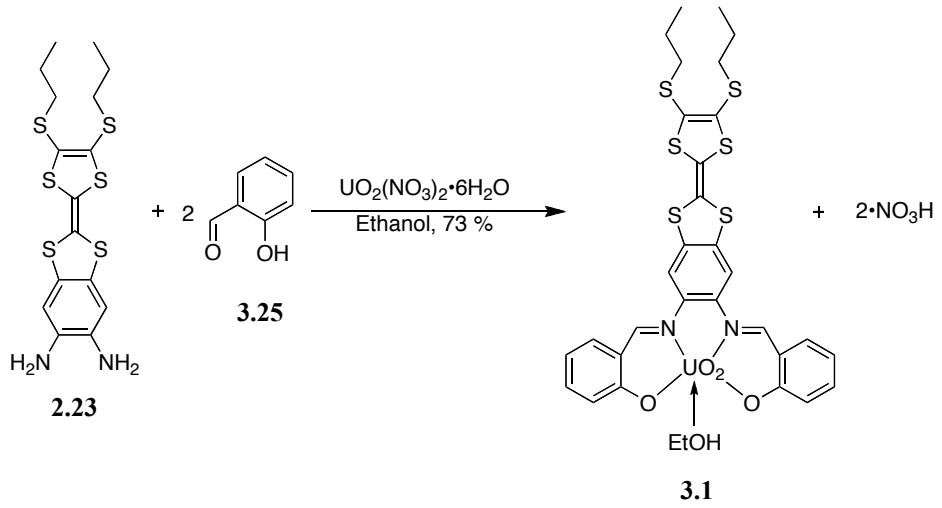

Scheme 3.1 Synthesis of (TTF-salphen)UO_2(EtOH) complex **3.1**.

3.5.1 ^{1}H NMR Comparative Study

The ^{1}H NMR spectrum (400 MHz) of **3.1** recorded in pyridine- d_5 at 298 K provided support for the formation of the uranyl complex. Comparing the spectra of the free-ligand **3.13** and that of the presumed uranyl complex **3.1**, revealed significant differences (Figure 3.15). Namely, the phenolic protons that appear as a broad singlet at 11.54 ppm in **3.13** are absent from the spectra of **3.1**. Also, the iminic protons at 8.88 ppm in free ligand **3.13** are substantially downshifted to 9.65 ppm in the uranyl complex. Presumably, this reflects the Lewis acidity of the bound uranyl cation. The spectrum of the uranyl complex **3.1** is also marked by a slight downfield shift in the aryl proton from the TTF-phenylene diamine, leading us to suggest that the electron withdrawing uranyl center could affect the redox properties of the TTF moiety. Finally, signals for free ethanol can be seen at 1.32 ppm and 3.91 ppm, in the spectrum of **3.1**. Such a finding is consistent with the notion that the stronger pyridine ligand has taken its place in filling the fifth equatorial coordination slot on the uranyl cation.

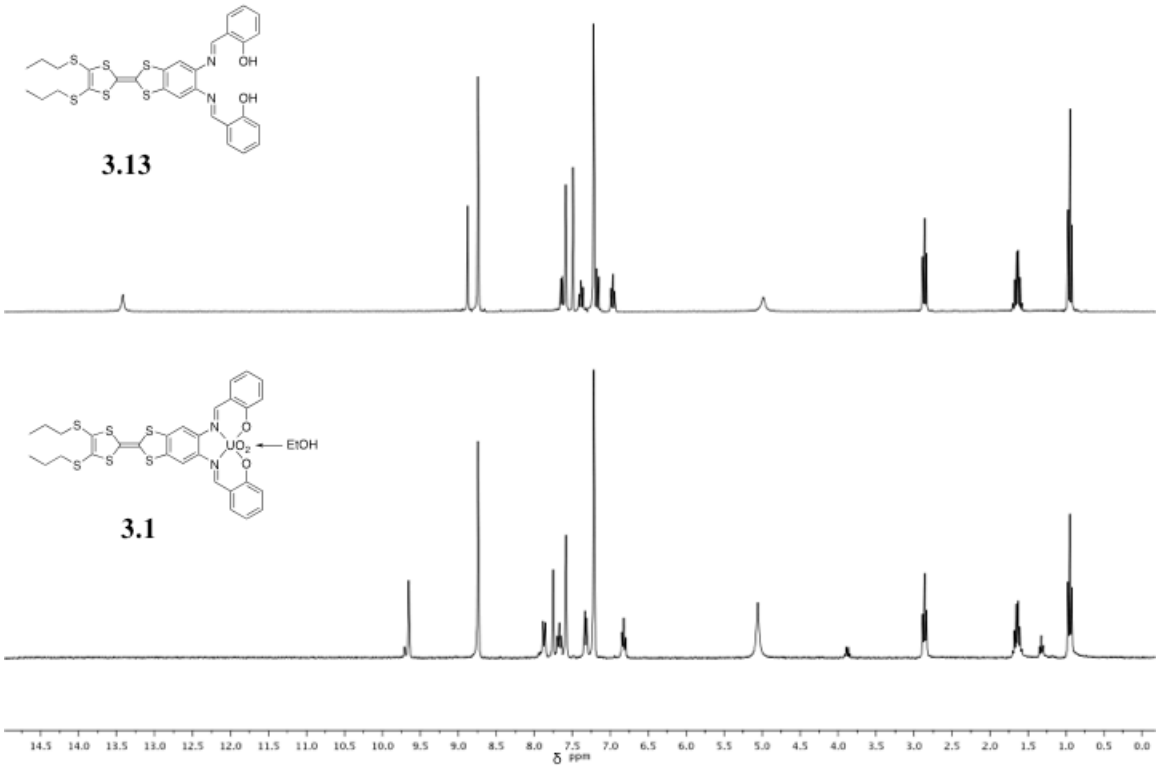

Figure 3.15 ^{1}H NMR spectra of **3.13** and **3.1** (400 MHz) recorded in pyridine-*d5* at 298 K.

3.5.2 X-ray Crystal Structure

Single crystals of complex **3.1** were grown as red blocks via slow evaporation from a CH_2Cl_2/MeOH solution. The resulting structure revealed a bound methanol (*i.e.*, (TTF-salphen)UO_2(HOMe)). In this complex, the ligand geometry around the central uranium ion is best described as pentagonal bipyramidal. The basic coordination mode is thus similar to what was observed in previous structures reported for (salophen)UO_2(L) (L = neutral ligand) complexes by Bandoli *et al*. and Ikeda and co-workers (Figures 3.16-3.17).[25,27] The U–O distances for the UO_2^{2+} cation of (TTF-salphen)UO_2(HOMe) (complex **3.1**) are 1.780(2) and 1.776(2) Å with an average of 1.778 Å (σ = 0.003 Å). These distances are consistent with those reported previously for many uranyl systems

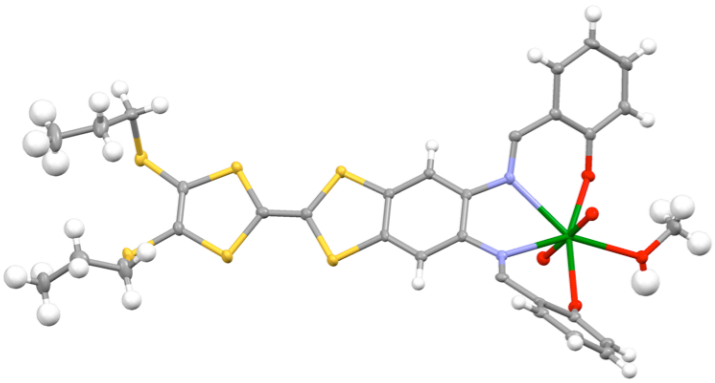

Figure 3.16 Top view of (TTF-salphen)UO_2(MeOH)•CH_2Cl_2 **3.1**. Solvent molecules (dichloromethane) have been omitted for clarity and the thermal ellipsoids are scaled to the 50% probability level.

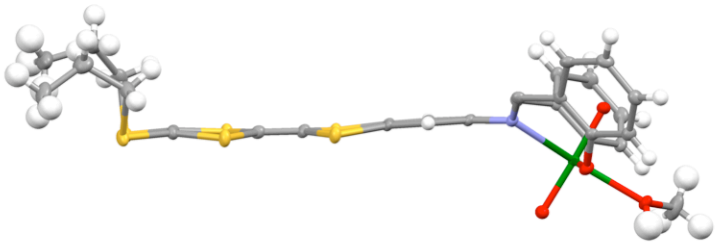

Figure 3.17 Side view of TTF-salphen(UO_2)MeOH•CH_2Cl_2 **3.1**. Solvent molecules of (dichloromethane) have been omitted for clarity and the thermal ellipsoids are scaled to the 50% probability level.

with uranyl distances and much shorter than the average U–O(salphen) 2.281 Å (σ = 0.056 Å) distance. The coordinating imine-to-uranyl U-N bond distances in (TTF-salphen)UO_2(HOMe) are 2.544(3) and 2.531(3) Å. Again, this is consistent with what has been seen in previous uranyl salophen complexes, *e.g.*, (salophen)UO_2(EtOH),[25] (salophen)UO_2(DMF),[27] and (salophen)UO_2(DMSO),[27] which have U-N distances of 2.54, 2.549(3), and 2.545(5) Å, respectively.

The extended structure of (TTF-salphen)UO_2(HOMe) (complex **3.1**) is unique in comparison to other uranyl salphen complexes. For example, previous solid state structures of uranyl salphen complexes that contain a solvent molecule occupying the fifth equatorial site are monomeric and void of any intermolecular interactions.[25,27] In contrast, uranyl salphen complexes without a solvent molecule in the fifth equatorial site often dimerize through μ:η^1:η^1 phenolic bridging interactions, as noted earlier in this chapter.[27] The present complex of (TTF-salphen)UO_2(HOMe) (**3.1**) contains a methanol molecule in the equatorial fifth ligand binding site. This coordinated methanol aids in the formation of an intermolecular dimer in the solid state structure via (HOMe)H•••O(TTF-salphen)$^{2-}$ hydrogen bonding interactions (Figure 3.18). These 2.615(3) Å hydrogen bonding distances are consistent with previously observed distances for (sp^3)C–O–H hydrogen bond donors to Ph-O-H hydrogen bond acceptors (2.84(1) Å).[31] The shorter distance in the case of (HOMe)H•••O(TTF-salphen)$^{2-}$ can be rationalized by the Lewis acidity of the coordinated uranyl, which renders the methanolic proton a stronger hydrogen bond donor.

An additional intermolecular interaction in the solid state was observed for (TTF-salphen)UO_2(HOMe) through the ligand units, which stack with eclipsed overlapping

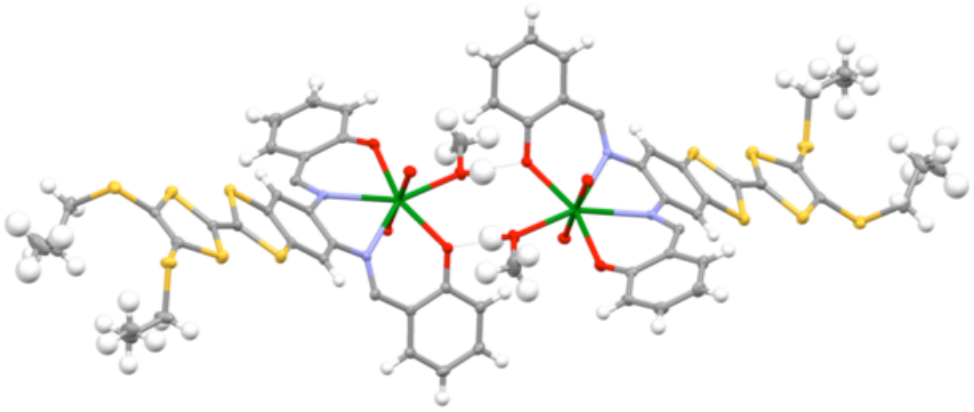

Figure 3.18 Hydrogen bonding dimer (TTF-salphen(UO_2)MeOH)$_2$•CH_2Cl_2 seen in the packing structure of **3.1**. Solvent molecules (dichloromethane) have been omitted for clarity and the thermal ellipsoids are scaled to the 50% probability level.

electron rich π-faces. The shortest distance observed between the ligand planes is 3.581(4) Å although there were no intermolecular short S•••S contacts between the TTF-units. This ligand-ligand "head-to-tail" arrangement, similar to that seen in previously reported in TTF-salphen 3*d*-4*f* heterobimetallic complexes,[21] leads us to suggest that an appreciable π•••π interaction exists between the two electron rich π-conjugated ring systems However, no evidence of this interaction was observed in the solution as inferred from an analysis of the ^{1}H and ^{13}C NMR spectrum recorded in d_5-pyridine at room temperature. Overall, the extended structure provides support for the notion that the methanol–phenoxide hydrogen bonding interactions work cooperatively with the ligand π•••π stacking interactions to arrange the (TTF-salphen)UO_2(HOMe) compounds into a tetrameric repeating unit.

The $(TTF\text{-}salphen)^{2-}$ unit in (TTF-salphen)UO_2(HOMe) does not adopt the "boat-like" conformation that is usually associated with most neutral TTF compounds. In fact, the observed planar TTF geometry is reminiscent of solid state structures associated with

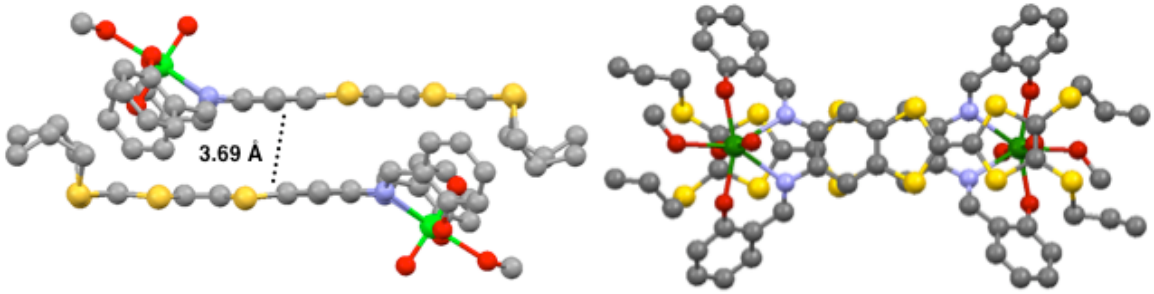

Figure 3.19 Ball and stick view of the π-π stacking dimer $[(TTFsalphen)UO_2(MeOH)]_2 \bullet CH_2Cl_2$ seen in the packing diagram associated with the X-ray structure of **3.1**. Solvent molecules (dichloromethane) and hydrogen atoms have been omitted for clarity.

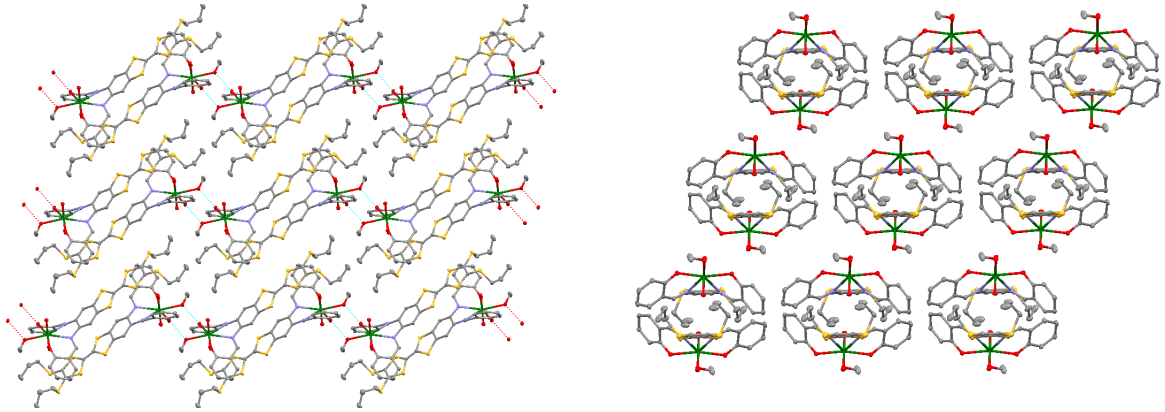

Figure 3.20 Views of the packing diagram for TTF-salphen$(UO_2)MeOH \bullet CH_2Cl_2$ **3.1** highlighting the formation of "head to tail" dimers between the TTF-salphen moieties and hydrogen bonding between the unidentate methanol ligand and the phenolic oxygen. Solvent molecules omitted for clarity.

one or more oxidized $TTF^{\bullet+}$ subunits. Despite the planarity of the TTF ligand in (TTF-salphen)UO_2(HOMe), the 1.341(5)Å C–C distance is consistent with a carbon double bond. Moreover, the observed diamagnetism of the complex leads us to suggest that the TTF-salphen ligand in (TTF-salphen)UO_2(HOMe) is best described as dianionic. On this basis, this compound was not carried forward for further tests of conductivity.

3.5.3 IR-Spectroscopy

IR-spectroscopic studies in a KBr matrix were also performed on compounds **3.1** and **3.13** (Figure 3.21). These studies were performed to characterize further the complex with the specific goal of a view to understanding the effect of the TTF-salphen ligand on uranyl stretching frequencies. When comparing the free ligand **3.13** with the uranyl complex **3.1** [(TTF-salphen)UO_2(HOEt)] there are two distinguishing differences (Figure 3.20). The first is a shift in the imine stretching frequency (ν_{C-N}) from 1610 cm^{-1} in the free ligand to 1601 cm^{-1} in the uranyl complex.

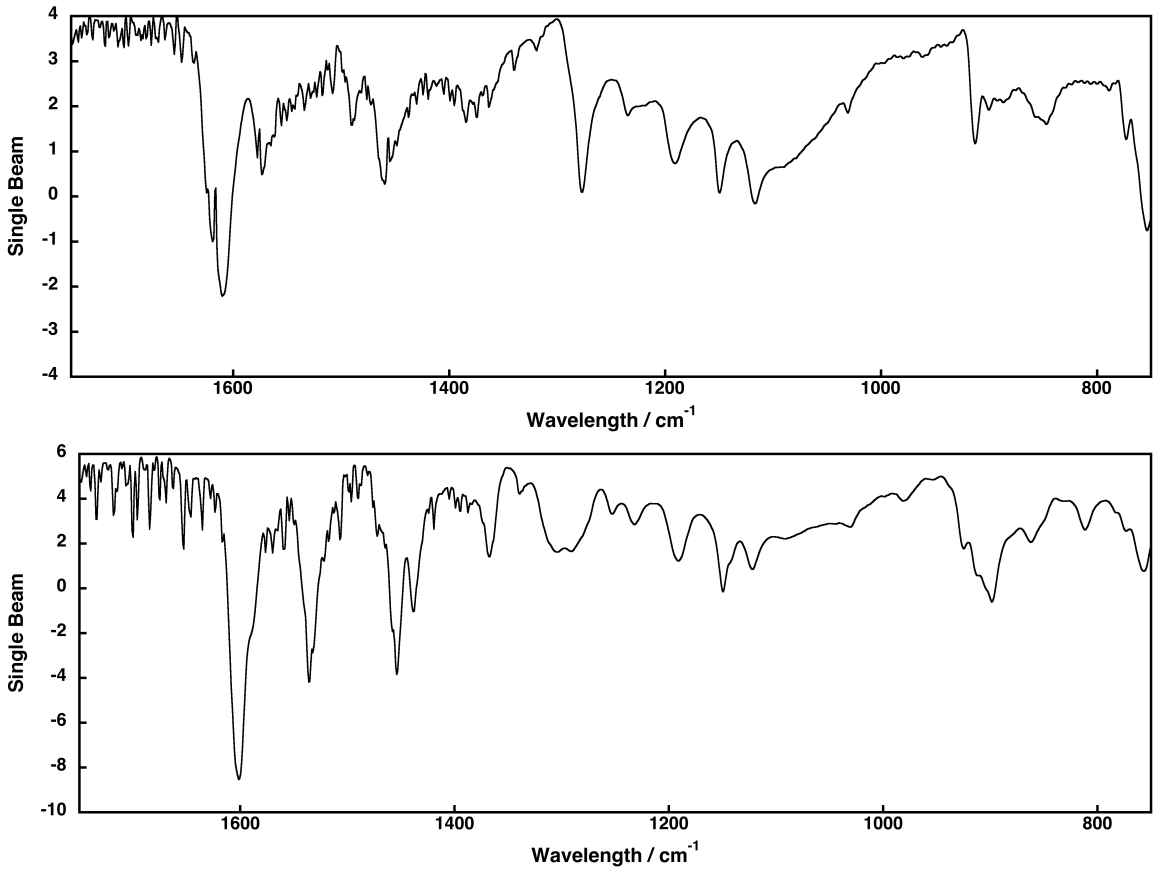

Figure 3.21 IR spectra of **3.13** (top) and **3.1** (bottom) as recorded in a KBr matrix.

Secondly, the IR spectrum of **3.1** has a feature at 899 cm^{-1} that is assigned to the asymmetric uranium-oxygen stretch ($\nu_{U\text{-}O}$). Such a feature is not present in the spectrum of the free ligand. These values are consistent with the IR spectra values reported by Ikeda[27] and coworkers for the parent (salophen)UO_2(DMSO) complex **3.24(DMSO)**, which has an imine stretching frequency ($\nu_{C\text{-}N}$) at 1605 cm^{-1} and an asymmetric uranium-oxygen stretch ($\nu_{U\text{-}O}$) at 897.

3.5.4 Electrochemical Studies

To characterize better the (TTF-salphen)UO_2(HOMe), electrochemical measurements were conducted using cyclic voltammetry (CV) with TBA·PF_6 (0.2 M) as the supporting electrolyte, and a glassy carbon and Pt as the working and counter electrodes, respectively. Potentials were measured against a Ag/AgCl reference electrode at 50 mV/s and referenced to a ferrocene/ferrocenium ion redox couple [$(C_5H_5)_2Fe/(C_5H_5)_2Fe^{1+}$] (Figure 3.22). The electrochemical measurements were carried out in a 10% DMSO / CH_2Cl_2 solvent mixture with the expectation – based on previous reports[27]– that DMSO would displace the methanol ligand. The anticipated DMSO adduct would ensure no hydrogen bonding interactions, as observed in the solid state structure of (TTF-salphen)UO_2(HOMe), and guard against dimer formation known to occur when uranyl salphen compounds are dissolved in non-coordinating solvents.[27b] The cyclic voltamagram of (TTF-salphen)UO_2(HOMe) (in 10% DMSO / CH_2Cl_2) was anticipated to be complicated given the presence of a TTF substituent, which can be oxidized twice, and a UO_2^{2+} cation that can be reduced by one electron. Figure 3.21 provides a comparison of the cyclic voltamagrams of (TTF-salphen)(HOMe), (salophen)UO_2(DMSO), a similar complex that lacks a redox active salphen ligand, and the free-ligand, (TTF-salphen)H_2. In the voltammogram of the free ligand, two reversible waves are observed with $E_{1/2}$ values of 120 mV and 500 mV, respectively. These features are attributed to quasireversible TTF/TTF^{1+} and TTF^{1+}/TTF^{2+} oxidations. The peak potential separations (E_p) for these oxidations are 115 mV and 124 mV. As expected, the spectrum of (salphen)UO_2(DMSO) contains a single quasi-reversible wave at -1540 mV attributable to the quasi-reversible UO_2^{2+}/UO_2^{1+} one electron reduction, and one uncoupled second oxidation peak at 1100 mV.

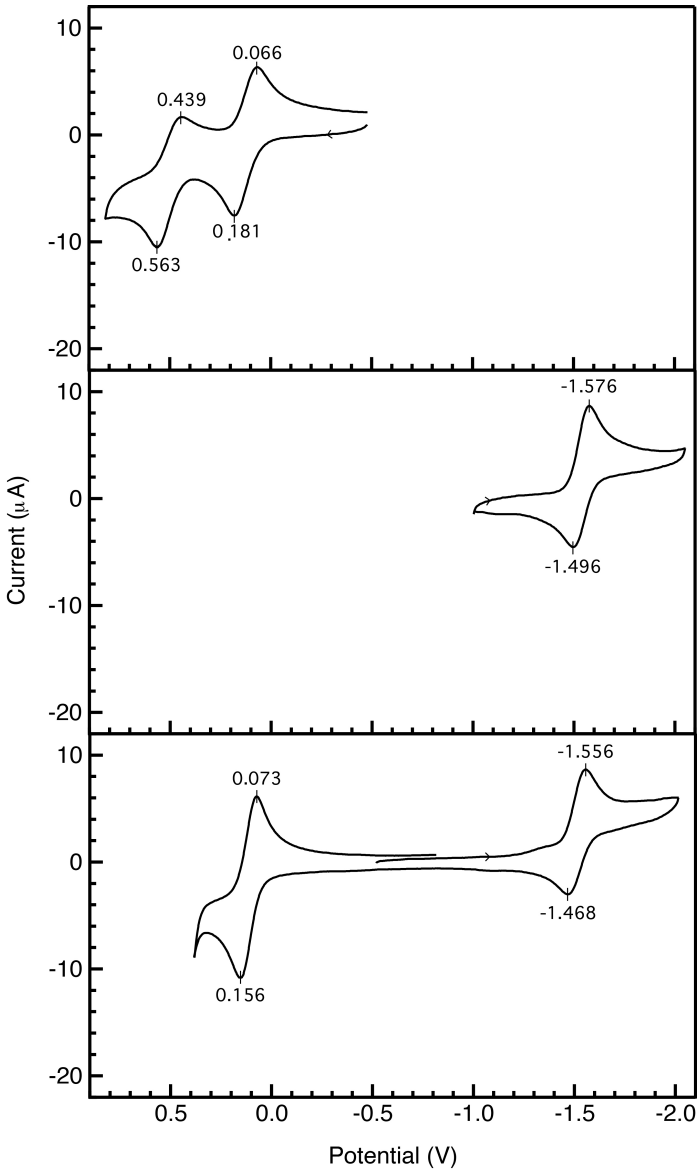

Figure 3.21 Cyclic voltamagram of (TTF-salphen)H_2 (*top*) in CH_2Cl_2, (salphen)UO_2(EtOH) in a mixture of DMSO (10%) / CH_2Cl_2 (*middle*), and (TTF-salphen)UO_2(HOMe) in a mixture of DMSO (10%) / CH_2Cl_2. The measurements were performed using a glassy carbon working electrode at a scan rate of 50 mV/s with TBA•PF_6 as the supporting electrolyte. Potentials are referenced to $(C_5H_5)_2Fe/(C_5H_5)_2Fe^{1+}$.

This is consistent with the mixed-solvent electrochemical data reported by Ikeda and co-workers, in which the electrochemical reduction of (salphen)UO_2^{2+}(DMSO) in a DMSO + CH_2Cl_2 mixture is accompanied by a dissociation of the coordinated DMSO from the [(salphen)UO_2^{1+}(DMSO)]$^-$ complex.[27a] In contrast, the new complex of this report spectrum of (TTF-salphen)UO_2(HOMe) is characterized by three redox processes. Two of these processes are observed upon scanning in the positive direction. Specifically, a quasi-reversible single-electron oxidation at 110 mV and a second single-electron oxidation process at 380 mV are observed. The similarity of these waves to that of the free ligand leads us to assign them, respectively, to a reversible oxidation of (TTF-salphen)$^{2-}$ moiety to the corresponding radical cation, and a second oxidation to the dication, which is irreversible under these conditions. The third redox process at 1510 mV is similar to that of (salphen)UO_2(DMSO) and best described as a quasi-reversible single-electron UO_2^{2+}/UO_2^{1+} reduction.

3.6 FUTURE DIRECTIONS

The successful formation of (TTF-salphen)UO_2(HOEt) has provided an initial entry point that may allow a merging of TTF chemistry with actinide science. In order to expand upon the results reported in this Chapter the substitution of the uranyl center for a later actinyl is the next logical step. While the salen^{2-} ligand platform has been reported to form complexes with NpO_2^{2+},[28] the more rigid salophen^{2-} has not been explored as a ligand for transactinide coordination.

The TTF-salphen^{2-} ligand discussed in this chapter could potentially be used to stabilize complexes containing transuranic actinyl cations (Figure 3.22). Having a series of actinyl species coordinated to the TTF-salphen^{2-} is desirable for several reasons.

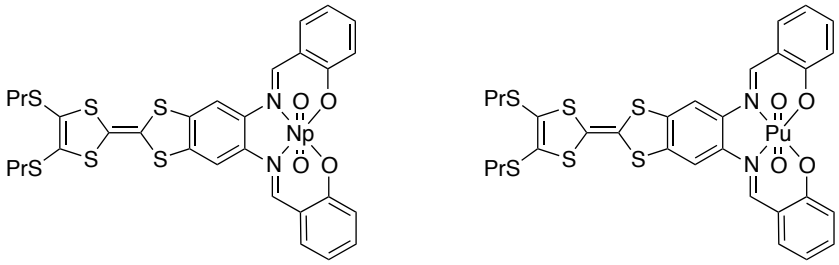

3.25 **3.26**

Figure 3.22 Proposed (TTF-salphen)NpO_2 **3.25** and (TTF-salphen)PuO_2 **3.26.**

Specifically, it would allow the redox properties of the TTF unit to be explored as a function of coordinated actinyl. Such a study, in turn, could provide further insights into the covalent nature of actinide-ligand bonding. In addition, since the uranyl cation has 0 5*f* electrons and is therefore diamagnetic, the coordination of a paramagnetic higher actinyls, such as NpO_2^{2+}, or PuO_2^{2+}, could allow for the development of TTF-actinide multifunctional materials.

Thus far, preliminary reactions of **2.23** and salicylaldehyde with $NpO_2(NO_3)_2$ in methanol were unsuccessful. It is suspected that the increased acidity of the neptunyl reaction vs. the uranyl reaction is causing hydrolosis of the imine bond or protonation of the TTF central double bond. Therefore, it is imperative to develop an acid free high-valent AnO_2^{2+} starting material.

Modification of the TTF-salphen ligand framework is also conceivable. For example, recent synthetic advances now allow preparation of symmetrical bis-phenylenediamine modified TTFs (**3.26**).[29] Decurtins and coworkers have condensed these electroactive tetraamines with diketo porphyrin precurors to synthesize novel symmetric porphyrin–tetrathiafulvalene–porphyrin triads where the TTF unit is fused to the porphyrins via quinoxaline linkers.[30] The synthesis of symmetric salphen–

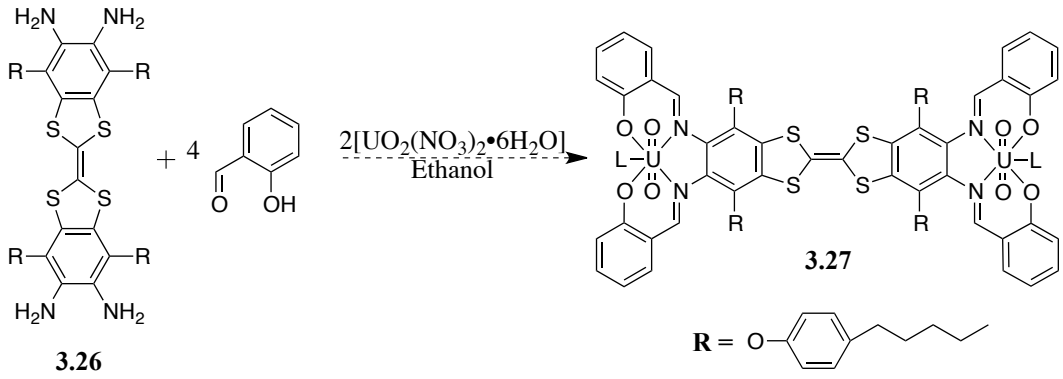

Figure 3.23 Proposed synthesis of ditopic TTF(salphen)$_2$(UO_2(L))$_2$ **3.27**.

tetrathiafulvalene–salphen triads would provide two tetradentate for actinyl coordination. Due to the fifth equatorial binding site located on the actinyl and ditopic nature of the proposed complexes, systems such as **3.27** could be used to form hybrid organic-inorganic coordination polymers upon choice of an appropriate bridging ligand.

References and Notes

1. (a) Lorcy, D.; Bellec, N.; Fourmigué, M.; Avarvari, N. *Coord. Chem. Rev.* **2009**, 1398. (b) Shatruk, M.; Ray, L. *Dalton. Trans.* **2010**, *39,* 11105.

2. (a) Zhou, B.; Idobata, Y.; Kobayashi, A.; Cui, H.; Kato, R.; Takagi, R.; Miyagawa, K.; Kanoda, K.; Kobayashi, H. *J. Am. Chem. Soc.* **2012**, *132*, 2385. (b) Zhang, B.; Zhang, Y.; Zhu, D. *Chem. Commun.* **2011**, *48*, 197. (c) Nishijo, J.; Judai, K.; Nishi, N. *Inorg. Chem.* **2011**, *50*, 3464. (d) Ouahab, L.; Enoki, T. *Eur. J. Inorg. Chem.* **2004**, 933. (e) Coronado, E.; Day, P. *Chem. Rev.* **2004**, *104*, 5419. (f) Coronado, E.; Galan-Mascaros, J. R.; Gomez-Garcia, C. J.; Laukhin, V. *Nature*, **2000**, *408*, 447.

3. (a) Imakubo, T.; Sawa, H.; Tajima, H.; Kato, R. *Synt. Met.* **1997**, 2047. (b) Dyachenko, O. A.; Kazheva, O. N.; Gritsenk, V. V.; Kushch, N. D. *Synt. Met.* **2001**, 1017. (c) Otsuka, T.; Cui, H.; Kobayashi, A.; Misaki, Y.; Kobayashiz, H. *J. Solid State Chem.* **2002**, *168*, 444. (d) Tamura, M.; Yamanaka, K.; Mori, Y.; Nishio, Y.; Kajita, K.; Mori, H.; Tanaka, S.; Yamaura, J. –I.; Imakubo, T.; Kato, R.; Misaki, Y.; Tanaka, K. *Synt Met.* **2001**, 442. (e) Pointillart, F.; Bourdolle, A.; Cauchy, T.; Maury, O.; Gal, Y. L.; Golhen, S.; Cador, O.; Ouahab, L. *Inorg. Chem.* **2011**, *51*, 978. (f) Pointillart, F.; Cauchy, T.; Maury, O.; Gal, Y. L.; Golhen, S.; Cador, O.; Ouahab, L. *Chem. Eur. J.* **2010**, *16*, 11926. (g) Pope, S. J. A.; Burton-Pye, B. P.; Berridge, R.; Khan, T.; Skabara, P. J.; Faulkner, S. *Dalton. Trans.* **2006**, 2907. (h) Faulkner, S.; Burton-Pye, B. P.; Khan, T.;Martin, L. R.; Wray, S. D.; Skabara, P. J. *Chem. Commun.* **2002**, 1668. (i) Pointillart, F.; Gal, Y. L.; Golhen, S.; Cador, O.; Ouahab, L. *Inorg. Chem.* **2009**, *48*, 4631. (j) Pointillart, F.; Klementieva, S.; Kuropatov, V.; Gal, Y. L.; Golhen, S.; Cador, O.; Cherkasov, V.; Ouahab, L. *Chem. Commun.* **2012**, *48*, 714. (k) Pointillart, F.; Maury, O.; Gal, Y. L.; Golhen, S.; Cador, O.; Ouahab, L. *Inorg. Chem.* **2009**, *48*, 7422. (l) Pointillart, F.; Gal, Y. L.; Golhen, S.; Cador, O.; Ouahab, L. *Chem. Eur. J.* **2011**, *17*, 10397.

4. C. E. Housecroft and A. G. Sharpe, Inorganic Chemistry, 3rd edition, 2008, Pearson Education Ltd., Gosport, UK.

5. For examples of actinides bound to redox-active ligands see: (a) Monreal, M. J. and Diaconescu, P. L. *J. Am. Chem. Soc.* **2010**, *132*, 7676. (b) Diaconescu, P. L., Arnold, P. L., Baker, T. A., Mindiola, D. J., and Cummins, C. C. *J. Am. Chem. Soc.* **2000**, 122, 6108. (c) Kraft, S. J., Fanwick, P. E., and Bart, S. C. *Inorg. Chem.* **2010**, *49*, 1103. (d) Schelter, E. J., Wu, R. L., Scott, B. L., Thompson, J. D., Cantat, T., John, K. D., Batista, E. R., Morris, D. E., and Kiplinger, J. L. *Inorg. Chem.* **2010**, *49*, 924. (e) Camp, C.; Mougel, V.; Horeglad, P.; Pécaut, J.; Mazzanti, M. *J. Am. Chem. Soc.* **2010**, *132*,17374

6. Rivera, N. M.; Engler, E. M.; Schumaker, R. R.; *J. Chem. Soc., Chem. Commun.* **1979**, 184.

7. (a) Gemmell, C.; Kilburn, J. D.; Ueck, H.; Underhill, A. E. *Tetrahedron Lett*., **1992**, *33*, 3923. (b) Gemmell, C.; Janairo, G. C.; Kilburn, J. D.; Ueck, H.; Underhill, A. E. *J. Chem. Soc., Perkin Trans. 1*, **1994**, 2715. (c) Becher, J.; Lau, J.; Leriche, P.; Mørk, P.; Svenstrup, N. *J. Chem. Soc., Chem. Commun*., **1994**, 2715. (d) Svenstrup, N.; Rasmussen, K. M.; Hansen, T. K.; Becher, J. *Synthesis*, **1994**, 809.

8. Tanaka, H.; Okano, Y.; Kobayashi, H.; Suzuki, W.; Kobayashi, A. *Science*, **2001**, *291*, 285.

9. (a) Isomura, E.; Tokuyama, K. I.; Nishinaga, T.; Iyoda, M. *Tetrahedron Lett*., **2007**, *48*, 5895. (b) Fourmigué, M.; Batail, P. *Bull. Soc. Chim. Fr*., **1992**, *129*, 29. (c) Yuan, M.; Ülgüt, B.; McGuire, M.; Takada, K.; DiSalvo, F. J.; Lee, S; Abruña, H. *Chem. Mater*., **2006**, *18*, 4296.

10. Jia, C.; Liu, S.-X.; Ambrus, C.; Neels, A.; Labat, G.; Decurtins, S. *Inorg. Chem*. **2006**, 45, 3152.

11. Green, D. C. *J. Chem. Soc., Chem. Commun*., **1977**, 161. (b) Ebihara, M.; Nomura, M.; Sakai, S.; Kawamura, T. *Inorg. Chim. Acta*, **2007**, *360*, 2345.

12. (a) Bellec, N.; Lorcy, D.; *Tetrahedron Lett*., **2001**, *42*, 3189. (b) Massue, J.; Bellec, N.; Chopin, S.; Levillain, E.; Roisnel, T.; Clérac, R.; Lorcy, D. *Inorg. Chem*., **2005**, *44*, 8740. (c) Bellec, N.; Massue, J.; Roisnel, T.; Lorcy, D. *Inorg. Chem. Commun*., **2007**, *10*, 1172.

13. (a) Jia, C.; Liu, S. X.; Tanner, C.; Leiggener, C.; Neels, A.; Sanguinet, L.; Levillain, E.; Leutwyler, S.; Hauser, A.; Decurtins, S. *Chem.–Eur. J*., **2007**, *13*, 3804. (b) Goze, C.; Leiggener, C.; Liu, S. X.; Sanguinet, L.; Levillain, E.; Hauser, A.; Decurtins, S. *ChemPhysChem*, **2007**, *8*, 1504. (c) Wu, J. C.; Liu, S. X.; Keene, T. D.; Neels, A.; Mereacre, V.; Powell, A. K.; Decurtins, S. *Inorg. Chem*., **2008**, *47*, 3452.

14. Ran, Y. F.; Bluma, C.; Liu, S-X.; Sanguinet, L.; Levillain, E.; Decurtins, S., *Tetrahedron*, **2011**, *67*,1623.

15. Bang, K. S.; Nielsen, M. B.; Zubarev, R.; Becher, J. *Chem. Commun*., **2000**, 215.

16. Bivaud, S.; Balandier, J-Y.; Chas, N.; Allain, M.; Goeb, S.; Sallé, M. *J. Am. Chem. Soc*., **2012**, *134*, 11968.

17. Ichikawa, S.; Mori, H. *Inorg. Chem*., **2009**, *48*, 4643.

18. Parker, D. *Coord. Chem. Rev*. **2000**, *205*, 109. (b) Parker, D. *Chem. Soc. Rev*. **2004**, *33*, 156. (c) Eliseeva, S.V.; Bünzli, J.-C. G. *Coord. Chem. Rev*. **2010**, *39*, 189.

19. Bencini, A.; Benelli, C.; Caneschi, A.; Carlin, R. L.; Dei, A.; Gatteschi, D. *J. Amer. Chem. Soc*. **1985**, *107*, 8128

20. Andruh, M.; Costes, J.-P.; Diaz, C.; Gao, S. *Inorg. Chem.*, **2009**, *48*, 3342.

21. (a) Cosquer, G.; Pointillart, F.; Gal, Y.-L.; Golhen, S.; Cador, O.; Ouahab, L.; *Chem. Eur. J.* **2011**, *17*, 12502. (b) Cosquer, G.; Pointillart, F.; Guennic, B. L.; Gal, Y. L.; Golhen, S.; Cador, O.; Ouahab, L. *Inorg. Chem.* **2012**, *51*, 8488.

22. There are numerous reports where actinides show evidence of covalent bonding: (a) Diamond, R. M.; Street, K.; Seaborg, G. T. *J. Am. Chem. Soc.* **1954**, *76*, 1461. (b) Tatsumi, K.; Nakamura, A.; Hofmann, P.; Stauffert, P.; Hoffmann, R. *J. Am. Chem. Soc.* **1985**, *107*, 4440. (c) Pepper, M.; Bursten, B. E. *Chem. Rev.* **1991**, *91*, 719. (d) Kuchle, W.; Dolg, M.; Stoll, H.; Preuss, H. *J. Chem. Phys.* **1994**, *100*, 7535. (e) Gagliardi, L.; Willetts, A.; Skylaris, C. K.; Handy, N. C.; Spencer, S.; Ioannou, A. G.; Simper, A. M. *J. Am. Chem. Soc.* **1998**, *120*,11727. (f) Barros, N.; Maynau, D.; Maron, L.; Eisenstein, O.; Zi, G.; Andersen, R. A. *Organometallics* **2007**, *26*, 5059. (g) Tassell, M. J.; Kaltsoyannis, N. *Dalton Trans.* **2010**, *39*, 6719. (h) Kirker, I.; Kaltsoyannis, N. *Dalton Trans.* **2011**, 40, 124.

23. (a) Clark, D. L. *The Chemical Complexities of Plutonium*, Los Alamos Science, **2000**, *26*, 364. (b) Denning, R. G. *J. Phys. Chem. A.* **2007**, *111*, 4125. (c) Denning, R. G.; Green, J. C.; Hutchings, T. E.; Dallera, C.; Tagliaferri, A.; Giarda, K.; Brookes, N. B.; Braicovich, L. *J. Chem. Phys.,* **2002**, *117*, 8008. (d) Clark, D. L.; Hobart, D. E.; Neu, M. P.; *Chem. Rev.* **1995**, *95*, 25.

24. Sessler, J. L.; Melfi, P. J.; Dan Pantos, G. *Coord. Chem. Rev.*, **2006**, *250*, 816.

25. Bandoli, G.; Clemente, D. A.; Croatto, U.; Vidali, M.; Vigato, P. A.; *Chem. Commun.* **1971**, 1330.

26. (a) Wroblewski, W.; Wojciechowski, K.; Dybko, A.; Brzozka, Z.; Egberink, R J. M.; Snellink-Rüel, B. H. M.; Reinhoudt, D. N. *Sens. Actuators B*, **2001**, *78*, 315. (b) Wroblewski, W.; Wojciechowski, K.; Dybko, A.; Brzozka, Z.; Egberink, R J. M.; Snellink-Rüel, B. H. M.; Reinhoudt, D. N. *Anal. Chim. Acta*, **2001**, *432*, 79. (c) Ion, A. C.; Antonisse, M. M. G.; Snellink-Rüel, B. H. M.; Reinhoudt, D. N. *Russ. J. Gen. Chem.*, **2001**, *71*, 159.

27. (a) Takao, K.; Ikeda, Y. *Inorg. Chem.* **2007**, *46*, 1550. (b)Mizuoka, K.; Kim, S-Y.; Hasegawa, M.; Hoshi, T.; Uchiyama, G.; Ikeda, Y. *Inorg. Chem.* **2003**, *42*, 1030.

28. Chuguryan, D. G.; Dzyubenko, V. I.; Grigoriev, M. S.; Yanovskii, A. I.; Struchkov, Y. T. *Radiokhimiya*, **1988**, *30*, 41.

29. Jia, H-P.; Ding, J.; Ran, Y. F.; Liu, S. X.; Blum, C. Petkova, I.; Hauser, A.; Decurtins, S. *Chem. Asian J.* **2011**, *6*, 33121.

30. Jia, H.; Schmid, B.; Liu, S-X.; Jaggi, M.; Monbaron, P.; Bhosale, S. V.; Rivadehi, S.; Langford, S. J.; Sanguinet, L.; Levillain, E.; El-Kouly, M. E.; Morita, Y.; Fukuzumi, S.; Decurtins, S. *Chem. Phys. Chem.* **2012**, *13*, 3370.

Chapter 4: Tetrathiafulvalene diindolylquinoxaline: a dual signaling anion receptor with phosphate selectivity

4.1 INTRODUCTION

Tetrahedral oxyanion recognition and sensing is of current interest due to the diverse roles that such anions play in biological systems and in the environment.[1] Within this general framework, the ability to monitor the phosphate anion is of particular importance due *inter alia* to the ubiquitous use of phosphates as fertilizers and the role such species can play in the eutrophication of waterways.[2] This is providing an incentive to develop receptors that can selectively bind and sense phosphate. To date a variety of receptor systems, running the gamut from metal complexes to small molecules employing hydrogen bonding, have been put forward for this purpose.[3] While a number of these have proven effective under appropriately chosen conditions, there remains a critical need for systems that display high selectivity and which function with high reliability. The use of so-called dual signaling systems, which allow phosphate anion detection via more than one read-out mode, thereby lowering the likelihood of false positives, could help address this need. Systems that permit phosphate anion detection via both optical and electrochemical means are rare.[4] This Chapter describes the preparation and spectroscopic characterization of a new TTF-modified diindolylquinoxaline (TTF-DIQ) **4.1**. In contrast to previously reported DIQ systems, this new receptor allows for the detection of dihydrogen phosphate anions in dichloromethane using a dual optical/electrochemical readout approach.

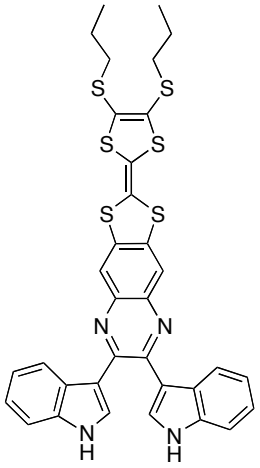

4.1

Figure 4.1 Tetrathiafulvalene-fused diindolylquinoxaline (TTF-DIQ) **4.1**.

As detailed below, the anion binding ability and selectivity of **4.1** has been examined using various techniques including UV-Vis, fluorescence, and ^{1}H-NMR spectroscopies. Additionally, perturbations in the electrochemical features of **4.1** are seen upon anion binding, as monitored via cyclic voltammetry. Structurally, the free receptor and dihydrogen phosphate complex were characterized in the solid state by means of single X-ray crystallographic analyses. TTF-DIQ **4.1** behaves as a 1:1 receptor for the dihydrogen phosphate anion, giving unique electrochemical and fluorescent readouts in the presence of dihydrogen phosphate.

4.2 SMALL MOLECULE PHOSPHATE RECEPTORS

The phosphate anion is an important constituent of energy processes that occur in biological systems as well as a major environmental pollutant that demands careful monitoring.[1,2] Inorganic-based detection methods and enzymatic recognition protocols can give rise to toxic heavy metal waste or require access to specialized equipment. There is thus incentive to design synthetic phosphate receptors, small molecule systems that provide improved methodologies for the detection, extraction, and transport of biologically and environmentally important phosphates.[5] Despite the extensive library of reported synthetic phosphate receptors, the area of phosphate recognition continues to present a challenge to the supramolecular chemistry community due to the relatively large size of the phosphate anion, as well as its inherent high hydrophilicity[6] and complex acid/base properties.[1b] In order to confront this challenge, synthetic receptors employing hydrogen bonding units, electrostatic interactions, van der Waals forces, π-surface interactions, shape complementarity, and metal coordination have been employed alone or in concert.[7] Such receptors have given rise to various detection methods that operate colorimetrically, optically, electrochemically, calorimetrically, and via nuclear magnetic resonance.

A full review of small molecule phosphate recognition is beyond the scope of this dissertation. However, a brief survey of small molecules designed to detect phosphate electrochemically, including efforts towards anion detection through the use of tetrathiafulvalene-based receptors, is appropriate and is provided below.

4.2.1 Electrochemical Phosphate Recognition Using Metal Cations

Small molecule systems that are capable of signaling the presence of phosphate anions typically rely on perturbations of oxidation potentials as monitored via cyclic

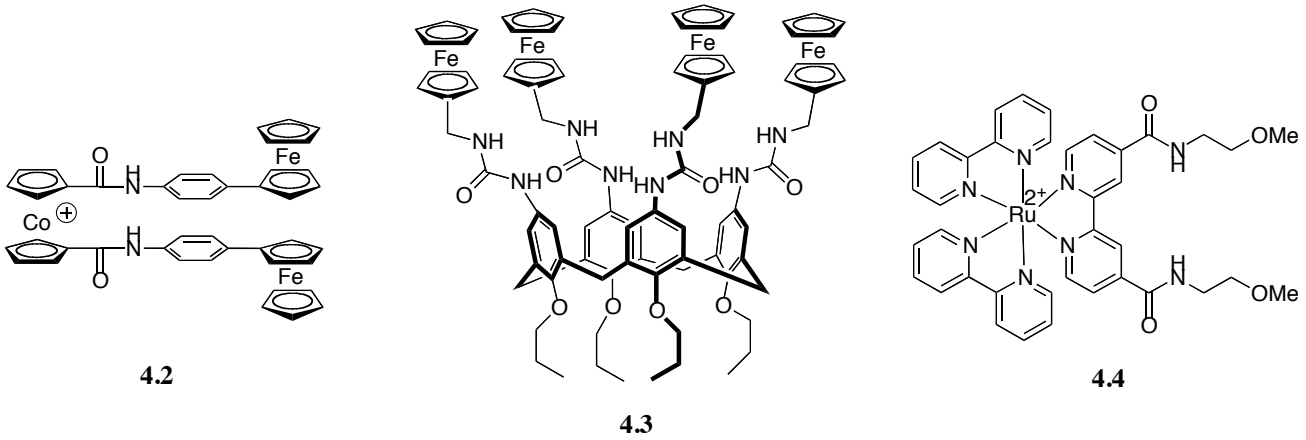

4.2 **4.3** **4.4**

Figure 4.2 Metallocene appended dihydrogen phosphate receptors **4.2** & **4.3** and amide functionalized $[Ru(bpy)_3]^{2+}$ **4.4**.

voltammetry. Often, the receptor itself is not redox active and therefore relies on a reporter group, such as cobaltocenium, ruthenium(II), or ferrocenyl, which are tethered to the binding site and give rise to the monitored electrochemical changes. (Figure 4.2).[8] One early example, reported in 1993 by Beer and co-workers, consisted of ferrocene and cobaltacene-appended amide-based receptors, such as **4.2**, which proved capable of effecting the electrochemical based detection of dihydrogen phosphate via cyclic-voltammetry.[9] Later, more advanced systems were reported in which metallocene-based units were appended to known phosphate recognition units, such as calixarenes, as seen in system **4.3**.[10] In an effort to increase the reliability of the signaling unit, Beer *et al*. introduced the dual luminescent/electrochemical reported group $[Ru(bpy)_3]^{2+}$ into various amide functionalized phosphate receptors. Compound **4.4** is an example of a dual mode phosphate receptor, displaying an electrochemical response as well as emission band shifts, a finding attributed to the increased structural rigidity of the bound anion complex vs the free receptor.[11]

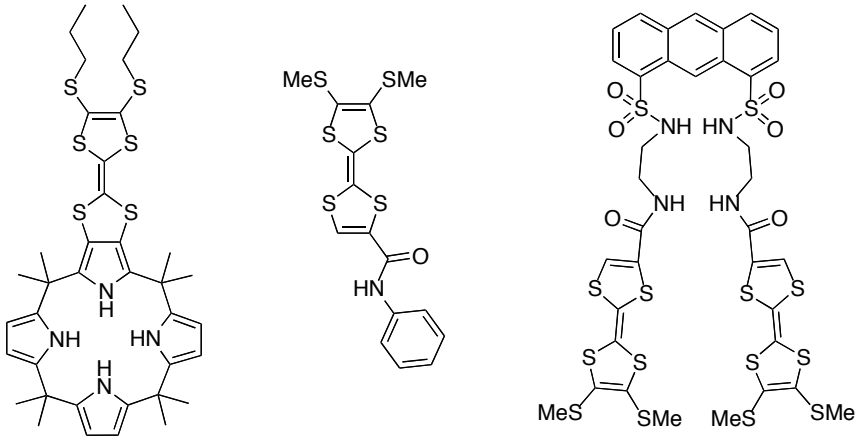

4.5 **4.6** **4.7**

Figure 4.3 Tetrathiafulvalene-based electrochemical anion receptors.

4.2.2 Tetrathiafulvalene Anion receptors

Tetrathiafulvalene (TTF) **1**, a classic organic redox active unit, has been exploited extensively in recent years as a supramolecular signaling and switching unit. However, it is still relatively unexplored as an electrochemical sensor element in the field of anion recognition. A seminal report by Becher *et al*. described a mono-TTF-calix[4]pyrrole **4.5** that proved capable of recognizing halide anions, as opposed to phosphate, electrochemically via shifts in the first oxidation potential.[12] Later, Zhu *et al*. developed the amide-based TTF phosphate sensor **4.6** and the dual signaling sensor **4.7**.[13] However, these latter receptors, although elegant and effective, did not function as selective dual signaling systems, giving rise to optical selectivity for fluoride but electrochemical selectivity for phosphate.

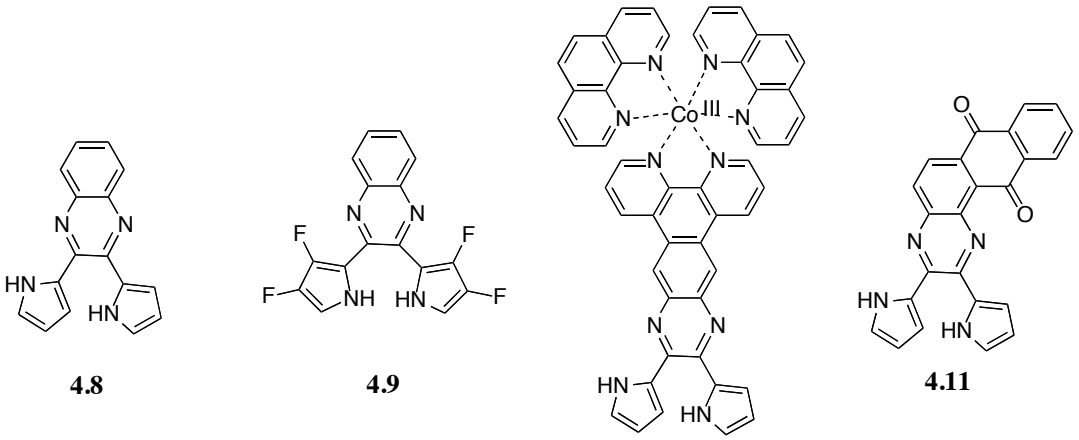

Figure 4.4 DPQ **4.8** and examples of DPQ derivatives **4.9**-**4.11**.

4.3 QUINOXALINE-BASED ANION RECEPTORS

In 1999 the Sessler group reported the use of 2,3-dipyrrol-2‘-ylquinoxaline (DPQ) **4.8** as a colorimetric anion sensor with fluoride selectivity that functioned in dichloromethane and DMSO.[14] While **4.8** was known in the literature since 1911, it had never been considered as being a possible colorimetric anion sensor.[15] Due to the pyrrrolic NH groups, built in quinoxaline ring, and synthetic ease of preparation, DPQ represented a new class of cheap and effective anion receptors that gave naked eye fluoride detection as well as providing fluorescent emission signaling.

Following the initial report of the parent DPQ, **4.8**, several attempts to augment its efficacy were described in the literature. These include, efforts to increase the binding affinity by appending electron withdrawing fluoro-groups to the beta-positions of the pyrrole rings (**4.9**),[16] advanced analogs with fused phenanthroline and related Co(II) complexes (**4.10**),[17] and quinone fused systems (**4.11**) by Anzenbacher and co-workers.[18]

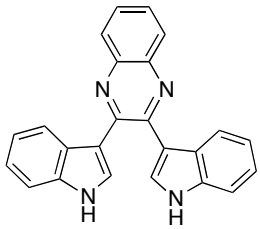

4.12

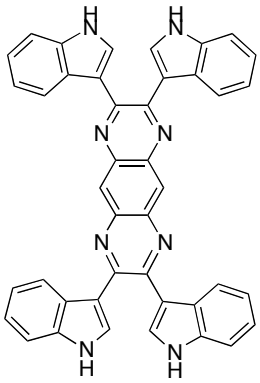

4.13

Figure 4.5 Dihydrogen phosphate receptor DIQ **4.2** and ditopic DIQ **4.13**.

Furthermore, Anzenbacher *et al*. also reported conjugated DPQ-polythiophene polymers that show reversible anion-specific changes that could be monitored both colorimetrically and through changes in conductivity.[19]

In 2006, Sessler and co-workers substituted the α–connected pyrrole units in DPQ with indole moieties connected through the 3 positions to give the 2,3-diindol-3'yl quinoxaline (DIQ) **4.12**.[20] The result of this alteration was an effective larger binding site leading to a change in anion binding selectivity, with dihydrogen phosphate showing the highest association constant with the new receptor. System **4.12** also represents one of the few neutral receptor systems bound to dihydrogen phosphate that has been characterized by X-ray crystallography. In the solid state it contains a self-associated network of dihydrogen phosphate anions surrounded by bound DIQ molecules. Wang and Yan further elaborated DIQ in a ditopic fashion (**4.13**). They used their system to explore the possibility of creating anion-directed metal free coordination polymers based on an infinite arrangements of receptors and phosphate networks.[21]

4.4 Design and Strategy

In the following sections, the synthesis of a tetrathiafulvalene-fused diindolylquinoxaline **4.1** will be described. The covalent introduction of a TTF moiety into the molecular framework of known dihydrogen phosphate selective anion receptor **4.12** demonstrates how a longstanding recognition unit can be elaborated into an electrochemical sensor. Prior to this work, the diindolylquinoxaline was known only as a selective recognition system for dihydrogen phosphate. Addition of a TTF unit, conjugated through the aromatic quinoxaline backbone, would, it was thought, allow for anion binding events taking place at the indolic N-H sites to be electronically communicated to TTF system. This communication would alter the electron density of the redox units and conceivably change the potentials at which the molecule is oxidized. A goal was to test this hypothesis. Towards this end, it was also deemed important to determine whether the inherent anion recognition strength and selectivity of the binding site mirrored that of DIQ and that the presumably altered electronics of receptor **4.1** do not have a serious effect on these characteristics.

4.5 Synthesis and Characterization

Receptor **4.1** requires a very short synthesis as illustrated in Scheme 4.1. TTF-diamine **2.24** and the diketone **4.14** were dissolved in a 1:1 solution of ethanol/acetic acid and heated at reflux overnight. The resulting solution was concentrated *in vacuo* and subject to column chromatography over silica gel to give **4.1** as a purple solid in 22% yield. Conveniently, these conditions are identical to those required for the synthesis of the parent DIQ **4.12**. In fact, one only needs to replace *o*-phenylenediamine by TTF-phenylenediamine **2.24**. A high-resolution ESI mass spectrum showed an exact mass at m/z 685.07110, a value that corresponds to the expected M^+ (calcd mass ($C_{34}H_{29}N_4S_6$)

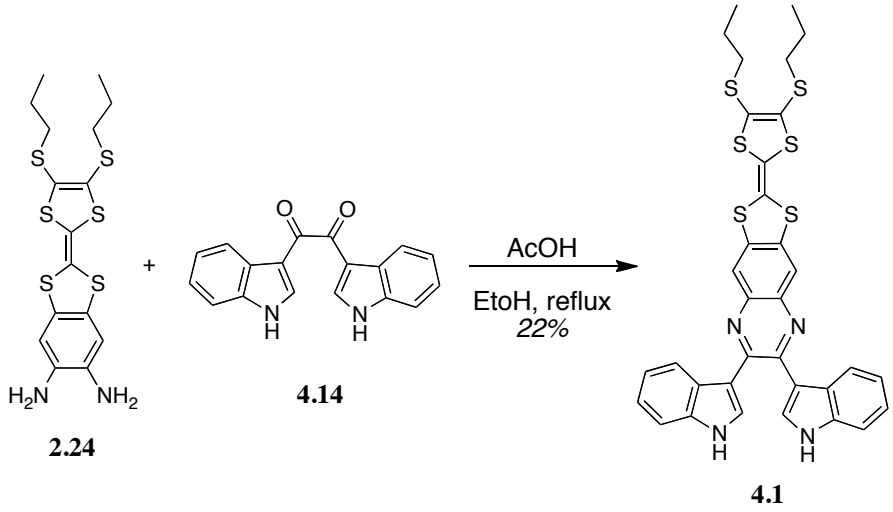

2.24 **4.14** **4.1**

Scheme 1 Preparation of TTF-DIQ **4.1**.

M^+685.07216). Further evidence for the proposed structure came from the ^1H and ^{13}C NMR (400 mHz) spectra, recorded in CD_2Cl_2 at 298 K.

4.5.1 X-ray Crystal Structure

Single crystals of **4.1** grew as red needles from an NMR tube of **4.1** in CD_2Cl_2 layered with ethanol. The resulting structure shows a nearly planar aromatic backbone and two indole units that are forced into a perpendicular conformation, presumably due to the steric repulsion arising from the nature of the connection between the two indoles and the quinoxaline (Figure 4.6). Unfortunately, the structure has high disorder around the quinoxaline ring. Repeated attempts to regrow better crystals of publication quality were unsuccessful.

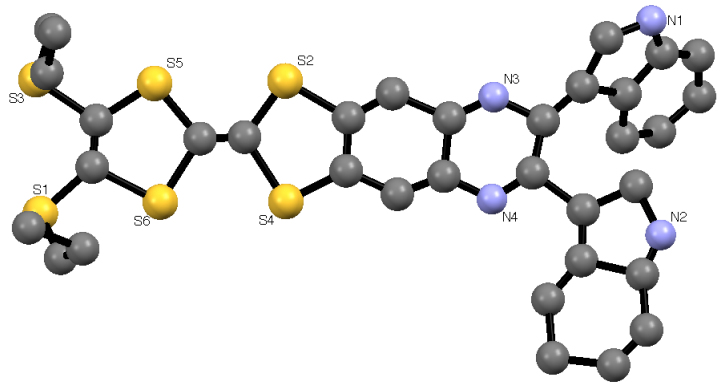

Figure 4.6 X-ray structure of **4.1**. Hydrogen atoms are omitted for clarity. Sulfur atoms are shown in yellow, nitrogen atoms in blue, and carbon in gray.

The packing structure of **4.1** shows a head-to-head π-π arrangement of the TTF-DIQ units with the shortest contact of 3.30 Å between the planes (Figure 4.7). There are no solvent molecules in the lattice of **4.1**, at least at the level of preliminary refinement.

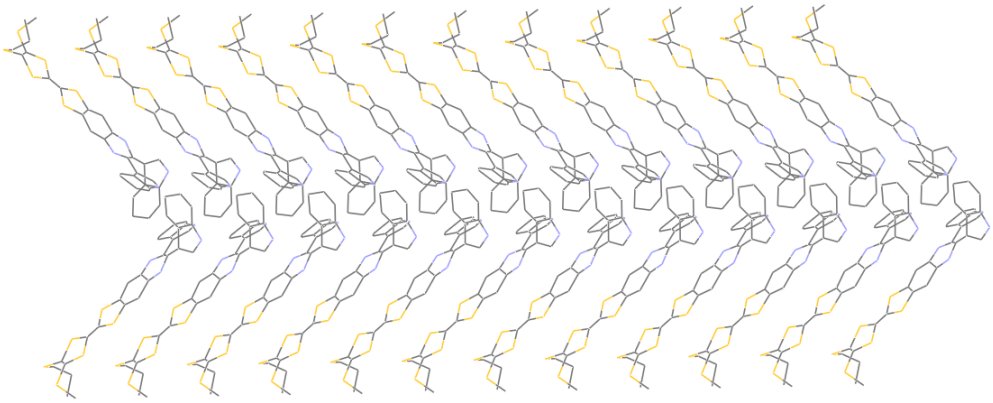

Figure 4.7 Packing structure of **4.1**. Hydrogen atoms have been omitted for clarity.

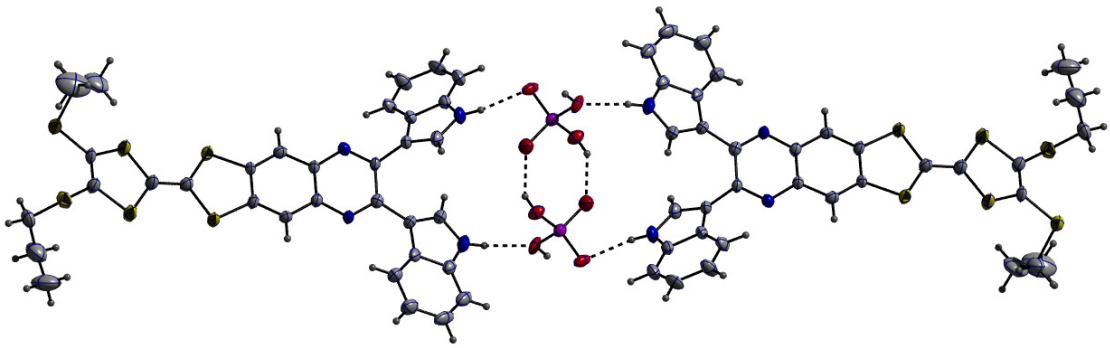

Figure 4.8 Single crystal X-ray structure of **4.1**·TBA·H_2PO_4. Top: view of the 2:2 complex formed between the receptor and the bound anion. The TBA counter cations have been omitted for clarity and the thermal ellipsoids are scaled to 30% probability level.

Based on the phosphate containing aggregate present in the solid-state structures of related *bis*-indole receptors bound to dihydrogen phosphate,[22] attempts were made to grow crystals of the bound anion to the neutral host **4.1**. The structure of the complex formed from receptor **4.1** and TBA·H_2PO_4, determined by X-ray diffraction analysis, is shown in Figure 4.8. It reveals a self-associated network wherein two molecules of receptor **4.1** interact with two dihydrogen phosphate anions. This self-association behavior, in which interactions between the individual dihydrogen phosphate anions are seen, is similar to what was observed in the case of the ditopic system **4.13** recently reported by Yan,[21] as well as previous studies in which the phosphate anion serves as both a hydrogen-bond donor and acceptor in a cooperative manner.[22]

The expanded packing diagram of receptor **4.1** and TBA·H_2PO_4 shows an extended network of alternating TTF-DIQ units flanking what can be considered as infinite self-assembled phosphate chains (Figure 4.9 left). The nature of the arrangement is similar to the infinite phosphate chain that exists in the complex of dinitro-substituted

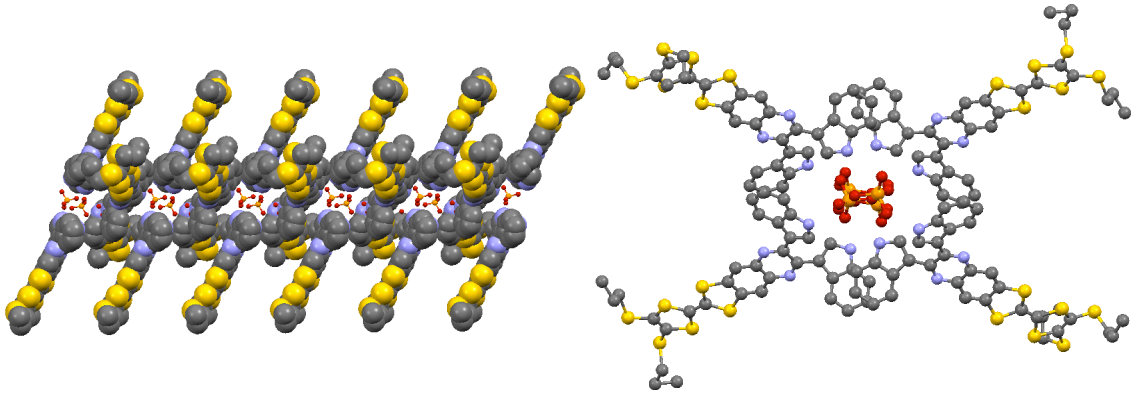

Figure 4.9 Left: Expanded structure of **4.1**·TBA·H_2PO_4. Right: View of packing structure looking down the infinite chain of dihydrogen phosphate.

DIQ **4.12** and TBA·H_2PO_4. From the side view of the expanded structure it is possible to see that two receptors line up across from one another (Figure 4.9 left). Both are hydrogen bonding with two molecules of dihydrogen phosphate. The next two dihydrogen phosphate anions in the chain then hydrogen bond with two more molecules of **4.1** that are rotated 90 degrees with respect to the previous TTF-DIQ entities. This perpendicular ordering between the pairs of TTF-DIQ units is more easily seen when viewing the network down the infinite self-assembled chain of dihydrogen phosphate (Figure 4.9 right).

4.5.2 UV-VIS BINDING STUDIES

In order to compare the binding affinity of the new TTF-DIQ with the parent unfunctionalized DIQ receptor (**4.12**), association constants (K_a) of receptor **4.1** with various anions were determined via UV-vis titrations carried out in dichloromethane using the corresponding tetrabutylammonium (TBA) salts. Equilibrium constants were calculated using the standard 1:1 binding equation for optical titrations originally taken

X^-	K_a [M^{-1}] [a]
F^-	3.6×10^3
$H_2PO_4^-$	6.5×10^3
BzO^-	9.5×10^2
HSO_4^-	3.7×10^2
Cl^-	1.1×10^3

Table 4.1 Anion binding constants determined by UV-Vis spectroscopic. [a] Errors < ±10%. All anions used in the form of their respective tetrabutylammonium (TBA) salts.

from Connors,[23] with the equation being fit using Origin version 7.5. As expected given the analogous nature of the binding site present in these two DIQ-based systems, the new TTF-functionalized system (**4.1**) was found to display good selectivity and affinity for $H_2PO_4^-$ ($K_a = 6.5 \times 103\ M^{-1}$; $K_{a(H2PO4-)}/\ K_{a(F-)} = 1.8$; cf. Table 4.1). In fact, the recorded K_a values for all anions tested proved similar for **4.1** and **4.12**, with the exception of chloride, which was found to bind more strongly to **4.1** than **4.12** by roughly an order of magnitude. Nevertheless, this latter species was bound less well than $H_2PO_4^-$ (for **4.1**: $K_{a(H2PO4-)}/\ K_{a(Cl-)} = 5.9$). It is worth noting that the affinity of receptor **4.1** for dihydrogen phosphate is the highest reported so far for a TTF-functionalized anion receptor.[13] It is also the only TTF-based system to display phosphate anion selectivity under solution phase conditions. Although system **4.1** functions in dichloromethane, a recent report from the Anzenbacher group has served to reveal that receptors that function in organic media can be useful in sensing anions under aqueous conditions.[24]

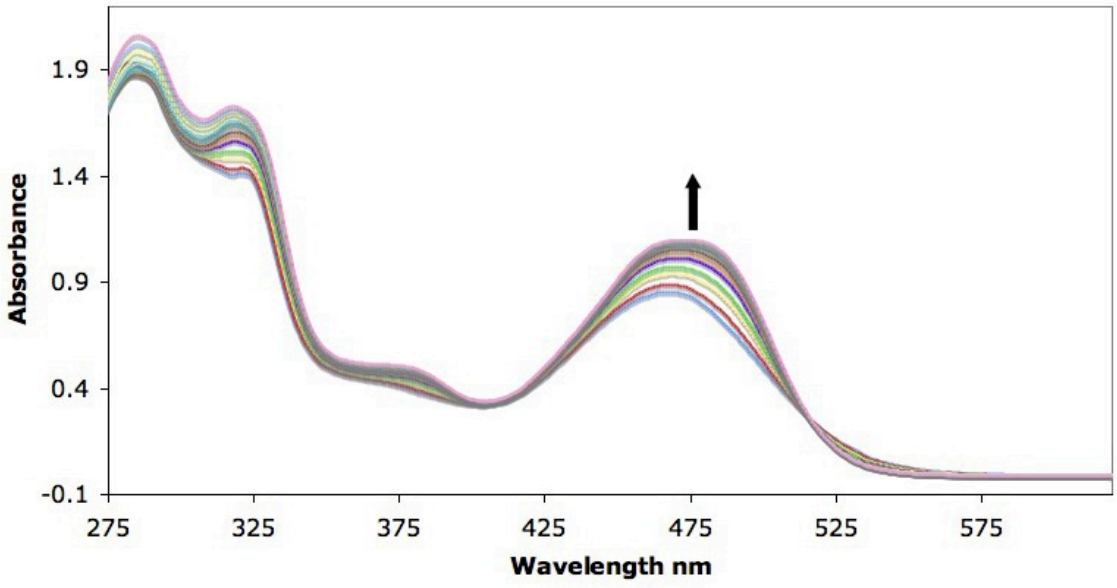

Figure 4.10 Typical UV-vis spectral changes observed during the $H_2PO_4^-$ binding titrations of **4.1** (50 μM) in CH_2Cl_2 at 296 K. [$H_2PO_4^-$] = 0.0 - 3 mM.

1-TBAH_2PO_4

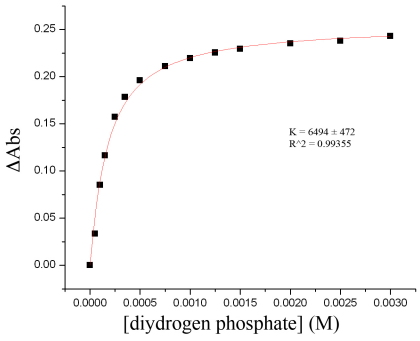

1-TBAOBz

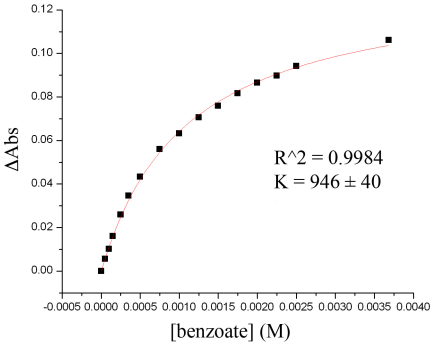

1-TBACl

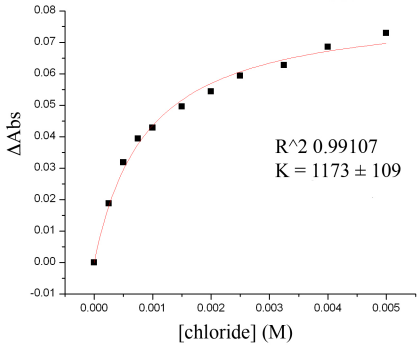

1- $TBAHSO_4$

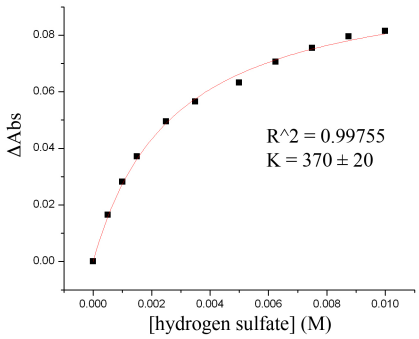

1-TBAF

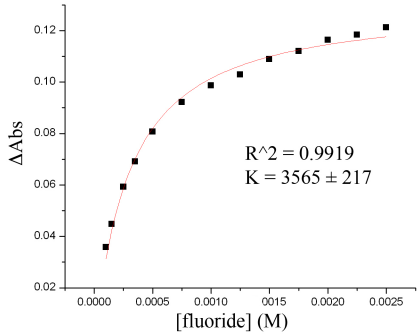

Figure 4.11 Anion binding isotherms for **4.1** (50 μM) titrated with various anions (TBA^+-X^-) in CH_2Cl_2.

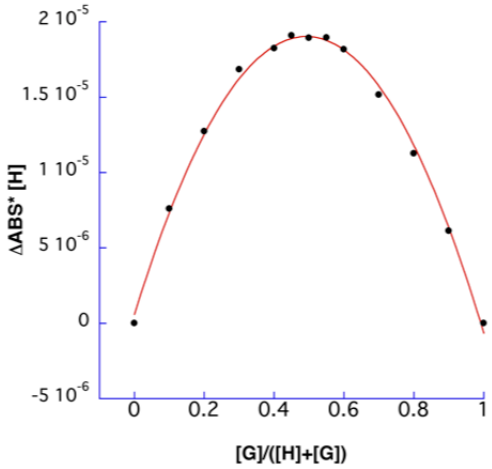

Figure 4.12 Job plot for the interaction of **4.1** and TBA•H_2PO_4. This plot shows changes expected for a 1:1 complexation stoichiometry.

Support for the proposed 1:1 dihydrogen phosphate binding stoichiometry came from curve fittings and the use of so-called Job plots.[23] A stock solution of the host was prepared as described for the K_a determination experiments. The guest stock solution was prepared by dissolving 1-2 equivalents of the TBA salts of the anions in question in the same solvent (dichloromethane) as the one used for the host stock solution.

4.5.3 FLUORESCENCE PROPERTIES OF TTF-DIQ

A attractive feature of receptor **4.1** is its expected ability to sense anions via fluorescence quenching of the quinoxaline emission. This postulate was tested in dichloromethane using various TBA salts. As shown in Figure 4.13, quenching is observed in the presence of $H_2PO_4^-$, with the effect increasing as a function of dihydrogen phosphate anion concentration. Under the same conditions, only a slight quenching is observed upon addition of F^-, and no noticeable decrease in intensity is seen in the

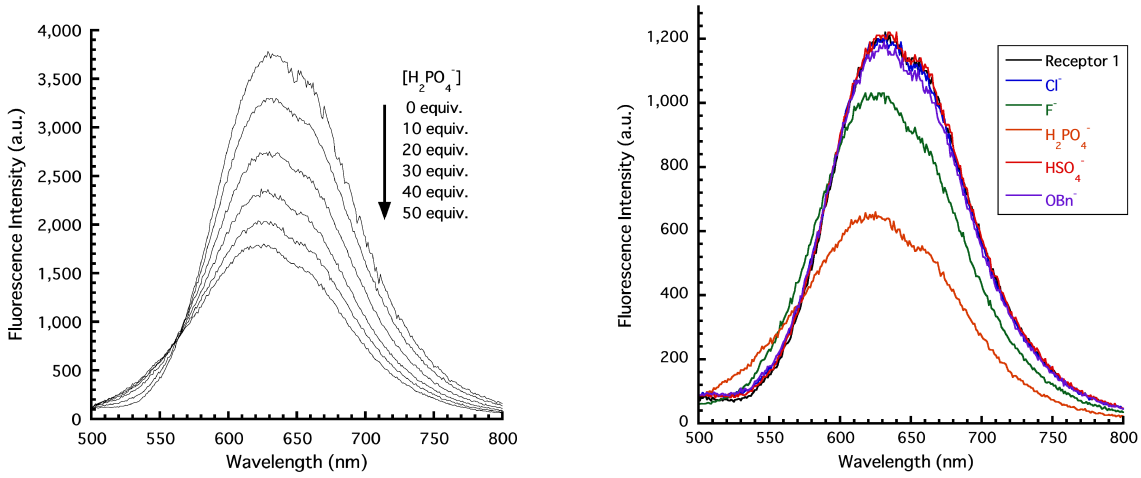

Figure 4.13 Left: Fluorescent emission spectra of **4.1** (2.0 × 10–6 M) recorded in dichloromethane (λ_{ex} = 468 nm) before and after the addition of up to 50 equiv. of TBA· H_2PO_4. Right: Fluorescent emission spectra of receptor **4.1** (1.5×10^{-6} M) recorded upon the addition of 50 equiv. of various tetrabutylammonium anion salts in dichloromethane (λ_{ex} = 468 nm).

presence of 50 equiv of Cl^-, BzO^-, or HSO_4^- (Figure 4.13). In contrast, a significant decrease is observed in the presence of $H_2PO_4^-$.

4.6.4 Electrochemical Anion Recognition Experiments

The TTF-DIQ, receptor **4.1**, was designed with the goal of detecting anions, specifically dihydrogen phosphate, electrochemically. In particular, it was expected that the direct link between the DIQ anion binding site and the redox active TTF moiety would allow the presence of anions to be sensed via changes in the redox potential of the latter subunit. In order to test this possibility, cyclic voltammetric (CV) analyses were carried out. In accord with design expectations, changes in E_1^{ox} were observed upon addition of dihydrogen phosphate (Figure 4.14). Specifically, the addition of two

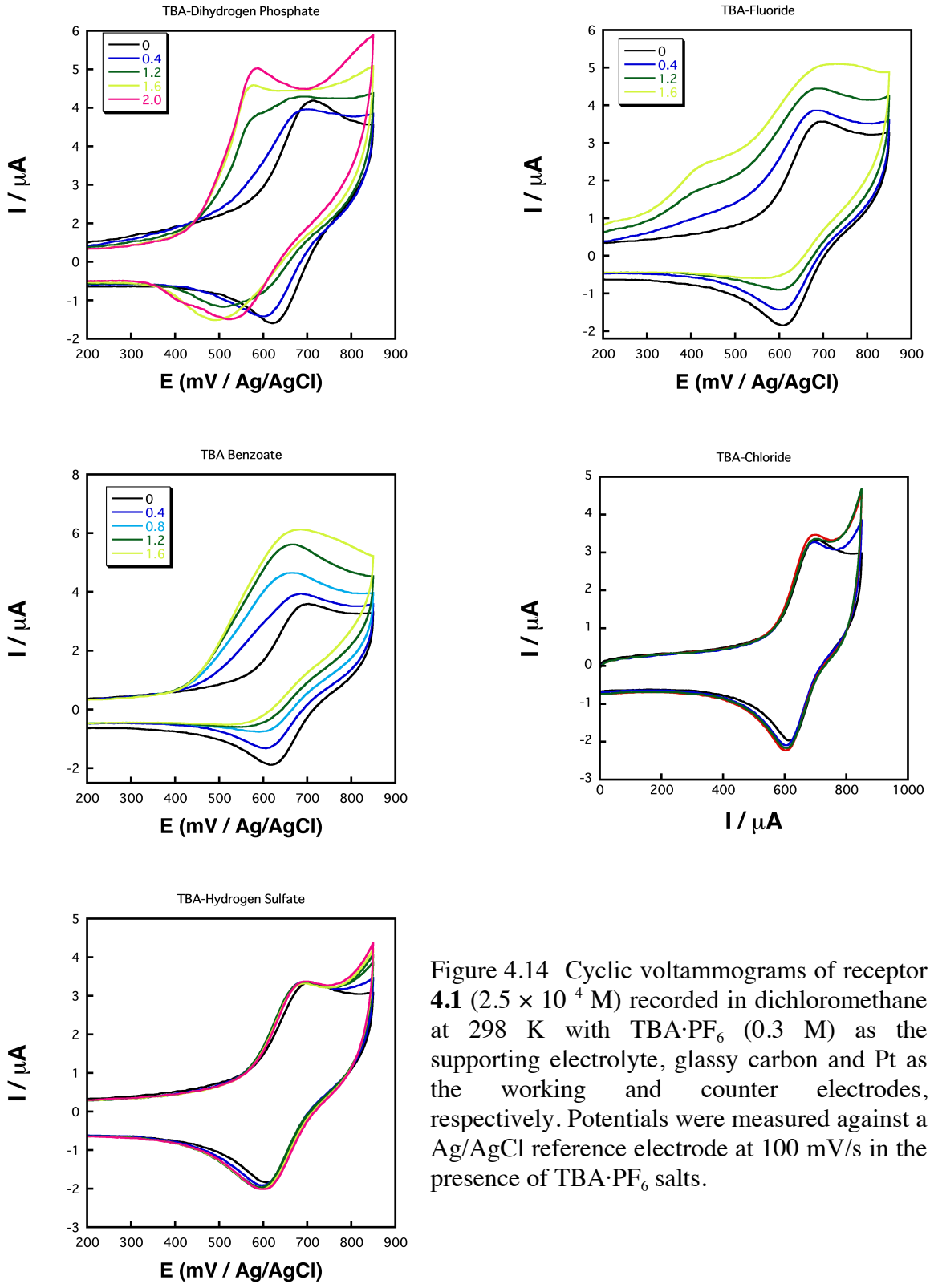

Figure 4.14 Cyclic voltammograms of receptor **4.1** (2.5×10^{-4} M) recorded in dichloromethane at 298 K with TBA·PF_6 (0.3 M) as the supporting electrolyte, glassy carbon and Pt as the working and counter electrodes, respectively. Potentials were measured against a Ag/AgCl reference electrode at 100 mV/s in the presence of TBA·PF_6 salts.

X^-	$^a\Delta E_1^{ox}$ /mV
F^-	-280[b]
$H_2PO_4^-$	-110
BzO^-	-10
HSO_4^-	0
Cl^-	0

Table 4.2 ΔE for first redox potentials of the complexes **1**·X (X = anion) determined *via* CV (2.5×10^{-4} M) recorded in dichloromethane at 298 K with TBA·PF_6 (0.3 M) as the supporting electrolyte, glassy carbon and Pt as the working and counter electrodes, respectively. Potentials were measured against a Ag/AgCl reference electrode at 100 mV/s. [a]ΔE_1^{ox} calculated for first oxidation potential after addition of 2 equiv. of anions. [b]Value after suspected deprotonation.

equivalents of this phosphate anion (as the TBA salt) yielded a cathodic shift of 110 mV in the first oxidation wave ascribed to the TTF subunit. The reduction wave decreased in intensity upon the addition of dihydrogen phosphate and shifted to more positive potentials. These findings are consistent with the suggestion that upon binding to receptor **4.1**, negative charge from the dihydrogen phosphate anion extends into the TTF core. This makes the molecule as a whole easier to oxidize and harder to reduce, as has been proposed for previous TTF-based anion receptors governed by hydrogen bonding.

The addition of chloride, benzoate, and hydrogen sulfate to dichloromethane solutions of **4.1** produced only modest changes in the $E^1_{1/2}$ values, while the addition of fluoride caused a broadening and splitting in the CV features (Table 4.2). This latter finding is attributed to deprotonation of the indole N–H moieties by the basic fluoride anion under the conditions of the CV experiments.

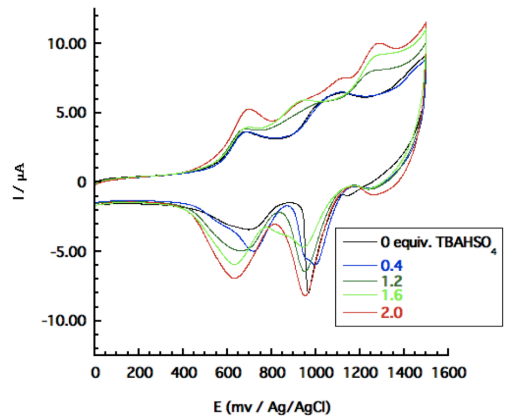

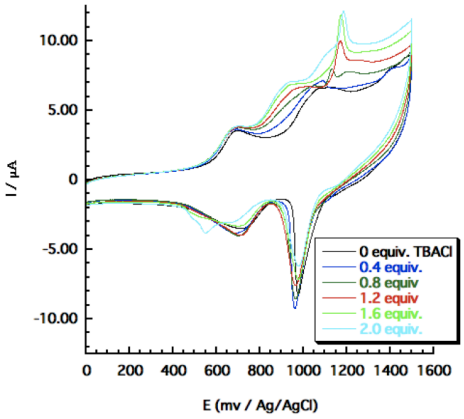

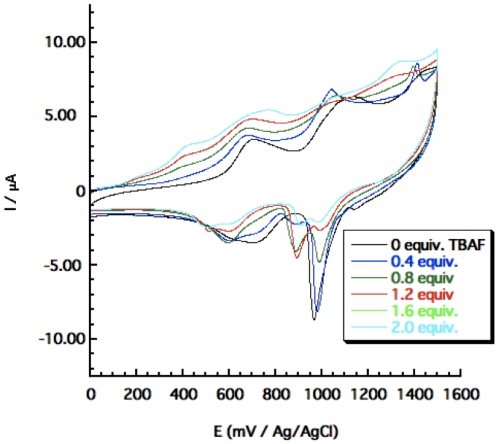

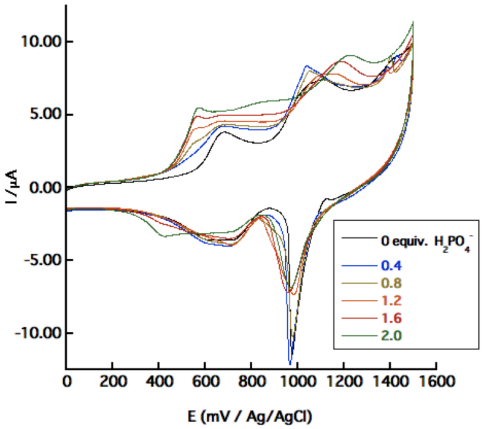

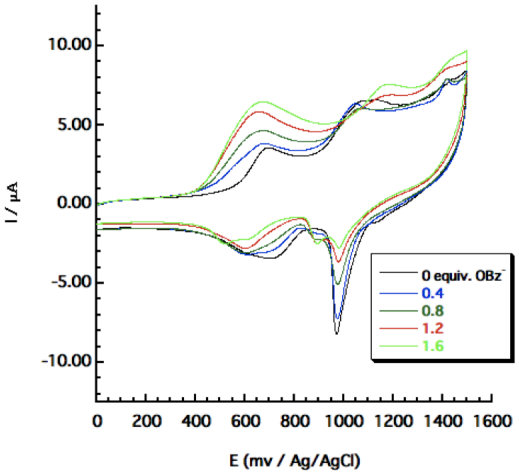

Figure 4.15 Cyclic voltammograms of receptor **4.1** (2.5×10^{-4} M) recorded in dichloromethane at 298 K with TBA·PF_6 (0.3 M) as the supporting electrolyte, glassy carbon and Pt as the working and counter electrodes, respectively. Potentials were measured against a Ag/AgCl reference electrode at 100 mV/s in the presence of various TBA·PF_6 salts.

The full CV scans show more complicated behavior (Figure 4.15). In the presences of increasing amounts of TBA•F and TBA•OBz for example, the oxidations become irreversible. The CV of **4.1** and TBA•Cl shows a new irreversible oxidation process after the first oxidation. After two equivalents of TBA•HSO_4 the CV shape of **4.1** is slightly different but the peak potentials remain relatively unchanged. Via CV, the complex of **4.1** and TBA•HSO_4 appears as a new redox process as evidenced by both the first and second oxidation events. Whereas the first oxidation becomes more favorable due to the increased electron density across the receptor, the second oxidation process is displaced anodically. Presumably, the formation of a 2:2 receptor to anion complex is stabilizing and thus harder to oxidize.

4.5.5 ^{1}H-NMR Spectroscopic Experiments

In an effort to understand more fully the interactions between receptor **4.1** and various anions, ^{1}H NMR spectroscopic studies were carried out in dichloromethane-d_2 (Figure 4.16). In the presence of 1.5 equiv of various TBA salts, the signals for the N–H protons of the indole moieties displayed dramatic shifts upon the addition of dihydrogen phosphate (3.88 ppm downfield shift). The addition of benzoate anion also gave a noticeable shift (1.9 ppm), while chloride and sulfate produced only slight downfield shifts. These findings are consistent with anion-dependent changes in the electron density of the receptor taking place upon anion addition. The disappearance of the N–H signal seen upon fluoride introduction is consistent with deprotonation of the indole N-H proton. Further evidence for this deprotonation was obtained by carrying out analogous ^{1}H NMR spectroscopic experiments in DMSO-d_6 (Figure 4.17). In this more polar solvent, the N–H signal also disappears upon the addition of $TBAH_2PO_4$, while a broadening of the other

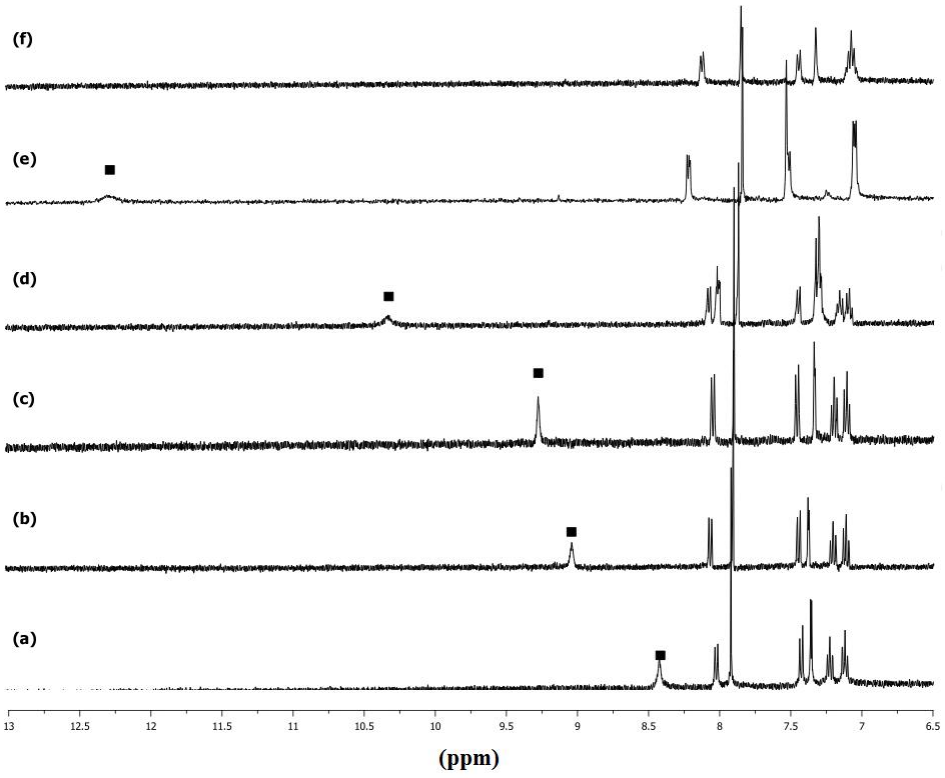

Figure 4.16 Partial ^{1}H NMR spectra (400 MHz) recorded in dichloromethane-d_2: (a) free receptor **4.1**; (b) receptor **4.1** + 1.5 equiv. HSO_4^-; (c) receptor **4.1** + 1.5 equiv. Cl^-; (d) receptor **4.1** + 1.5 equiv. BzO^-; (e) receptor **4.1** + 1.5 equiv. $H_2PO_4^-$; (f) receptor **4.1** + 1.5 equiv. F^-. All anions were studied as their TBA salts. ■ designates the N-H signal of the DIQ moiety.

aromatic signals is also observed. In dichloromethane-d_2 these changes are only seen upon fluoride anion addition and are consistent with what was found by Wang and Yan in the case of system **4.13**.[21]

The relative strengths of the hydrogen bonding interactions between receptor **4.1** and various anions inferred from these NMR spectroscopic analyses, can be used to explain the respective pertubations in the CV titrations . For example, the phosphate and

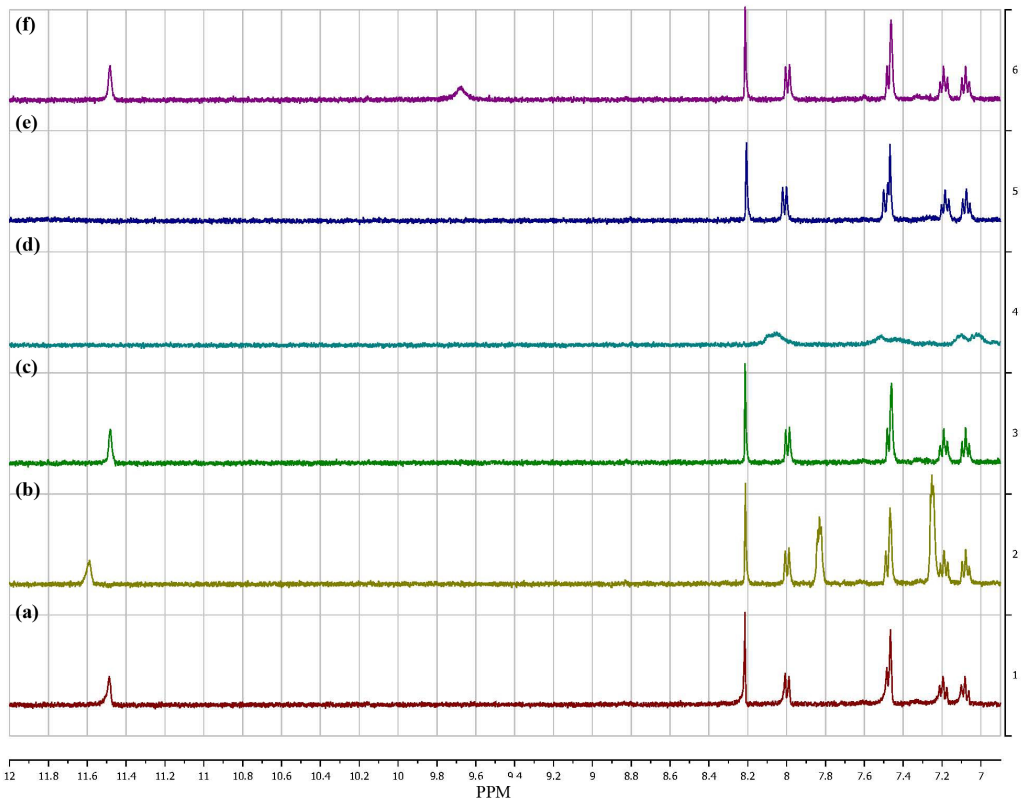

Figure 4.17 Partial ^{1}H NMR spectra (400 MHz) recorded in DMSO-d_6: (a) free receptor **4.1**; (b) receptor **4.1** + 2 equiv. BzO^- ; (c) receptor **4.1** + 2 equiv. Cl^- ; (d) receptor **4.1** + 2 equiv. F^-; (e) receptor **4.1** + 1.5 equiv. $H_2PO_4^-$; (f) receptor **4.1** + 1.5 equiv HSO_4^-. All anions used in the form of their TBA salts. Note the disappearance of the N-H signal and the broadening of the resonances associated with the aromatic protons that is observed upon the addition of fluoride anion.

benzoate anions give rise to the greatest downfield shifts of the indole N–H signals; they also produce the largest cathodic displacements in the first, TTF-centered oxidation potential. Thus, concordant results are obtained from these two disparate measurement methods.

4.6 CONCLUSIONS

In summary, a new TTF-functionalized diindolyl-quninoxaline receptor, **4.1**, has been prepared. In contrast to previously reported DIQ systems, this new receptor allows for the detection of dihydrogen phosphate anions in dichloromethane using a dual optical/electrochemical readout approach. In the presence of TBAF, changes are seen that are thought to reflect deprotonation, rather than hydrogen bond mediated receptor–anion interactions. These effects can be readily distinguished via spectroscopic means. We thus propose that receptors, such as **4.1**, that combine a redox active TTF moiety with recognition subunits that permit an optical response will have a role to play in the recognition, detection, and sensing of the dihydrogen phosphate anion

Finally, although **4.1** shows no evidence of solution phase self assembly in the presence of dihydrogen phosphate, the solid state evidence leads us to suggest anion induced long-range ordering of TTF-subunits could emerge as a new strategy for constructing conductive molecular wires and nanostructures.

4.7 FUTURE DIRECTIONS

The tetrahedral anion recognition chemistry of TTF based receptors in is still in its infancy. Nonetheless, the findings reported in the present Chapter allow one to envision several directions for further investigations.

For instance, there are several known macrocyclic frameworks comprised of Schiff-base linkages that demonstrate tetrahedral anion binding properties. Specifically, the pyridine 2,6-dicarboxamide dipyrromethane macrocycles **4.15-4.16** reported by Sessler and co-workers function as efficient dihydrogen phosphate or hydrogen sulfate receptors, depending on the connectivity of the dipyrromethane *meso*-carbon (Figure 4.18).[25] Whereas **4.16** shows 2:1 anion-to-receptor stoichiometry and selectivity for

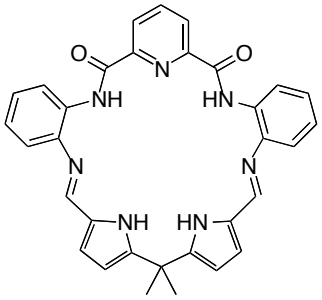

4.15

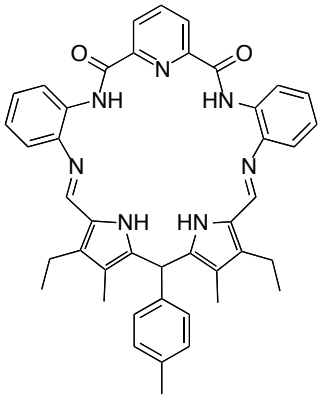

4.16

Figure 4.18 Pyridine 2,6-dicarboxamide dipyrromethane macrocyclic receptors **4.15-4.16**.

dihydrogen phosphate, the more rigid system **4.17** displays selectivity for hydrogen-sulfate and binds most anions with a 1:1 stoichiometry. Presumably, this is due to the tolyl group acting as a "pseudo lid" for the macrocycle cavity.

These structurally similar macrocycles offer the potential for TTF modification through the Schiff-base units (Figure 4.19). Addition of TTF could potentially enhance the known anion affinities by providing a larger hydrophobic pocket. They would also provide an electrochemical handle through which anion binding events could presumably be monitored by CV.

Modification of macrocycles **4.16** and **4.17** by use of TTF-annulated Schiff-base subunits would offer several advantages over the TTF-DIQ receptors reported in this Chapter. Namely, the macrocycles in question bind dihydrogen phosphate much more effectively than does TTF-DIQ **4.1** (K_a 10^5 vs. K_a 10^3 M^{-1}). The macrocycles **4.16** and **4.17** also function as anion receptors in more polar solvents, such as acetonitrile. This represents an advantage over **4.1**, which functions well as an anion receptor only in

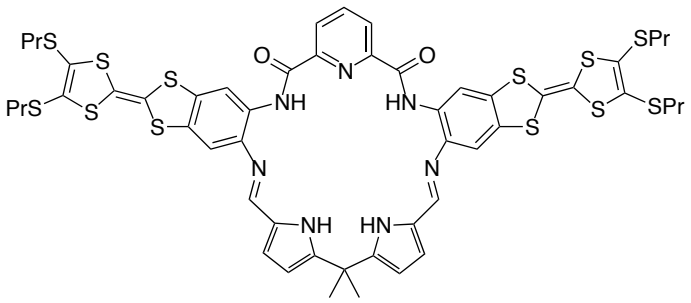

4.18

Figure 4.19 TTF-modified pyridine 2,6-dicarboxamide dipyrromethane macrocyclic receptor **4.18**.

dichloromethane. This increased binding strength presumably reflects the fact that the pyridine 2,6-dicarboxamide dipyrromethane macrocycles offer more anion binding sites. They also provide and an increased macrocyclic hydrophobic effect, which shields the anion from solvent molecules.

References and Notes

1. (a) Adams, R. L. P.; Knowler, J. T.; Leader, D. P. *The Biochemistry of the Nucleic Acids*, 10th ed.; Chapman and Hall: New York, **1986**. (b) Sessler, J. L.; Katayev, E. A.; Ustynyuk, Y. A. *Coord. Chem. Rev*., 2006, **250**, 3004. (c) Hruska, K.; Teitlebaum, S. *New Engl. J. Med*. **1995**, *333*, 166. (d) Block, G. A.; Port, F. K. Am. J. *Kidney Dis*. **2000**, *35*, 1226. (e) Delmez, J. A.; Slatopolsky, E. Am. *J. Kidney Dis*. **1992**, *19*, 303.

2. (a) Sessler, J.; Gale, P. A.; Cho W.-S. *Anion Receptor Chemistry*; The Royal Society of Chemistry: Cambridge, U.K., **2006**. (b) Mason, C. F. *Biology of Freshwater Pollution*; Longman: New York, **1991**. (c) *Phosphorus in the Global Environment: Transfers, Cycles, and Management*; Tiessen, H., Ed.; Wiley: New York, **1995**.

3. Hargrove, A. E.; Nieto, S.; Zhang, T.; Sessler, J. L.; Anslyn, E. V. *Chem. Rev*. **2011**, *111*, 6603.

4. (a) Szemes, F.; Hesek, D.; Chen, Z.; Dent, S. W.; Drew, M. G. B.; Goulden, A. J.; Graydon, A. R.; Grieve, A.; Mortimer, R. J.; Wear, T. J.; Weightman, J. S.; Beer, P. D. *Inorg. Chem*. **1996**, *35*, 5868 (b) Aldakov, D.; Anzenbacher, Jr., P.; *J. Am. Chem. Soc*., **2004**, *126*, 4752 (c) Anzenbacher, Jr., P.; Palacios, M. A.; Jusikova, K. Marquez, M.; *Org. Lett*., **2005**, *7*, 5027.

5. (a) Fiske, C. H.; Subbarow, Y. *J. Biol. Chem*. **1925**, *66*, 375. (b) Gee, A.; Deitz, V. R. *Anal. Chem*. **1953**, *25*, 1320. (c) Duff, E. J.; Stuart, J. L. *Analyst* **1971**, 96, 802. (c) Shida, J.; Matsuo, T. *Bull. Chem. Soc. Jpn*. **1980**, *53*, 2868. (d) Worsfold, P. J.; Gimbert, L. J.; Mankasingh, U.; Omaka, O. N.; Hanrahan, G.; Gardolinski, P. C. F. C.; Haygarth, P. M.; Turner, B. L.; Keith-Roach, M. J.; McKelvie, I. D. *Talanta* **2005**, *66*, 273. (e) Guilbault, G. G.; Nanjo, M. *Anal. Chim. Acta* **1975**, *78*, 69. (f) Gajovic, N.; Habermuller, K.; Warsinke, A.; Schuhmann, W.; Scheller, F. W. *Electroanalysis* **1999**, *11*, 1377. (g) Kubo, I.; Inagawa, M.; Sugawara, T.; Arikawa, Y.; Karube, I. *Anal. Lett*. **1991**, *24*, 1711 (h) Amine, A.; Palleschi, G. *Anal. Lett*. **2004**, *37*, 1. (i) Luque de Castro, M. D.; Quiles, R.; Fernández-Romero, J. M.; Fernández, E. *Clin. Chem*. **1995**, *41*, 99 (j) Schulz, D. W.; Passonneau, J. V.; Lowry, O. H. *Anal. Biochem*. **1967**, *19*, 300.

6. Marcus, Y. *Biophys. Chem*. **1994**, *51*, 111.

7. (a) Antonisse, M. M. G.; Reinhoudt, D. N. *Chem. Commun*. **1998**, 443 (b) Snowden, T. S.; Anslyn, E. V. Curr. Opin. *Chem. Biol*. **1999**, *3*, 740 (c) Beer, P. D.; Gale, P. A. *Angew. Chem., Int. Ed*. **2001**, *40*, 486 (d) Aoki, S.; Kimura, E. *Rev. Mol. Biotechnol*. **2002**, *90*, 129 (e) Hartley, J. H.; James, T. D.; Ward, C. J. *J. Chem. Soc., Perkin Trans. 1* **2000**, 3155.

8. Beer, P. D.; Bayly, S. R. *Top. Curr. Chem.* **2005**, *255*, 125.

9. Beer, P. D.; Chen, Z.; Goulden, A. J.; Graydon, A.; Stokes, S. E.; Wear, T. *J. Chem. Soc., Chem. Commun.* **1993**, 1834.

10. Evans, A. J.; Matthews, S. E.; Cowley, A. R.; Beer, P. D. *Dalton Trans.* **2003**, 4644.

11. Duff, T.; Grussing, A.; Thomas, J.-L.; Duati, M.; Vos, J. G. *Polyhedron* **2003**, *22*, 775.

12. Becher, J.; Nielsen, K. A.; Jeppeson, J. O.; Levillian, E. *Angew. Chem., Int. Ed.*, **2003**, *42*, 187.

13. (a) Zhu, D.; Xu, W.; Lu, H.; Zhang, D.; Chen, C.; *Org. Lett.*, **2005**, *7*, 4629. (b) Lu, H.; Xu, W.; Zhang, D.; Zhu, D. *Chem. Commun.*, **2005**, 4777.

14. Black, C. B.; Andrioletti, B.; Try, A. C.; Ruiperez, C.; Sessler, J. L. *J. Am. Chem. Soc.*, **1999**, *121*, 10438.

15. (a) Oddo, B. Gazz. *Chim. Ital.* **1911**, *41*, 248. (b) Behr, D.; Brandänge, S.; Lindström, B. *Acta Chem. Scand.* **1973**, *27*, 2411.

16. Anzenbacher, P.; Try, A. C.; Miyaji, H.; Jursikova, K.; Lynch, V. M.; Marquez, M.; Sessler, J. L. *J. Am. Chem. Soc.* **2000**, *122*, 10268.

17. Mizuno, T.; Wei, W.-H.; Eller, L. R.; Sessler, J. L. *J. Am. Chem. Soc.* **2002**, *124*, 1134.

18. Anzenbacher, P., Jr.; Palacios, M. A.; Jursíková, K.; Marquez, M. *Org. Lett.* **2005**, *7*, 5027.

19. Aldakov, D.; Anzenbacher, P., Jr. *J. Am. Chem. Soc.* **2004**, *126*, 4752.

20. Sessler, J. L.; Cho, D-G.; Lynch, V. *J. Am. Chem. Soc.* **2006**, *128*, 16518.

21. Wang, T.; Yan, X. P. *Chem.–Eur. J.*, **2010**, *16*, 4639.

22. (a) Caltagirone, C.; Gale, P. A.; Hiscock, J. R.; Hursthouse, M. B.; Light, M. E.; Tizzard, G. J. *Supramol. Chem.* **2009**, *21*, 125. (b) Amendola, V.; Boicchi, M.; Esteban-Gomez, D.; Fabrizzi, L.; Monzani, E. *Org. Biomol. Chem.* **2005**, *3*, 2632.

23. Connors, K. A. *Binding Constants*, John Wiley, New York, **1987**

24. Palacios, M. A.; Nishiyabu, R.; Marquez, M.; Anzenbacher, Jr., P. *J. Am. Chem. Soc.*, **2007**, *129*, 7538.

25. (a) Sessler, J. L.; Katayev, E.; Pantos, G. D.; Ustynyuk, Y. A. *Chem. Commun.*, **2004**, 1276. (b) Sessler, J. L.; Katayev, E.; Pantos, G. D.; Scherbakov, P.; Reshetova, M. D.; Khrustalev, V. N.; Lynch, V. M.; Ustynyuk, Y. A. *J. Am. Chem. Soc.* **2005**, *127*, 11442.

Chapter 5

Experimental Procedures

5.1 General Procedures

Prior to use, all glassware was soaked in KOH-saturated isopropyl alcohol for ca. 12 h and then rinsed with water and acetone before being thoroughly dried. Tetrahydrofuran (THF) was dried by passage through two columns of activated alumina. Acetonitrile, methanol and dimethylformamide were dried by passage through two columns of molecular sieves. Toluene was dried by passage through one column of Q-5 reactant and one column of neutral alumina. When used as reaction medium, Dichloromethane was freshly distilled from CaH_2. Dichloromethane used for chromatographic purifications was purchased from Fisher Scientific and used as received. Triethylamine was distilled over barium oxide. Hexanes were purchased from Fisher Scientific and used as received.

Unless otherwise stated, reagents and metal salts were purchased commercially (Aldrich, Acros, TCI, or Strem) and used as received. Precursors and reagents that could not be obtained from commercial sources were prepared according to previously published procedures, with the references for the preparation being cited in the main text.

Solutions were stirred magnetically.

Column chromatography purifications were carried out using Silicycle Silia Flash® P60 grade silica gel (40-63 μm) Silica gel plates for analytical thin layer chromatography were purchased from Silicycle, Inc.

Nuclear magnetic resonance (NMR) spectra were recorded on a Varian Mercury 400 MHz, a Varian Inova 500 MHz, or a Brüker AC 300 MHz spectrometer. Chemical shifts (δ) are reported in ppm and referenced to the solvent. All other deuterated NMR solvents were purchased from Cambridge Isotope Labs and used as received.

Electrochemistry was done on a CV-50W Voltammetric Analyzer.

UV-visible spectra were recorded at room temperature on a Beckman DU-640 spectrophotometer. Low- and high-resolution mass spectra were obtained at the Mass Spectrometry Facility of the Department of Chemistry and Biochemistry, University of Texas at Austin.

Fluorescence spectra were recorded on Horiba Jobin Yvon Nanolog.

Elemental combustion analyses were performed by UC Berkeley Microanalytical Laboratory.

5.2 SYNTHETIC DETAILS AND CHARACTERIZATION DATA

TTF-Schiff-base calixpyrrole 2.1 [$C_{58}H_{61}N_8S_{12}$]: A mixture of **2.24** (100 mg, 0.231 mmol) and **2.23** (53 mg, 0.231 mmol) in methanol was warmed until most of the solids had dissolved. Para-toluene sulfonic acid monohydrate (88 mg, 0.463 mmol) was added slowly in portions to the solution over one hour. The reaction mixture was allowed to stir for 1 hour. Triethylamine (0.25 mL) was slowly added to the solution causing precipitation of a yellow/orange solid, which was filtered, washed with methanol, and dried in vacuo to afford the title compound **2.1** (225 mg, 78%) as a light orange solid. ^{1}H NMR ($CDCl_3$): δ = 8.0 (s, N-H, 4H), 6.85 (s, Ar-H, 4H), 6.46 (d, *J* = 3.7 Hz, C-H pyrrole, 4H), 6.06 (d, *J* = 3.7 Hz, C-H pyrrole, 8H), 2.77 (t, *J* = 7.3 Hz, -S-$\mathbf{CH_2}CH_2CH_3$, 8H), 1.78 (s, meso-CH_3, 12H), 1.63 (m, -S-$CH_2\mathbf{CH_2}CH_3$, 8H), 0.99 (t, *J* = 7.4 Hz, -S-$CH_2CH_2\mathbf{CH_3}$, 12H) ppm. HRMS (ESI) m/z calcd for $(C_{58}H_{61}N_8S_{12})^+$1253.16661, found 1253.16622.

***Bis*-Pd(II) Complex 2.2 [$C_{58}H_{57}N_8Pd_2S_{12}$]**: Palladium acetate (33mg, 0.160 mmol) was added to a solution of free ligand **2.1** (100 mg, 0.08 mmol) dissolved in CH_2Cl_2 (15 mL). After 30 minutes, triethylamine (0.2 mL) was added to the reaction mixture and the solution was allowed to stir at room temperature overnight. Pentane (50 mL) was added to the reaction and a brown solid precipitated, which was filtered and purified via column chromatography (silica gel, eluent: CH_2Cl_2/hexanes 2:1) to yield the title **2.2** compound as a red solid (35 mg, 30%). ^{1}H NMR ($CDCl_3$): δ = 7.26 (s, N-H, 4H), 6.80 (d, *J* = 3.8 Hz, C-H pyrrole, 4H), 6.66 (s, Ar-H, 4H), 6.23 (d, *J* = 3.7 Hz, C-H pyrrole, 4H), 2.79 (m, -S-$\mathbf{CH_2}CH_2CH_3$, 8H), 1.66 (m, -S-$\mathbf{CH_2}CH_2CH_3$, 8H), 1.62 (s,

meso-CH_3, 6H), 1.54 (s, meso-CH_3, 6H), 1.00 (*t*, *J* = 7.3 Hz, -S-CH_2CH_2**CH_3**, 12H) ppm; ^{13}C NMR (CDCl3): δ = 159.1, 153.1, 141.3, 136.4, 135.1, 127.4, 119.7, 117.1, 112.6, 108.8, 108.3, 43.5, 38.1, 32.4, 30.6, 29.7, 23.2, 13.3 ppm, HRMS (MALDI) m/z ($C_{58}H_{57}N_8Pd_2S_{12}$) found 1463.92879. This compound was also characterized by X-ray diffraction analysis (see Appendix A).

TTF-salphen(UO_2)EtOH 3.1 [$C_{32}H_{32}N_2O_5S_6U$]: A stock solution (1 mL) of salicylaldehyde (0.12 mmol in ethanol) was added to flask that contained **2** (25 mg, 0.06 mmol) and $UO_2(NO_3)_2$•$6H_2O$ (30 mg, 0.06 mmol) dissolved in ethanol (10 mL). The solution was stirred at room temperature (12 h), during which time a dark orange precipitate was formed. The precipitate was isolated via vacuum filtration, washed with cold ethanol (10 mL, 3x), and dried in vacuo (10 to afford **1** without further purification in *73%* yield. ^{1}H NMR (pyridine-d_5): δ 9.62 (s, NH, 2H), 7.84 (d, *J* = 8.6 Hz, 2H), 7.72 (s, Ar-H, 2H) 7.64 (t, *J* = 7.5, 7.59 Hz, 2H) 7.29 (d, *J* = 8.3 Hz, 2H) 6.79 (t, *J* = 7.3, 7.48 Hz, 2H) 2.82 (t, *J* = 7.1 Hz, -S-**CH_2**CH_2CH_3, 4H) 1.61 (m, *J* = 7.10, 7.47 Hz, -S-CH_2**CH_2**CH_3, 4H) 0.92 (t, *J* = 7.4Hz, -S-CH_2CH_2**CH_3**, 6H) ppm; ^{13}C NMR (pyridine-d_5): δ 171.21, 166.62, 146.32, 137.08, 136.41, 128.25, 124.96, 121.36, 118.12, 114.13, 112.16, 111.05, 38.33, 23.39, 13.10 ppm. Anal. Calc. [$C_{59}H_{66}N_4O_7S_{12}U$ • CH_3CH_2OH]: C, 40.24; H, 3.38; N, 2.93; S, 20.15. Found C, 39.18; H, 3.34; N, 2.96; S, 20.01. This compound was also characterized by X-ray diffraction analysis (see Appendix A).

TTF-DIQ 4.1 [$C_{34}H_{28}N_4S_6$]: TTF-Diamine (5,6-Diamino-2-(4,5-bis(propylthio)-1,3-dithio-2-ylidene)benzo[*d*]-1,3-dithiole) **2.23** (161mg, 0.23mmol) and the **4.14** diketone (90mg, 0.37mmol) were dissolved in 50mL EtOH and 50mL acetic acid and refluxed overnight. The resulting solution was concentrated in vacuo and subject to

column chromatography (silica gel, CH_2Cl_2/EtOAc (7/1, v/v)) to give **1** as a purple solid (47mg, 22%). ^{1}H NMR (DCM-*d2*) δ 8.42 (s, N-H, 2H), 8.02 (d, J= 8.5 Hz, 2H), 7.92 (s, Ar-H, 2H), 7.43 (d, *J* = 8.13 Hz, 2H), 7.36 (s, 2H), 7.23 (t, J= 7.02, 6.96 Hz, 2H), 7.12 (t, J= 8.11, 6.99 Hz, 2H), 2.84 (t, J=7.09, 7.32, -S-propyl, 4H), 2.84 (m, -S-propyl, 4H), 1.03(t, J=7.31, 7.34 Hz, -S-propyl, 6H) ppm; ^{13}C NMR (DMSO-*d6*) δ 149.661, 138.431, 137.728, 136.160, 128.131, 126.930, 125.978, 121.956, 121.260, 120.374, 120.117, 113.905, 111.891, 110.880, 110.733, 37.449, 22.673, 12.777 ppm. MS *m/z*: 685.07 [M^+]. This compound was also characterized by X-ray diffraction analysis (see Appendix A).

Appendix A

Crystallographic Experimental Methods

A.1 General Procedures

The X-ray data refinements for crystal structures of **2.2**, **2.2**$^{\bullet+}$**,** and **4.1** reported in the present dissertation were performed by Dr. Vincent M. Lynch of the X-ray Diffraction Laboratory, Department of Chemistry and Biochemistry, University of Texas at Austin.

The X-ray data refinements for crystal structure **4.1•TBA-H_2PO_4** reported in the present dissertation were performed by Dr. Jung Su Park at the University of Texas at Austin.

Dr. Brian L. Scott of the Chemistry Division, Los Alamos National Laboratory performed the X-ray data refinements for the crystal structure of **3.1** reported in the present dissertation.

This Appendix describes the experimental methods used by Dr. Lynch, Dr. Park, and Dr. Scott in obtaining each of these structures. Relevant data tables for all the refinements are included.

A.2 EXPERIMENTAL DETAILS

***Bis*-Pd(II) Complex 2.2 [$C_{58}H_{57}N_8Pd_2S_{12}$]**: Crystals grew as large orange prisms by vapor diffusion of hexanes into a methylene chloride solution of the complex. The data crystal had approximate dimensions; 0.30 x 0.28 x 0.25 mm. The data were collected on a Nonius Kappa CCD diffractometer using a graphite monochromator with MoKa radiation (l = 0.71073Å). A total of 427 frames of data were collected using w-scans with a scan range of 1.2° and a counting time of 59 seconds per frame. The data were collected at 153 K using an Oxford Cryostream low temperature device. Details of crystal data, data collection and structure refinement are listed in Table A.1. Data reduction were performed using DENZO-SMN.[1] The structure was solved by direct methods using SIR97[2] and refined by full-matrix least-squares on F^2 with anisotropic displacement parameters for the non-H atoms using SHELXL-97.[3] The hydrogen atoms were calculated in ideal positions with isotropic displacement parameters set to 1.2xUeq of the attached atom (1.5xUeq for methyl hydrogen atoms).

The function, $\Sigma w(|F_o|^2 - |F_c|^2)^2$, was minimized, where $w = 1/[(s(F_o))^2 + (0.0657*P)^2 + (3.3734*P)]$ and $P = (|F_o|^2 + 2|F_c|^2)/3$. $R_W(F^2)$ refined to 0.116, with R(F) equal to 0.0406 and a goodness of fit, S, = 1.06. Definitions used for calculating R(F),$R_W(F^2)$ and the goodness of fit, S, are given below.[4] The data were checked for secondary extinction effects but no correction was necessary. Neutral atom scattering factors and values used to calculate the linear absorption coefficient are from the International Tables for X-ray Crystallography (1992).[5] All figures were generated using SHELXTL/PC.[6]

***Bis*-Pd(II) Complex 2.2$^{\bullet+}$ [$(C_{58}H_{57}N_8Pd_2S_{12})^{\bullet+}$]**: : Crystals grew as clusters of thin, dark red laths by vapor diffusion of hexanes into a 1:1 solution of toluene/acetonitrile. The data were collected on a Rigaku AFC12 diffractometer with a Saturn 724+ CCD using a graphite monochromator with MoKα radiation (λ = 0.71075Å). A total of 860 frames of data were collected using ω-scans with a scan range of 0.5° and a counting time of 75 seconds per frame. The data were collected at 100 K using a Rigaku XStream low temperature device. Details of crystal data, data collection and structure refinement are listed in Table 1. Data reduction were performed using the Rigaku Americas Corporation's Crystal Clear version 1.40.[11] The structure was solved by direct methods using SIR97[2] and refined by full-matrix least-squares on F^2 with anisotropic displacement parameters for the non-H atoms using SHELXL-97.[3] Structure analysis was aided by use of the programs PLATON98[12] and WinGX.[13] The hydrogen atoms were calculated in ideal positions with isotropic displacement parameters set to 1.2xUeq of the attached atom (1.5xUeq for methyl hydrogen atoms).

A large solvent void centered around -0.2, -0.16, 0 was found. Very little chemical sense could be made of this void and the utility Squeeze[14] in Platon98 was used to try to remove the effects of this solvent region from the diffraction data. In addition to this solvent void, some of the atoms of the n-propyl groups could not be localized in sensible positions. Apparently, these atoms are dynamically disordered and were excluded from the model. Four regions of the asymmetric unit contained the anion. Two of these resided on crystallographic three-fold rotation axes and two were located on general positions. If fully occupied, the anion count would be 1.333 ClO4- anions per Pd dimer. However, one ClO4- anion, composed of atoms Cl1c, O1c, O2c, O3c and O4c were not fully occupied. The site appeared to be partially occupied by a molecule of methanol. The site occupancy factors for the two components refined to approximately

54% ClO4- and 46% methanol. This number is not to be considered a firm accounting but more of an estimate.The contents of the solvent void was not considered in the reporting of the unit cell contents.

The function, $\Sigma w(|F_o|^2 - |F_c|^2)^2$, was minimized, where $w = 1/[(\sigma(F_o))^2 + (0.078*P)^2]$ and $P = (|F_o|^2 + 2|F_c|^2)/3$. $R_W(F^2)$ refined to 0.270, with R(F) equal to 0.119 and a goodness of fit, S, = 1.32. Definitions used for calculating R(F), $R_W(F^2)$ and the goodness of fit, S, are given below.[4] The data were checked for secondary extinction effects but no correction was necessary. Neutral atom scattering factors and values used to calculate the linear absorption coefficient are from the International Tables for X-ray Crystallography (1992).[5] All figures were generated using SHELXTL/PC.[6] Tables of positional and thermal parameters, bond lengths and angles, torsion angles and figures are found elsewhere.

TTF-salphen(UO_2)EtOH 3.1 [$C_{32}H_{32}N_2O_5S_6U$]: Single crystals were grown as red blocks by slow evaporation of a concentrated solution of **3.1** in an equimolar solution of dichloromethane and methanol. Crystals of **3.1** were mounted in a nylon cryoloop from Paratone-N oil. The data were collected on a Bruker D8 diffractometer, with APEX II charge-coupled-device (CCD) detector, and Cryo Industries of America Cryocool G2 low temperature device (120 K). The instrument was equipped with graphite monochromatized MoKα X-ray source (λ= 0.71073 Å), and a 0.5 mm monocapillary. A hemisphere of data was collected using ω scans, with 10-second frame exposures and 0.5º frame widths. Data collection and initial indexing and cell refinement were handled using APEX II[7] software. Frame integration, including Lorentz-polarization corrections, and final cell parameter calculations were carried out using SAINT+[8] software. The data were corrected for absorption using redundant reflections and the SADABS[9] program. Decay of reflection intensity was not observed as monitored via analysis of redundant

frames. The structure was solved using Direct methods and difference Fourier techniques. All hydrogen atom positions were idealized, and rode on the atom they were attached to. The final refinement included anisotropic temperature factors on all non-hydrogen atoms. Structure solution, refinement, graphics, and creation of publication materials were performed using SHELXTL[10].

TTF-DIQ 4.1 [$C_{34}H_{28}N_4S_6$]: Single crystals were grown as yellow needles from a solution of **4.1** in dichloromethane layered with ethanol over the course of one week at ambient temperature. The data were collected on a Rigaku AFC12 diffractometer with a Saturn 724+ CCD using a graphite monochromator with MoKa radiation (l = 0.71075Å). A total of 202 frames of data were collected using w-scans with a scan range of 1° and a counting time of 160 seconds per frame. The data were collected at 100 K using a Rigaku XStream low temperature device. Details of crystal data, data collection and structure refinement are listed in Table 1. Data reduction were performed using the Rigaku Americas Corporation's Crystal Clear version 1.40.[11] The structure was solved by direct methods using SIR97[2] and refined by full-matrix least-squares on F^2 with anisotropic displacement parameters for the non-H atoms using SHELXL-97.[3] Structure analysis was aided by use of the programs PLATON98[12] and WinGX.[13] The hydrogen atoms were calculated in ideal positions with isotropic displacement parameters set to 1.2xUeq of the attached atom (1.5xUeq for methyl hydrogen atoms). The function, $\Sigma w(|F_o|^2 - |F_c|^2)^2$, was minimized, where $w = 1/[(s(F_o))^2 + (0.2*P)^2]$ and $P = (|F_o|^2 + 2|F_c|^2)/3$. $R_W(F^2)$ refined to 0.596, with R(F) equal to 0.260 and a goodness of fit, S, = 1.15. Definitions used for calculating R(F), $R_W(F^2)$ and the goodness of fit, S, are given below.[4] The data were checked for secondary extinction effects but no correction was necessary. Neutral atom scattering factors and values used to calculate the linear

absorption coefficient are from the International Tables for X-ray Crystallography (1992).[5] All figures were generated using SHELXTL/PC.[6] Tables of positional and thermal parameters, bond lengths and angles, torsion angles and figures are found elsewhere.

TTF-DIQ 4.1•TBAH_2PO_4 [$C_{34}H_{28}N_4S_6$]: Single crystals were grown as orange laths from equimolar mixtures of **4.1** and **TBA•H_2PO_4** in acetone, into which diethylether was slowly diffused over the course of one week at ambient temperature. X-ray crystallographic data was collected at –50 °C on a Rigaku SCX-Mini diffractometer using a monochromatized MoKα source (λ = 0.71070 Å) equipped with a Mercury CCD area detector. The frame data was integrated and corrected for absorption effects using the Rigaku/MSC CrystalClear program package.[11] The structures were solved by direct methods and refined by full-matrix least-squares on F^2 with anisotropic displacement parameters for the non-H atoms using SHELXL-97.[3] The function, $w(|Fo|^2 - |Fc|^2)^2$, was minimized, where $w = 1/[((Fo))^2 + (X*P)^2 + (Y*P)]$ and $P = (|Fo|^2 + 2|Fc|^2)/3$ and the parameters, X and Y, are suggested during the refinement process. The hydrogen atoms were calculated in ideal positions with isotropic displacement parameters set to 1.2xUeq of the attached atom (1.5xUeq for methyl hydrogen atoms). Neutral atom scattering factors and values used to calculate the linear absorption coefficient are from the International Tables for X-ray Crystallography (1992). All the calculations were carried out with the SHELXTL program.[6]

A.3 CRYSTALLOGRAPHIC DATA TABLES

Table A.1 Crystal data and structure refinement parameters for complex **2.2**

Empirical formula	C60 H60 Cl4 N8 Pd2 S12	
Formula weight	1632.48	
Temperature	153(2) K	
Wavelength	0.71069 Å	
Crystal system	Monoclinic	
Space group	P21/n	
Unit cell dimensions	a = 18.0698(6) Å	a= 90.000(5)°.
	b = 18.8957(7) Å	b= 96.632(2)°.
	c = 19.9815(7) Å	g = 90.000(5)°.
Volume	6776.9(4) $Å^3$	
Z	4	
Density (calculated)	1.600 Mg/m^3	
Absorption coefficient	1.104 mm^{-1}	
F(000)	3312	
Crystal size	0.30 x 0.28 x 0.25 mm	
Theta range for data collection	2.16 to 27.48°.	
Index ranges	-23<=h<=23, -24<=k<=24, -25<=l<=25	
Reflections collected	30338	
Independent reflections	15512 [R(int) = 0.0287]	
Completeness to theta = 27.48°	99.8 %	
Absorption correction	Semi-empirical from equivalents	
Max. and min. transmission	1.06 and 0.934	
Refinement method	Full-matrix least-squares on F^2	
Data / restraints / parameters	15512 / 0 / 759	
Goodness-of-fit on F^2	1.058	
Final R indices [I>2sigma(I)]	R1 = 0.0406, wR2 = 0.1078	
R indices (all data)	R1 = 0.0585, wR2 = 0.1162	
Largest diff. peak and hole	1.232 and -0.708 $e.Å^{-3}$	

Table A.2 Crystal data and structure refinement parameters for complex **2.2**$^{\bullet+}$

Empirical formula	C58 H56 Cl1.10 F0 N8 O4.40 Pd2 S12	
Formula weight	1572.02	
Temperature	100(2) K	
Wavelength	0.71075 Å	
Crystal system	Hexagonal	
Space group	R-3c	
Unit cell dimensions	a = 38.862(12) Å	a= 90°.
	b = 38.862(12) Å	b= 90°.
	c = 110.96(4) Å	g = 120°.
Volume	145124(79) Å^3	
Z	72	
Density (calculated)	1.295 Mg/m^3	
Absorption coefficient	0.836 mm^{-1}	
F(000)	57449	
Theta range for data collection	1.52 to 24.22°.	
Index ranges	-38<=h<=0, 0<=k<=44, 0<=l<=128	
Reflections collected	25898	
Independent reflections	25898	
Completeness to theta = 24.22°	99.6 %	
Refinement method	Full-matrix-block least-squares on F^2	
Data / restraints / parameters	25898 / 326 / 1428	
Goodness-of-fit on F^2	1.320	
Final R indices [I>2sigma(I)]	R1 = 0.1191, wR2 = 0.2475	
R indices (all data)	R1 = 0.2272, wR2 = 0.2698	
Largest diff. peak and hole	1.474 and -0.775 e.Å^{-3}	

Table A.3 Crystal data and structure refinement parameters for complex **3.1**

Empirical formula	$C_{31.50}\ H_{28}\ Cl\ N_2\ O_5\ S_6\ U$	
Formula weight	980.40	
Temperature	120(1) K	
Wavelength	0.71073 Å	
Crystal system	Triclinic	
Space group	P -1	
Unit cell dimensions	a = 9.7141(6) Å	a= 82.010(1)°.
	b = 12.0383(7) Å	b= 75.098(1)°.
	c = 16.5610(10) Å	g = 68.090(1)°.
Volume	1734.35(18) $Å^3$	
Z	2	
Density (calculated)	1.877 Mg/m^3	
Absorption coefficient	5.161 mm^{-1}	
F(000)	952	
Crystal size	0.20 x 0.16 x 0.06 mm^3	
Theta range for data collection	1.83 to 28.36°.	
Index ranges	-12<=h<=12, -15<=k<=15, -21<=l<=21	
Reflections collected	19573	
Independent reflections	7907 [R(int) = 0.0238]	
Completeness to theta = 25.00°	99.7 %	
Absorption correction	Semi-empirical from equivalents	
Max. and min. transmission	0.7471 and 0.4251	
Refinement method	Full-matrix least-squares on F^2	
Data / restraints / parameters	7907 / 0 / 436	
Goodness-of-fit on F^2	1.089	
Final R indices [I>2sigma(I)]	R1 = 0.0248, wR2 = 0.0577	
R indices (all data)	R1 = 0.0289, wR2 = 0.0590	
Largest diff. peak and hole	1.058 and -0.765 $e.Å^{-3}$	

Table A.4 Crystal data and structure refinement parameters for complex **4.1**

Empirical formula	C34 H28 N4 S6	
Formula weight	684.96	
Temperature	100(2) K	
Wavelength	0.71075 Å	
Crystal system	Monoclinic	
Space group	P21/n	
Unit cell dimensions	a = 15.053(5) Å	a= 90°.
	b = 5.388(3) Å	b= 96.815(5)°.
	c = 39.209(12) Å	g = 90°.
Volume	3158(2) $Å^3$	
Z	4	
Density (calculated)	1.441 Mg/m^3	
Absorption coefficient	0.466 mm^{-1}	
F(000)	1424	
Theta range for data collection	3.03 to 24.99°.	
Index ranges	-16<=h<=15, -3<=k<=6, -21<=l<=46	
Reflections collected	6668	
Independent reflections	3900 [R(int) = 0.3524]	
Completeness to theta = 24.99°	70.2 %	
Absorption correction	Semi-empirical from equivalents	
Max. and min. transmission	1.00 and 0.299	
Refinement method	Full-matrix least-squares on F^2	
Data / restraints / parameters	3900 / 264 / 399	
Goodness-of-fit on F^2	1.148	
Final R indices [I>2sigma(I)]	R1 = 0.2599, wR2 = 0.4818	
R indices (all data)	R1 = 0.4963, wR2 = 0.5963	
Largest diff. peak and hole	0.969 and -0.879 $e.Å^{-3}$	

Table A.5 Crystal data and structure refinement parameters for complex **4.1•TBA-PF_6**

Empirical formula	C104 H142 N10 O9.50 P2 S12
Formula weight	2130.94
Temperature	223(2) K
Wavelength	0.71075 A
Crystal system, space group	Triclinic, P-1
Unit cell dimensions	a = 15.186(3) A alpha = 92.706(5) deg.
	b = 16.853(3) A beta = 90.213(5) deg.
	c = 25.923(5) A gamma = 91.252(5) deg.
Volume	6625(2) A^3
Z, Calculated density	2, 1.068 Mg/m^3
Absorption coefficient	0.271 mm^-1
F(000)	2268
Crystal size	0.20 x 0.14 x 0.11 mm
Theta range for data collection	3.00 to 25.00 deg.
Limiting indices	-18<=h<=18, -20<=k<=20, -30<=l<=30
Reflections collected / unique	57121 / 23245 [R(int) = 0.1273]
Completeness to theta = 25.00	99.7 %
Absorption correction	Semi-empirical from equivalents
Max. and min. transmission	0.9708 and 0.9477
Refinement method	Full-matrix least-squares on F^2
Data / restraints / parameters	23245 / 121 / 1299
Goodness-of-fit on F^2	1.074
Final R indices [I>2sigma(I)]	R1 = 0.0849, wR2 = 0.1794
R indices (all data)	R1 = 0.1803, wR2 = 0.2042
Largest diff. peak and hole	0.498 and -0.345 e.A^-3

References and Notes

1. DENZO-SMN. (1997). Z. Otwinowski and W. Minor, Methods in Enzymology, **276**: Macromolecular Crystallography, part A, 307 – 326, C. W. Carter, Jr. and R. M. Sweets, Editors, Academic Press.
2. SIR97. (1999). A program for crystal structure solution. Altomare A., Burla M.C., Camalli M., Cascarano G.L., Giacovazzo C. , Guagliardi A., Moliterni A.G.G., Polidori G.,Spagna R. J. Appl. Cryst. 32, 115-119.
3. Sheldrick, G. M. (1994). SHELXL97. Program for the Refinement of Crystal Structures. University of Gottingen, Germany.
4. $R_w(F^2) = \{\Sigma w(|F_o|^2 - |F_c|^2)^2/\Sigma w(|F_o|)^4\}^{1/2}$ where w is the weight given each reflection. $R(F) = \Sigma(|F_o| - |F_c|)/\Sigma|F_o|\}$ for reflections with $F_o > 4(\sigma(F_o))$. $S = [\Sigma w(|F_o|^2 - |F_c|^2)^2/(n - p)]^{1/2}$, where n is the number of reflections and p is the number of refined parameters.
5. International Tables for X-ray Crystallography (1992). Vol. C, Tables 4.2.6.8 and 6.1.1.4, A. J. C. Wilson, editor, Boston: Kluwer Academic Press.
6. Sheldrick, G. M. (1994). SHELXTL/PC (Version 5.03). Siemens Analytical X-ray Instruments, Inc., Madison, Wisconsin, USA.
7. APEX II 1.08, **2004**, Bruker AXS, Inc., Madison, Wisconsin 53719.
8. SAINT+ 7.06, **2003**, Bruker AXS, Inc., Madison, Wisconsin 53719.
9. SADABS 2.03, **2001**, George Sheldrick, University of Göttingen, Germany.
10. SHELXTL 5.10, **1997**, Bruker AXS, Inc., Madison, Wisconsin 53719.
11. CrystalClear 1.40, Rigaku Americas Corporation, The Woodlands, TX, 2008.
12. Spek, A. L. (1998). PLATON, A Multipurpose Crystallographic Tool. Utrecht University, The Netherlands.
13. WinGX 1.64. (1999). An Integrated System of Windows Programs for the Solution, Refinement and Analysis of Single Crystal X-ray Diffraction Data. Farrugia, L. J. J. Appl. Cryst. 32. 837-838.
14. Sluis, P. v. d. and Spek, A. L. (1990). SQUEEZE. Acta Cryst. A46, 194-201.

Comprehensive Bibliography

- Letheby, H. *J. Chem. Soc.*, **1862**, *15*, 161.
- Akamatu, H.; Inokuchi, H.; Matsunaga, Y. *Nature,* **1954**, *173,* 168.
- Jérome, D.; *Chem Rev*. **2004**, *104*, 5565.
- (a) Acker, D. S.; Blomstrom, D. C., *J. Am. Chem. Soc.,* **1962**, *84*, 3370. (b) Burarov, L.; Fedutin, D.; Shchegolev, I. *Zh. Eksp. Teor. Fiz.* **1970**, *59*, 1125. (c) Shchegolev, I. *Phys. Status Solidi A* **1972**, *12*, 9.
- TTF was actually first synthesized in 1965 and known as bis-1,3-Dithiolium, but only later realized to possess strong electron donating ability. Prinzbach, H.; Berger, H.; Luttringhaus, A. *Angew. Chem. Int. Ed. Engl.* **1965**, *4*, 435.
- Three research groups independently and almost simultaneously reported the synthesis and associated studies of TTF (a) Wudl, F.; Smith, G. M.; Hufnagel, E. J. *J. Chem. Soc., Chem. Commun*. **1970**, 1453. (b) Coffen, D. L.; Chambers, J. Q.; Williams, D. R.; Garrett, P. E.; Canfield, N. D. *J. Amer. Chem. Soc*. **1971**, 109. (c) Hünig, S.; Kiesslich, G.; Scheutzow, D.; Zahradnik, R.; Carsky, P. *Int. J. Sulfur Chem. Part C*, **1971**, *6*, 109.
- Wudl, F.; Wobschall, D.; Hafnagel, E. *J. Am. Chem. Soc*. **1972**, *94*, 670.
- Ferraris, J.; Cowan, D. O.; Walatka, V. V., Jr.; Perlstein, J. H. *J. Am. Chem. Soc*. **1973**, *95*, 948.
- Coleman, L. B.; Cohen, M. J.; Sandman, D. J.; Yamagishi, F. G.; Garito, A. F.; Heeger, A. J. *Solid State Commun*. **1973**, *12*, 1125.
- (a) Yamada, J.-I., Sugimoto, T., Eds. *TTF Chemistry: Fundamentals and Applications of Tetrathiafulvalene*; Springer: Berlin, Germany, 2004. (b) Rovira, C. *Chem. Rev*. **2004**, *104*, 5289. (c) Mas-Torrent, M.; Hadley, P.; Bromley, S. T.; Crivillers, N.; Veciana, J.; Rovira, C. *Appl. Phys. Lett*. **2005**, *86*, 02110. (d) Mas-Torrent, M.; Durkut, M.; Hadley, P.; Ribas, X.; Rovira, C. *J. Am. Chem. Soc*. **2004**, *126*, 984. (e) Mas-Torrent, M.; Hadley, P.; Bromley, S. T.; Ribas, X.; Tarres, J.; Mas, M.; Molins, E.; Veciana, J.; Rovira, C. *J. Am. Chem. Soc*. **2004**, *126*, 8546. (f) Dressel, Mm; Drichko, N. *Chem. Rev*. **2004**, *104*, 5869. (g) Bendikov, M.; Wudl, F. Perepichka, D. F. *Chem. Rev*. **2004**, *104*, 4891. (h) Talham, D. R.; *Chem. Rev*. **2004**, *104*, 5479. (i) Kartsovnik, M. V. *Chem. Rev*. **2004**, *104*, 5737. (j) Gieser, U.; Schlueter, J. A. *Chem. Rev*. **2004**, *104*, 5203. (k) Enoki, T. Miyazaki, A. *Chem. Rev*. **2004**, *104*, 5449. (l) Shibaeva, R. P.; Yagubskii, E. B. *Chem. Rev*. **2004**, *104*, 5347. (m) Fourmigué, M.; Batail, P. *Chem. Rev*. **2004**, *104*, 5379. (n) Iyoda, M.; Hasegawa, M.; Miyake, Y. *Chem. Rev*. **2004**, *104*, 5085. (o) Yamada, J. I.; Akutsu, H.; Nishikawa, H.; Kikuchi, K. *Chem. Rev*. **2004**, *104*, 5057. (p) Kobayashi, H.; Cui, H. B.; Kobayashi, A. *Chem.*

Rev. **2004**, *104*, 5265. (q) Kobayashi, A.; Fujiwara, E.; Kobayashi, H. *Chem*. *Rev*. **2004**, *104*, 5243. (r) Mori, T. *Chem*. *Rev*. **2004**, *104*, 4947. (s) Fabre, J. M.; *Chem*. *Rev*. **2004**, *104*, 5133.

- Jérome, D.; Mazaud, A.; Ribault, M.; Bechgaard, K. *J*. *Phys*., *Lett*. **1980**, *41*, L-95.

- (a) Urayama, H.; Yamochi, H.; Saito, G.; Nozawa, K; Sugano, T.; Kinoshita, M.; Sato, S.; Oshima, K.; Kawamoto, A.; Tanaka, J. *Chem*. *Lett*. **1988**, 55. (b) Kini, A. M.; Geiser, U.; Wang, H. H.; Carlson, K. D.; Williams, J. M.; Kwok, W. K.; Vandervoot, K. G.; Thompson, J. E.; Stupka, D. L.; Jung, D.; Whangbo, M. H. *Inorg*. *Chem*. **1990**, *29*, 2555. (c) Williams, J. M.; Kini, A. M.; Wang, H. H.; Carlson, K. D.; Geiser, U.: Montgomery, L. K.; Pyrka, G. J.; Watkins, D. M.; Kommers, J. M.; Boryshuk, S. J.; Strieby Crouch, A. V.; Kwok, W. K.; Schirber, J. E.; Overmyer, D. L.; Jung, D.; Whangbo, M. H. *Inorg*. *Chem*. **1990**, *29*, 3272. (d) Williams, J. M.; Schultz, A. J. Geiser, U.: Carlson, K. D.; Kini, A. M.; Wang, H. H.; Kowk, W. K.; Whangbo, M. H.; Schirber, J. E. *Science,* **1991**, *252*, 1501. (e) Schlueter, J. A.; Williams, J. M.; Geiser, U.; Dudek, J. D.; Sirchio, S. A.; Kelly, M. E.; Gregar, J. S.; Kwok, W. K.; Fendrich, J. A.; Schirber, J. E.; Bayless, W. R.; Naumenn, D.; Roy, T. *J*. *Chem*. *Soc*., *Chem*. *Commun*. **1995**, 1311. (f) Williams, J. M.; Ferraro, J. R.; Thorn, R. J.; Carlson, K. D. Geiser, U.; Wang, H. H.; Kini, A. M.; Whangbo, M. H. *Organic Superconductors (Including Fullerenes) Synthesis, Structure, Properties, and Theory*; Prentice-Hall, Inc., New Jersey, 1992.

- Wudl, F. *Acc*. *Chem*. *Res*. **1984**, *17*, 227.

- (a) Jorgensen, T.; Hansen, T. K.; Becher, J. *Chem*. *Soc*. *Rev*. **1994**, *23*, 41. (b) Nielsen, M. B.; Lomholt, C.; Becher, J. *Chem*. *Soc*. *Rev*. **2000**, *29*, 153.

- (a) Thomas, G. A.; Wudl, F.; DiSalvo, F.; Walsh, W. M., Jr.; Rupp, L. W.; Schafer, D. E. *Solid State Commun*. **1976**, *20*, 1009. (b) Wudl, F.; Schafer, D. E.; Walsh, W. M., Jr.; Rupp, L. W.; DiSalvo, F. J.; Waszczak, J. V.; Kaplan, M. L.; Thomas, G. A. *J*. *Chem*. *Phys*. **1977**, *66*, 377. (c) Wudl, F. *J*. *Amer*. *Chem*. *Soc*. **1975** *97*, 1962. (d) Somoano, R. B.; Gupta, A.; Hadek, V.; Novotny, M.; Jones, M.; Datta, T.; Deck, S. R.; Hermann, A. M. *Phys*. *Rev*. *B* **1977**, *15*, 595. (e) Kobayashi, H.; Kobayashi, K. *Bull*. *Chem*. *Soc*. *Jpn*. **1977**, *50*, 3127.

- (a) Bozio, R.; Zanon, I.; Girlando, A.; Pecile, C. *J*. *Chem*. *Phys*. **1979**, *71*, 2282. (b) Torrance, J. B.; Scott, B. A.; Welber, B.; Kaufman, F. B.; Seiden, P. E. *Phys*. *Rev*. *B* **1979**, *19*, 730. (c) Khodorkovsky, V.; Shapiro, L.; Krief, P.; Shames, A.; Mabon, G.; Gorgues, A.; Giffard, M. *Chem*. *Commun*. **2001**, 2736. (d) Rosokha, S. V.; Kochi, J. K. *J*. *Am*. *Chem*. *Soc*. *2007*, 129, 828.

- (a) Yakushi, K.; Nishimura, S.; Sugano, T.; Kuroda, H.; Ikemoto, I. *Acta Crystallogr*. *B* **1980**, *36*, 358. (b) Kathirgamanathan, P.; Mazid, M. A.;

Rosseinsky, D. R. *J. Chem. Soc., Perkin Trans. 2* **1982**, 593. (c) Kondo, K.; Matsubayashi, G.; Tanaka, T.; Yoshioka, H.; Nakatsu, K. *J. Chem. Soc., Dalton Trans*. **1984**, 379. (d) Pyrka, G. J.; Fernando, Q.; Inoue, M. B.; Inoue, M. *Inorg. Chim. Acta* **1989**, *156*, 257. (e) Umeya, M.; Kawata, S.; Matsuzaka, H.; Kitagawa, S.; Nishikawa, H.; Kikuchi, K.; Ikemoto, I. *J. Mater. Chem*. **1998**, *8*, 295. (f) Tanaka, K.; Kunita, T.; Ishiguro, F.; Naka, K.; Chujo, Y. *Langmuir* **2009**, *25*, 6929.

- (a) Huchet, L.; Akoudad, S.; Levillain, E.; Roncali, J.; Emge, A.; Bäuerle, P. *J. Phys. Chem. B* **1998**, *102*, 7776. (b) Spanggard, H.; Prehn, J.; Nielsen, M. B.; Levillain, E.; Allain, M.; Becher, J. *J. Am. Chem. Soc*. **2000**, *122*, 9486.
- An in depth description of the various TTF-dimer stabilization strategies is given in Chapter 3.
- Hankache, J.; Wenger, O. S.; *Chem. Rev*. **2011**, *111*, 5138.
- (a) Davydov, A. S.; *Theory of Molecular Exitons* (Plenum, New York, 1971). (b) Craig, D. P.; Walmsley, S. H. *Exitons in Molecular Crystals* (Benjamin, New York, 1968).
- Phillips, T. E.; Kistenmacher, T. J.; Ferraris, J. P.; Cowan, D. O. *J. Chem. Soc., Chem. Commun*. **1973**, 471.
- Bejger, C.; Davis, C. M.; Park, J-S.; Lynch, V. M.; Love, J. B.; Sessler, J. L. *Org. Lett*., **2011**, *13*, 4902.
- Bejger, C.; Park, J-S.; Silver, E. S.; Sessler, J. L. *Chem. Commun*., **2010**, *46*, 7745.
- For Reviews on TTF-cyclophanes and TTF-oligimeric systems see: (a) Jeppesen, J. O.; Nielsen, M. B.; Becher, J. *Chem. Rev*. **2004**, *104*, 5115. (b) Iyoda, M.; Hasegawa, M.; Miyake, Y.; *Chem. Rev*. **2004**, *104*, 5085.
- (a) Hasegawa, M.; Iyoda, M. *Chem. Soc. Rev*. **2010**, *39*, 2420. (b) Amabilino, D. B.; Puigmartí-Luis, J. *Soft Matter* **2010**, *6*, 1605. (c) Canevet,, D.; Sallé, M.; Zhang, G.; Zhu, D. *Chem. Commun*. **2009**, 2245. (d) Iyoda, M.; Hasegawa, M.; Enozawa, E. *Chem. Lett*. **2007**, *36*, 1402.
- See Chapter 1 reference 12f.
- Urayama, H.; Yamochi, H.; Saito, G.; Nozawa, K. Sugano, T.; Kinoshita, M.; Sato, S.; Oshima, K.; Kawamoto, A.; Tanaka, J. *Chem. Lett*. **1988**, 55.
- Ziganshina, A. Y.; Ko, Y-H.; Jeon, W-S.; Kim, K. *Chem. Commun*. **2004**, 806.
- Yoshizawa, M.; Kumazawa, K.; Fujita, M. *J. Am. Chem. Soc*. **2005**, *127*, 13456.
- Martí-Rujas, J.; Islam, N.; Hashizume, D.; Izumi, F.; Fujita, M.; Song, H. J.; Choi, H. C.; Kawano, M. *Angew. Chem. Int. Ed*. **2011**, *50*, 6105.

- Bertho-Thoraval, F; Robert, A.; Souizi, A.; Boubekeur, K.; Batail, P. *J. Chem. Soc., Chem. Commun.* **1991**, 843.
- Lyskawa, J.; Sallé, M.; Balandie, J-Y.; Le Derf, F.; Levillain, E.; Allain, M.; Viel, P.; Palacin, S. *Chem. Commun.* **2006**, 2233.
- Hasegawa, M.; Daigoku, K.; Hashimoto, K.; Nishikawa, H.; Iyoda, M. *Bull. Chem. Soc. Jpn.* **2012**, *85*, 51.
- Nakamura, K.; Takashima, T.; Shirahata, T.; Hino, S.; Hasegawa, M.; Mazaki, Y.; Misaki, Y. *Org. Lett.* **2011**, *13*, 3122.
- Park, J. S.; Karnas, E.; Ohkubo, K.; Chen, P.; Kadish, K. M.; Fukuzumi, S.; Bielawski, C. W.; Hudnall, T. W.; Lynch, V. M.; Sessler, J. L. *Science* **2010**, *329*, 1324.
- (a) Coskun, A.; Spruell, J. M.; Barin, G.; Fahrenbach, A. C.; Forgan, R. S.; Colvin, M. T.; Carmieli, R.; Benítez, D.; Tkatchouk, E.; Friedman, D. C.; Sarjeant, A. A.; Wasielewski, M. R.; Goddard, W. A., III; Stoddart, J. F. *J. Am. Chem. Soc.*, **2011**, *133*, 4538. (b) Spruell, J. M.; Coskun, A.; Friedman, D. C.; Forgan, R. S.; Sarjeant, A. A.; Trabolsi, A.; Fahrenbach, A. C.; Barin, G.; Paxton, W. F.; Dey, S. K.; Olson, M. A.; Benítz, D.; Tkatchouk, E.; Colvin, M. T.; Carmielli, R.; Caldwell, S. T.; Rosair, G. M.; Hewage, S. G.; Duclairoir, F.; Seymour, J. L.; Slawin, A. M. Z.; Goddard, W. A., III; Wasielewski, M. R.; Cooke, G.; Stoddard, J. F. *Nat. Chem.* **2010**, *2*, 870.
- Takase, M.; Yoshia, N.; Nishinaga, T.; Iyoda, M. *Org. Lett.* **2011**, *13*, 3896.
- Cheng, P-N.; Chiang, P-T.; Chiu, S-H. *Chem. Commun.* **2005**, 1285. (b) Chiang, P-T.; Chen, N-C.; Lai, C-C.; Chiu, S-H. *Chem. Eur. J.* **2008**, *14*, 6546.
- Saad, A.; Barriére, F.; Levillain, E.; Vanthuyne, N.; Jeannin, O.; Fourmigué, M. *Chem. Eur. J.* **2010**, 16, 8020.
- Enozawa, H.; Hasegawa, M.; Takamatsu, D.; Fukui, K-I.; Iyoda, M. *Org. Lett.* **2006**, *8*, 1917.
- (a) Terech, P.; Weiss, R. G. *Chem. Rev.* **1997**, *97*, 3133. (b) Fages, F. *Low Molecular Mass Gelators* In *Topics in Current Chemistry* Ed.; Springer: Berlin, Heidelberg, New York, 2005; Vol. 256.
- Akutagawa, T.; Kakiuchi, K.; Hasegawa T.; Noro, S.; Nakamura, T.; Hasegawa, H.; Mashiko, S.; Becher, J. *Angew. Chem. Int. Ed.* **2005**, *44*, 7283.
- Puigmartí-Luis, J.; Laukhin, V.; Pérez del Pino, A.; Vidal-Gancedo, J.; Rovira, C.; Laukhina, E.; Amabalino, D. B. *Angew. Chem. Int. Ed.* **2007**, *46*, 238.
- Jørgensen, M.; Bechgaard, K. *J. Org. Chem.* **1984**, *59*, 5877.

- Kitahara, T.; Shirakawa, M.; Kawano, S.; Beginn, U.; Fujita, N.; Shinkai, S. *J. Am. Chem. Soc.* **2005**, *127*, 14980.
- Gale, P. A.; Sessler, J. L.; Král, V.; Lynch, V. *J. Am. Chem. Soc.* **1996**, *118*, 5184.
- Baeyer, A. *Ber. Dtsch Chem. Ges.* **1886**, *19*, 2184.
- Floriani, C.; Floriani-Moro, R. *Porphyrin Handbook* **2000**, *3*, 385.
- Gale, P. A.; Anzenbacher, P., Jr.; Sessler, J. L. *Coord. Chem. Rev* **2001**, *222*, 57.
- Sessler, J. L.; Cho, W-S; Dudek, S. P.; Hicks, L.; Lynch, V. M.; Huggins, M. T. *Journal of Porphyrins and Phthalocyanines **2003**, 7*, 97.
- 28. (a) Givaja, G.; Blake, A. J.; Wilson, C.; Schröder, M.; Love, J. B. *Chem. Commun.* **2003**, 2508. (b) Givaja, G.; Blake, A. J.; Wilson, C.; Schröder, M.; Love, J. B. *Chem. Commun.* **2005**, 4423. (c) Veauthier, J. M.; Tomat, E; Lynch, V. M.; Sessler, J. L.; Mirsaidov, U.; Markert, J. T. *Inorg. Chem.* **2005**, 44, 6736. (d) Tomat, E.; Cuesta, L.; Lynch, V. M.; Sessler, J. L. *Inorg. Chem.* **2007**, 46, 6224. (e) Givaja, G.; Volpe, M.; Leeland, J. W.; Edwards, M. A.; Young, T. K.; Darby, S. B.; Reid, S. D.; Blake, A. J.; Wilson, C.; Wolowska, J.; McInnes, E. J. L.; Schröder, M.; Love, J. B. *Chem.—Eur. J.* **2007**, 13, 3707. (f) Cuesta, L.; Tomat, E.; Lynch, V. M.; Sessler, J. L. *Chem. Commun.* **2008**, 3744. (g) Love, J. B. *Chem. Commun.* **2009**, 3154.
- (a) Collman, J. P.; Wagenknecht, P. S.; Hutchinson, J. E *Angew. Chem.* **1994**, *106*, 1620. (b) Dempsey, J. L.; Esswein, A. J.; Manke, D. R.; Rosenthal, J.; Soper, J. D.; Nocera, D. G. *Inorg. Chem.* **2005**, *44*, 6879. (c) Chang, C. J.; Loh, Z.-H.; Shi, C.; Anson, F. C.; Nocera, D. G. *J. Am. Chem. Soc.* **2004**, *126*, 10013. (d) Chang, C. J.; Deng, Y.; Shi, C.; Anson, F. C.; Nocera, D. G. *Chem. Commun.* **2000**, 1355. (e) Guilard, R.; Brandès, S.; Tardieux, C.; Tabard, A.; L'Her, M.; Miry, C.; Gouerec, P.; Knop, Y.; Collman, J. P. *J. Am. Chem. Soc.* **1995**, *117*, 11721. (f) Proniewicz, L. M.; Odo, J.; Goral, J.; Chang, C. K.; Nakamoto, C. K. *J. Am. Chem. Soc.* **1989**, *111*, 2105 (g) Durand, R. R.; Bencosme, Jr., C. S.; Collman, J. P.; Anson, F. C. *J. Am. Chem. Soc.* **1983**, *105*, 2710. (h) Collman, J. P.; Denisevich, P.; Konai, Y.; Marrocco, M.; Koval, C.; Anson, F. C. *J. Am. Chem. Soc.* **1980**, *102*, 6027. (i) Hodgkiss, J. M.; Chang, C. J.; Pistorio, B. J.; Nocera, D. G. *Inorg. Chem.* **2003**, *42*, 8270. (j) Pistorio, B. J.; Chang, C. J.; Nocera, D. G. *J. Am. Chem. Soc.* **2002**, *124*, 7884. (k) Rosenthal, J.; Luckett, T. D.; Hodgkiss, J. M.; Nocera, D. G. *J. Am. Chem. Soc.* 2006, **128**, 6546. (l) Rosenthal, J.; Pistorio, B. J.; Chng, L. L.; Nocera, D. G. *J. Org. Chem.* **2005**, *70*, 1885.
- Arnold, P. L.; Potter, N. A.; Carmichael, C. D.; Slawin, A. M. Z.; Roussel, P.; Love, J. B. *Chem. Commun.* **2010**, 1833. (b) Arnold, P. L.; Blake, A. J.; Wilson, C.; Love, J. B. *Inorg. Chem.* **2004**, *43*, 8206. (c) Arnold, P. L.; Patel, D.; Pécharman, A.-F.; Wilson, C.; Love, J. B. *Dalton Trans.* **2010**, *39*, 3501. (d)

Arnold, P. L.; Patel, D.; Wilson, C.; Love, J. B. *Nature* **2008**, *451*, 315. (e) Arnold, P. L.; Pécharman, A.-F.; Hollis, E.; Yahia, A.; Maron, L.; Parsons, S.; Love, J. B. *Nat. Chem.* **2010**, *2*, 1056. (f) Arnold, P. L.; Hollis, E.; White, F. J.; Magnani, N.; Caciuffo, R.; Love, J. B. *Angew. Chem., Int. Ed.* **2011**, *50*, 887.

- Leeland, J. W.; White, F. J.; Love, J. B. *J. Am. Chem. Soc.* **2011**, *133*, 7320.
- Jia, C.; Liu, S. X.; Tanner, C.; Leiggener, C.; Neels, A.; Sanguinet, L.; Levillain, E.; Leutwyler, S.; Hauser, A.; Decurtins, S. *Chem.–Eur. J.* **2007**, *13*, 3804.
- Spanggard, H.; Prehn, J.; Nielsen, M. B.; Levillain, E.; Allain, M.; Becher, J. *J. Am. Chem. Soc.* **2000**, 122, 9486.
- Wang, F. F.; Wang, F.; Wang, B. Q.; Wang, Y. F.; Ma, F.; Li, Z. R. *Sci. China Ser. B: Chem.* **2009**, *52*, 1980.
- Ma, B.; Li, J.; Djurovich, P.; Yousufuddin, M.; Bau, R.; Thompson, M. E. *J. Am. Chem. Soc.*, **2005**, *127*, 28.
- (a) Yamashita, Y.; Kobayashi, Y.; Miyashi, T. *Angew. Chem., Int. Ed. Engl.* **1989**, *28*, 1052. (b) Bryce, M. R.; Moore, A. J.; Hasan, M.; Ashwell, G. J.; Fraser, A. T.; Clegg, W.; Hursthouse, M. B.; Karaulov, A. I. *Angew. Chem., Int. Ed. Engl.* **1990**, *29*, 1450.
- (a) Lorcy, D.; Bellec, N.; Fourmigué, M.; Avarvari, N. *Coord. Chem. Rev.* **2009**, 1398. (b) Shatruk, M.; Ray, L. *Dalton. Trans.* **2010**, *39,* 11105.
- (a) Zhou, B.; Idobata, Y.; Kobayashi, A.; Cui, H.; Kato, R.; Takagi, R.; Miyagawa, K.; Kanoda, K.; Kobayashi, H. *J. Am. Chem. Soc.* **2012**, *132*, 2385. (b) Zhang, B.; Zhang, Y.; Zhu, D. *Chem. Commun.* **2011**, *48*, 197. (c) Nishijo, J.; Judai, K.; Nishi, N. *Inorg. Chem.* **2011**, *50*, 3464. (d) Ouahab, L.; Enoki, T. *Eur. J. Inorg. Chem.* **2004**, 933. (e) Coronado, E.; Day, P. *Chem. Rev.* **2004**, *104*, 5419. (f) Coronado, E.; Galan-Mascaros, J. R.; Gomez-Garcia, C. J.; Laukhin, V. *Nature*, **2000**, *408*, 447.
- (a) Imakubo, T.; Sawa, H.; Tajima, H.; Kato, R. *Synt. Met.* **1997**, 2047. (b) Dyachenko, O. A.; Kazheva, O. N.; Gritsenk, V. V.; Kushch, N. D. *Synt. Met.* **2001**, 1017. (c) Otsuka, T.; Cui, H.; Kobayashi, A.; Misaki, Y.; Kobayashiz, H. *J. Solid State Chem.* **2002**, *168*, 444. (d) Tamura, M.; Yamanaka, K.; Mori, Y.; Nishio, Y.; Kajita, K.; Mori, H.; Tanaka, S.; Yamaura, J. –I.; Imakubo, T.; Kato, R.; Misaki, Y.; Tanaka, K. *Synt Met.* **2001**, 442. (e) Pointillart, F.; Bourdolle, A.; Cauchy, T.; Maury, O.; Gal, Y. L.; Golhen, S.; Cador, O.; Ouahab, L. *Inorg. Chem.* **2011**, *51*, 978. (f) Pointillart, F.; Cauchy, T.; Maury, O.; Gal, Y. L.; Golhen, S.; Cador, O.; Ouahab, L. *Chem. Eur. J.* **2010**, *16*, 11926. (g) Pope, S. J. A.; Burton-Pye, B. P.; Berridge, R.; Khan, T.; Skabara, P. J.; Faulkner, S. *Dalton. Trans.* **2006**, 2907. (h) Faulkner, S.; Burton-Pye, B. P.; Khan, T.;Martin, L. R.;

Wray, S. D.; Skabara, P. J. *Chem. Commun.* **2002**, 1668. (i) Pointillart, F.; Gal, Y. L.; Golhen, S.; Cador, O.; Ouahab, L. *Inorg. Chem.* **2009**, *48*, 4631. (j) Pointillart, F.; Klementieva, S.; Kuropatov, V.; Gal, Y. L.; Golhen, S.; Cador, O.; Cherkasov, V.; Ouahab, L. *Chem. Commun.* **2012**, *48*, 714. (k) Pointillart, F.; Maury, O.; Gal, Y. L.; Golhen, S.; Cador, O.; Ouahab, L. *Inorg. Chem.* **2009**, *48*, 7422. (l) Pointillart, F.; Gal, Y. L.; Golhen, S.; Cador, O.; Ouahab, L. *Chem. Eur. J.* **2011**, *17*, 10397.

- C. E. Housecroft and A. G. Sharpe, Inorganic Chemistry, 3rd edition, 2008, Pearson Education Ltd., Gosport, UK.

- For examples of actinides bound to redox-active ligands see: (a) Monreal, M. J. and Diaconescu, P. L. *J. Am. Chem. Soc.* **2010**, *132*, 7676. (b) Diaconescu, P. L., Arnold, P. L., Baker, T. A., Mindiola, D. J., and Cummins, C. C. *J. Am. Chem. Soc.* **2000**, 122, 6108. (c) Kraft, S. J., Fanwick, P. E., and Bart, S. C. *Inorg. Chem.* **2010**, *49*, 1103. (d) Schelter, E. J., Wu, R. L., Scott, B. L., Thompson, J. D., Cantat, T., John, K. D., Batista, E. R., Morris, D. E., and Kiplinger, J. L. *Inorg. Chem.* **2010**, *49*, 924. (e) Camp, C.; Mougel, V.; Horeglad, P.; Pécaut, J.; Mazzanti, M. *J. Am. Chem. Soc.* **2010**, *132*,17374

- Rivera, N. M.; Engler, E. M.; Schumaker, R. R.; *J. Chem. Soc., Chem. Commun.* **1979**, 184.

- Gemmell, C.; Kilburn, J. D.; Ueck, H.; Underhill, A. E. *Tetrahedron Lett.*, **1992**, *33*, 3923. (b) Gemmell, C.; Janairo, G. C.; Kilburn, J. D.; Ueck, H.; Underhill, A. E. *J. Chem. Soc., Perkin Trans. 1*, **1994**, 2715. (c) Becher, J.; Lau, J.; Leriche, P.; Mørk, P.; Svenstrup, N. *J. Chem. Soc., Chem. Commun.*, **1994**, 2715. (d) Svenstrup, N.; Rasmussen, K. M.; Hansen, T. K.; Becher, J. *Synthesis*, **1994**, 809.

- Tanaka, H.; Okano, Y.; Kobayashi, H.; Suzuki, W.; Kobayashi, A. *Science*, **2001**, *291*, 285.

- Isomura, E.; Tokuyama, K. I.; Nishinaga, T.; Iyoda, M. *Tetrahedron Lett.*, **2007**, *48*, 5895. (b) Fourmigué, M.; Batail, P. *Bull. Soc. Chim. Fr.*, **1992**, *129*, 29. (c) Yuan, M.; Ülgüt, B.; McGuire, M.; Takada, K.; DiSalvo, F. J.; Lee, S; Abruña, H. *Chem. Mater.*, **2006**, *18*, 4296.

- Jia, C.; Liu, S.-X.; Ambrus, C.; Neels, A.; Labat, G.; Decurtins, S. *Inorg. Chem.* **2006**, 45, 3152.

- Green, D. C. *J. Chem. Soc., Chem. Commun.*, **1977**, 161. (b) Ebihara, M.; Nomura, M.; Sakai, S.; Kawamura, T. *Inorg. Chim. Acta*, **2007**, *360*, 2345.

- (a) Bellec, N.; Lorcy, D.; *Tetrahedron Lett.*, **2001**, *42*, 3189. (b) Massue, J.; Bellec, N.; Chopin, S.; Levillain, E.; Roisnel, T.; Clérac, R.; Lorcy, D. *Inorg. Chem.*, **2005**, *44*, 8740. (c) Bellec, N.; Massue, J.; Roisnel, T.; Lorcy, D. *Inorg. Chem. Commun.*, **2007**, *10*, 1172.

- Jia, C.; Liu, S. X.; Tanner, C.; Leiggener, C.; Neels, A.; Sanguinet, L.; Levillain, E.; Leutwyler, S.; Hauser, A.; Decurtins, S. *Chem.–Eur. J.*, **2007**, *13*, 3804. (b) Goze, C.; Leiggener, C.; Liu, S. X.; Sanguinet, L.; Levillain, E.; Hauser, A.; Decurtins, S. *ChemPhysChem*, **2007**, *8*, 1504. (c) Wu, J. C.; Liu, S. X.; Keene, T. D.; Neels, A.; Mereacre, V.; Powell, A. K.; Decurtins, S. *Inorg. Chem.*, **2008**, *47*, 3452.
- Ran, Y. F.; Bluma, C.; Liu, S-X.; Sanguinet, L.; Levillain, E.; Decurtins, S., *Tetrahedron*, **2011**, *67*,1623.
- Bang, K. S.; Nielsen, M. B.; Zubarev, R.; Becher, J. *Chem. Commun.*, **2000**, 215.
- Bivaud, S.; Balandier, J-Y.; Chas, N.; Allain, M.; Goeb, S.; Sallé, M. *J. Am. Chem. Soc.*, **2012**, *134*, 11968.
- Ichikawa, S.; Mori, H. *Inorg. Chem.*, **2009**, *48*, 4643.
- Parker, D. *Coord. Chem. Rev.* **2000**, *205*, 109. (b) Parker, D. *Chem. Soc. Rev.* **2004**, *33*, 156. (c) Eliseeva, S.V.; Bünzli, J.-C. G. *Coord. Chem. Rev.* **2010**, *39*, 189.
- Bencini, A.; Benelli, C.; Caneschi, A.; Carlin, R. L.; Dei, A.; Gatteschi, D. *J. Amer. Chem. Soc.* **1985**, *107*, 8128
- Andruh, M.; Costes, J.-P.; Diaz, C.; Gao, S. *Inorg. Chem.*, **2009**, *48*, 3342.
- (a) Cosquer, G.; Pointillart, F.; Gal, Y.-L.; Golhen, S.; Cador, O.; Ouahab, L.; *Chem. Eur. J.* **2011**, *17*, 12502. (b) Cosquer, G.; Pointillart, F.; Guennic, B. L.; Gal, Y. L.; Golhen, S.; Cador, O.; Ouahab, L. *Inorg. Chem.* **2012**, *51*, 8488.
- There are numerous reports where actinides show evidence of covalent bonding: (a) Diamond, R. M.; Street, K.; Seaborg, G. T. *J. Am. Chem. Soc.* **1954**, *76*, 1461. (b) Tatsumi, K.; Nakamura, A.; Hofmann, P.; Stauffert, P.; Hoffmann, R. *J. Am. Chem. Soc.* **1985**, *107*, 4440. (c) Pepper, M.; Bursten, B. E. *Chem. Rev.* **1991**, *91*, 719. (d) Kuchle, W.; Dolg, M.; Stoll, H.; Preuss, H. *J. Chem. Phys.* **1994**, *100*, 7535. (e) Gagliardi, L.; Willetts, A.; Skylaris, C. K.; Handy, N. C.; Spencer, S.; Ioannou, A. G.; Simper, A. M. *J. Am. Chem. Soc.* **1998**, *120*,11727. (f) Barros, N.; Maynau, D.; Maron, L.; Eisenstein, O.; Zi, G.; Andersen, R. A. *Organometallics* **2007**, *26*, 5059. (g) Tassell, M. J.; Kaltsoyannis, N. *Dalton Trans.* **2010**, *39*, 6719. (h) Kirker, I.; Kaltsoyannis, N. *Dalton Trans.* **2011**, 40, 124.
- Clark, D. L. *The Chemical Complexities of Plutonium*, Los Alamos Science, **2000**, *26*, 364. (b) Denning, R. G. *J. Phys. Chem. A.* **2007**, *111*, 4125. (c) Denning, R. G.; Green, J. C.; Hutchings, T. E.; Dallera, C.; Tagliaferri, A.; Giarda, K.; Brookes, N. B.; Braicovich, L. *J. Chem. Phys.,* **2002**, *117*, 8008. (d) Clark, D. L.; Hobart, D. E.; Neu, M. P.; *Chem. Rev.* **1995**, *95*, 25.

- Sessler, J. L.; Melfi, P. J.; Dan Pantos, G. *Coord. Chem. Rev.*, **2006**, *250*, 816.
- Bandoli, G.; Clemente, D. A.; Croatto, U.; Vidali, M.; Vigato, P. A.; *Chem. Commun*. **1971**, 1330.
- (a) Wroblewski, W.; Wojciechowski, K.; Dybko, A.; Brzozka, Z.; Egberink, R J. M.; Snellink-Rüel, B. H. M.; Reinhoudt, D. N. *Sens. Actuators B*, **2001**, *78*, 315. (b) Wroblewski, W.; Wojciechowski, K.; Dybko, A.; Brzozka, Z.; Egberink, R J. M.; Snellink-Rüel, B. H. M.; Reinhoudt, D. N. *Anal. Chim. Acta*, **2001**, *432*, 79. (c) Ion, A. C.; Antonisse, M. M. G.; Snellink-Rüel, B. H. M.; Reinhoudt, D. N. *Russ. J. Gen. Chem.*, **2001**, *71*, 159.
- (a) Takao, K.; Ikeda, Y. *Inorg. Chem*. **2007**, *46*, 1550. (b)Mizuoka, K.; Kim, S-Y.; Hasegawa, M.; Hoshi, T.; Uchiyama, G.; Ikeda, Y. *Inorg. Chem*. **2003**, *42*, 1030.
- Chuguryan, D. G.; Dzyubenko, V. I.; Grigoriev, M. S.; Yanovskii, A. I.; Struchkov, Y. T. *Radiokhimiya*, **1988**, *30*, 41.
- Jia, H-P.; Ding, J.; Ran, Y. F.; Liu, S. X.; Blum, C. Petkova, I.; Hauser, A.; Decurtins, S. *Chem. Asian J*. **2011**, *6*, 33121.
- Jia, H.; Schmid, B.; Liu, S-X.; Jaggi, M.; Monbaron, P.; Bhosale, S. V.; Rivadehi, S.; Langford, S. J.; Sanguinet, L.; Levillain, E.; El-Kouly, M. E.; Morita, Y.; Fukuzumi, S.; Decurtins, S. *Chem. Phys. Chem*. **2012**, *13*, 3370.
- (a) Adams, R. L. P.; Knowler, J. T.; Leader, D. P. *The Biochemistry of the Nucleic Acids*, 10th ed.; Chapman and Hall: New York, **1986**. (b) Sessler, J. L.; Katayev, E. A.; Ustynyuk, Y. A. *Coord. Chem. Rev.*, 2006, **250**, 3004. (c) Hruska, K.; Teitlebaum, S. *New Engl. J. Med*. **1995**, *333*, 166. (d) Block, G. A.; Port, F. K. Am. J. *Kidney Dis*. **2000**, *35*, 1226. (e) Delmez, J. A.; Slatopolsky, E. Am. *J. Kidney Dis*. **1992**, *19*, 303.
- (a) Sessler, J.; Gale, P. A.; Cho W.-S. *Anion Receptor Chemistry*; The Royal Society of Chemistry: Cambridge, U.K., **2006**. (b) Mason, C. F. *Biology of Freshwater Pollution*; Longman: New York, **1991**. (c) *Phosphorus in the Global Environment: Transfers, Cycles, and Management*; Tiessen, H., Ed.; Wiley: New York, **1995**.
- Hargrove, A. E.; Nieto, S.; Zhang, T.; Sessler, J. L.; Anslyn, E. V. *Chem. Rev*. **2011**, *111*, 6603.
- (a) Szemes, F.; Hesek, D.; Chen, Z.; Dent, S. W.; Drew, M. G. B.; Goulden, A. J.; Graydon, A. R.; Grieve, A.; Mortimer, R. J.; Wear, T. J.; Weightman, J. S.; Beer, P. D. *Inorg. Chem*. **1996**, *35*, 5868 (b) Aldakov, D.; Anzenbacher, Jr., P.; *J. Am. Chem. Soc.*, **2004**, *126*, 4752 (c) Anzenbacher, Jr., P.; Palacios, M. A.; Jusikova, K. Marquez, M.; *Org. Lett.*, **2005**, *7*, 5027.

- (a) Fiske, C. H.; Subbarow, Y. *J. Biol. Chem.* **1925**, *66*, 375. (b) Gee, A.; Deitz, V. R. *Anal. Chem.* **1953**, *25*, 1320. (c) Duff, E. J.; Stuart, J. L. *Analyst* **1971**, 96, 802. (c) Shida, J.; Matsuo, T. *Bull. Chem. Soc. Jpn.* **1980**, *53*, 2868. (d) Worsfold, P. J.; Gimbert, L. J.; Mankasingh, U.; Omaka, O. N.; Hanrahan, G.; Gardolinski, P. C. F. C.; Haygarth, P. M.; Turner, B. L.; Keith-Roach, M. J.; McKelvie, I. D. *Talanta* **2005**, *66*, 273. (e) Guilbault, G. G.; Nanjo, M. *Anal. Chim. Acta* **1975**, *78*, 69. (f) Gajovic, N.; Habermuller, K.; Warsinke, A.; Schuhmann, W.; Scheller, F. W. *Electroanalysis* **1999**, *11*, 1377. (g) Kubo, I.; Inagawa, M.; Sugawara, T.; Arikawa, Y.; Karube, I. *Anal. Lett.* **1991**, *24*, 1711 (h) Amine, A.; Palleschi, G. *Anal. Lett.* **2004**, *37*, 1. (i) Luque de Castro, M. D.; Quiles, R.; Fernández-Romero, J. M.; Fernández, E. *Clin. Chem.* **1995**, *41*, 99 (j) Schulz, D. W.; Passonneau, J. V.; Lowry, O. H. *Anal. Biochem.* **1967**, *19*, 300.
- Marcus, Y. *Biophys. Chem.* **1994**, *51*, 111.
- (a) Antonisse, M. M. G.; Reinhoudt, D. N. *Chem. Commun.* **1998**, 443 (b) Snowden, T. S.; Anslyn, E. V. Curr. Opin. *Chem. Biol.* **1999**, *3*, 740 (c) Beer, P. D.; Gale, P. A. *Angew. Chem., Int. Ed.* **2001**, *40*, 486 (d) Aoki, S.; Kimura, E. *Rev. Mol. Biotechnol.* **2002**, *90*, 129 (e) Hartley, J. H.; James, T. D.; Ward, C. J. *J. Chem. Soc., Perkin Trans. 1* **2000**, 3155.
- Beer, P. D.; Bayly, S. R. *Top. Curr. Chem.* **2005**, *255*, 125.
- Beer, P. D.; Chen, Z.; Goulden, A. J.; Graydon, A.; Stokes, S. E.; Wear, T. *J. Chem. Soc., Chem. Commun.* **1993**, 1834.
- Evans, A. J.; Matthews, S. E.; Cowley, A. R.; Beer, P. D. *Dalton Trans.* **2003**, 4644.
- Duff, T.; Grussing, A.; Thomas, J.-L.; Duati, M.; Vos, J. G. *Polyhedron* **2003**, *22*, 775.
- Becher, J.; Nielsen, K. A.; Jeppeson, J. O.; Levillian, E. *Angew. Chem., Int. Ed.*, **2003**, *42*, 187.
- (a) Zhu, D.; Xu, W.; Lu, H.; Zhang, D.; Chen, C.; *Org. Lett.*, **2005**, *7*, 4629. (b) Lu, H.; Xu, W.; Zhang, D.; Zhu, D. *Chem. Commun.*, **2005**, 4777.
- Black, C. B.; Andrioletti, B.; Try, A. C.; Ruiperez, C.; Sessler, J. L. *J. Am. Chem. Soc.*, **1999**, *121*, 10438.
- (a) Oddo, B. Gazz. *Chim. Ital.* **1911**, *41*, 248. (b) Behr, D.; Brandänge, S.; Lindström, B. *Acta Chem. Scand.* **1973**, *27*, 2411.
- Anzenbacher, P.; Try, A. C.; Miyaji, H.; Jursikova, K.; Lynch, V. M.; Marquez, M.; Sessler, J. L. *J. Am. Chem. Soc.* **2000**, *122*, 10268.
- Mizuno, T.; Wei, W.-H.; Eller, L. R.; Sessler, J. L. *J. Am. Chem. Soc.* **2002**, *124*, 1134.

- Anzenbacher, P., Jr.; Palacios, M. A.; Jursíková, K.; Marquez, M. *Org. Lett.* **2005**, *7*, 5027.
- Aldakov, D.; Anzenbacher, P., Jr. *J. Am. Chem. Soc.* **2004**, *126*, 4752.
- Sessler, J. L.; Cho, D-G.; Lynch, V. *J. Am. Chem. Soc.* **2006**, *128*, 16518.
- Wang, T.; Yan, X. P. *Chem.–Eur. J.*, **2010**, *16*, 4639.
- (a) Caltagirone, C.; Gale, P. A.; Hiscock, J. R.; Hursthouse, M. B.; Light, M. E.; Tizzard, G. J. *Supramol. Chem.* **2009**, *21*, 125. (b) Amendola, V.; Boicchi, M.; Esteban-Gomez, D.; Fabrizzi, L.; Monzani, E. *Org. Biomol. Chem.* **2005**, *3*, 2632.
- Connors, K. A. *Binding Constants*, John Wiley, New York, **1987**
- Palacios, M. A.; Nishiyabu, R.; Marquez, M.; Anzenbacher, Jr., P. *J. Am. Chem. Soc.*, **2007**, *129*, 7538.
- (a) Sessler, J. L.; Katayev, E.; Pantos, G. D.; Ustynyuk, Y. A. *Chem. Commun.*, **2004**, 1276. (b) Sessler, J. L.; Katayev, E.; Pantos, G. D.; Scherbakov, P.; Reshetova, M. D.; Khrustalev, V. N.; Lynch, V. M.; Ustynyuk, Y. A. *J. Am. Chem. Soc.* **2005**, *127*, 11442.
- DENZO-SMN. (1997). Z. Otwinowski and W. Minor, Methods in Enzymology, **276**: Macromolecular Crystallography, part A, 307 – 326, C. W. Carter, Jr. and R. M. Sweets, Editors, Academic Press.
- SIR97. (1999). A program for crystal structure solution. Altomare A., Burla M.C., Camalli M., Cascarano G.L., Giacovazzo C. , Guagliardi A., Moliterni A.G.G., Polidori G.,Spagna R. J. Appl. Cryst. 32, 115-119.
- Sheldrick, G. M. (1994). SHELXL97. Program for the Refinement of Crystal Structures. University of Gottingen, Germany.
- $R_w(F^2) = \{Sw(|F_o|^2 - |F_c|^2)^2/Sw(|F_o|)^4\}^{1/2}$ where w is the weight given each reflection. $R(F) = S(|F_o| - |F_c|)/S|F_o|\}$ for reflections with $F_o > 4(s(F_o))$. $S = [Sw(|F_o|^2 - |F_c|^2)^2/(n - p)]^{1/2}$, where n is the number of reflections and p is the number of refined parameters.
- International Tables for X-ray Crystallography (1992). Vol. C, Tables 4.2.6.8 and 6.1.1.4, A. J. C. Wilson, editor, Boston: Kluwer Academic Press.
- Sheldrick, G. M. (1994). SHELXTL/PC (Version 5.03). Siemens Analytical X-ray Instruments, Inc., Madison, Wisconsin, USA.
- APEX II 1.08, **2004**, Bruker AXS, Inc., Madison, Wisconsin 53719.
- SAINT+ 7.06, **2003**, Bruker AXS, Inc., Madison, Wisconsin 53719.
- SADABS 2.03, **2001**, George Sheldrick, University of Göttingen, Germany.

- SHELXTL 5.10, **1997**, Bruker AXS, Inc., Madison, Wisconsin 53719.
- CrystalClear 1.40, Rigaku Americas Corporation, The Woodlands, TX, 2008.
- Spek, A. L. (1998). PLATON, A Multipurpose Crystallographic Tool. Utrecht University, The Netherlands.
- WinGX 1.64. (1999). An Integrated System of Windows Programs for the Solution, Refinement and Analysis of Single Crystal X-ray Diffraction Data. Farrugia, L. J. J. Appl. Cryst. 32. 837-838.
- Sluis, P. v. d. and Spek, A. L. (1990). SQUEEZE. Acta Cryst. A46, 194-201.